CORTICAL FEEDBACK AND THE INTEGRATION OF SIGNALS ACROSS THE VISUAL FIELD

By

Gina Cantone

A dissertation submitted to the Graduate Faculty in Biology in partial fulfillment of the requirements for the degree of Doctor of Philosophy, The City University of New York

2005

This manuscript has been read and accepted for the Graduate Faculty in Biology in satisfaction of the dissertation requirements for the degree of Doctor of Philosophy.

Jonathan B. Levitt, Ph. D. June 21, 2005
Chair of Examining Committee Date

Richard L. Chappell, Ph. D. July 19, 2005
Executive Officer Date

Josh Wallman, Ph. D.

Christine Li, Ph. D.

Liesl B. Jones, Ph. D.

Micheal Hawken, Ph. D.
Supervisory Committee

Abstract

CORTICAL FEEDBACK AND THE INTEGRATION OF SIGNALS ACROSS THE VISUAL FIELD

By

Gina Cantone

Advisor: Jonathan B. Levitt

Mammalian cerebral cortex is comprised of many anatomically and physiologically distinct areas. Anatomical connections among these areas are a fundamental aspect of cortical architecture, yet many aspects of their organization and functional relevance remain poorly understood. We have studied the fine topographic organization of cortical feedback inputs to primary visual cortex (area 17) of the ferret (*Mustela putorius furo*). We made restricted injections of the anatomical tracer CTb into area 17, and mapped the distribution of retrogradely labeled cells throughout cerebral cortex. We found dense cell label in areas 18, 19, 21 and suprasylvian cortex (Ssy), and sparser connections from visual areas in lateral temporal and posterior parietal cortex. We then related the distribution of labeled cells to the map of visual space in each area, determined by electrophysiologically mapping receptive fields throughout cortex. In areas 18, 19, and 21 receptive fields of cells in the region containing labeled neurons overlapped those at the injection site, but spanned a greater distance in visual space than the receptive fields at the injection site. In electrophysiological experiments, we studied the physiological properties of single neurons in area 17. We directly measured the extent of visual space over which neuronal responses in the near-central representation of area

17 could be elicited or modified. We find for a proportion of cells that visual stimuli can evoke or modify responses over a region in visual space extending at least 35 º in diameter. This distance exceeds that spanned by monosynaptic connections within area 17, but is commensurate with the extent of feedback connections. We consistently found substantial feedback projections to area 17 arising from Ssy. Therefore we established the retinotopic organization in Ssy as a step in confirming the retinotopic precision of feedback connections arising from this area. Based on the retinotopic organization and receptive field size that it is likely that larger visuotopic extents converge onto less extensive regions of visual space in area 17 through feedback connections. These data are thus consistent with the suggestion that feedback connections in visual cerebral cortex contribute to response modulation by stimuli beyond the classical receptive field.

Acknowledgements

I thank my advisor Jonathan B. Levitt for his guidance and patience. I also thank Josh Wallman for his advice throughout the years, Jun Xiao for his help with this project and Blazej Andziak for his support.

Table of Contents

Title page……i

Approval page……ii

Abstract……iii

Acknowledgments……v

Table of Contents……vi

List of Tables……xi

List of Figures……xii

CHAPTER 1

BACKGROUND

General organization of cortex……1

Cortical connectivity and integration of visual information……4

Advantages in using ferret as model……7

Relevance to understanding cortical processing……10

CHAPTER 2

FEEDBACK CONNECTIONS TO FERRET STRIATE CORTEX: DIRECT EVIDENCE FOR VISUOTOPIC CONVERGENCE OF FEEDBACK INPUTS

2.1 INTRODUCTION……11

2.2 MATERIAL AND METHODS……12

Anatomical tracer injections ……12

Electrophysiological recording……14

Histological processing and identification of visual cortical areas……..…15

Cell counts and cell densities……..…20

Cortical magnification factors ……..…..…21

Determining cortical spread of retrogradely labeled cells……23

Determining retinotopic extents of retrogradely labeled cell..…….……... 28

2.3 RESULTS……..……...……30

Characteristics of retrograde label in extrastriate cortex…….……30

Direct evidence for retinotopic convergence of feedback connections…….46

Cortical magnification factors in extrastriate cortex …….50

Calculation of visuotopic extents corresponding to the cortical spreads of labeled fields……...54

2.4 DISCUSSION … ……62

Summary……62

Methodological considerations ……62

Factors governing the distribution of feedback connections and their functional relevance……..……..63

Comparisons to cat and primate……65

The role of feedback in modulatory surround effects…….…..……..…68

CHAPTER 3

EXTENT OF SUMMATION FIELDS OF NEURONS IN FERRET STRIATE CORTEX

3.1 INTRODUCTION…….……..……70

3.2 MATERIALS AND METHODS ……..…..……....…….……..…….. 71

S*urgical procedures*…….……...…..…….71

Recording methods and receptive field analysis…….…….…….72

Characterization of receptive fields…….…..…….…….….72

Data analysis…….……...……..…74

Histology and track reconstruction…….…….……..…76

3.3 RESULTS…….…….…...…..…….77

Classic receptive fields…….……...…….…….77

Spatial summation properties…….…….……..……87

Comparisons across cortical layers……..……94

Comparison of summation properties to MRF……..97

S*urround tuning*……..……101

Comparison to anatomical data.…….……..……..…106

3.4 DISCUSSION……...109

Summary…….…….109

Methodological considerations…….……..109

Minimum response fields…….111

Modulatory surround tuning…….……..….112

Laminar differences…….114

Possible anatomical substrates of summation……..……..….114

CHAPTER 4

RETINOTOPIC ORGANIZATION OF FERRET SUPRASYLVIAN CORTEX.

4.1 INTRODUCTION……..……...118

4.2 MATERIALS AND METHODS. ……..…..…….…..119

Electrophysiological recording…...……...119

Reconstruction of retrogradely labeled cells……..…….119

Reconstruction of recording sites in Ssy……..120

Calculating cortical magnification factors……..……121

Interpolation of retinotopic maps……..……..121

4.3 RESULTS ……126

Size and boundaries of Suprasylvian cortex……126

*Receptive fields in S*sy……..…….…..130

General trends in retinotopic organization of Ssy…….……..138

Extent of the representation of visual space……141

Connectional evaluation of retinotopic organization in Ssy ……..……145

Receptive field size and cortical magnification factor as a function of eccentricity……..……..…150

4.4 DISCUSSION……...…160

Summary…….…..……160

Defining suprasylvian cortex as a single visual area……..……160

Comparisons of Ssy with other visual areas in ferret cortex……..…….163

Comparisons with other species..……..…..165

Functional relevance of Ssy...…….…….……...166

CHAPTER 5

SUMMARY AND CONCLUSIONS ……..…..169

General Discussion…….169

Significance…….172

LITERATURE CITED…….175

List of Tables

CHAPTER 2

Table 1. Aggregate receptive field extents (ARFs) of injection cores and labeled fields……...58

List of Figures

CHAPTER 2

Figure 1. Multiple visual areas in ferret cortex……..……...……19

Figure 2. Relationship of the pattern of labeled cells to retinotopic organization in areas 17, 18, 19 and 21…….…….…….27

Figure 3. Brightfield photomicrographs of parasagittal brain sections showing labeling in cortex after a CTb injection in area 17……..……33

Figure 4. Serial reconstructions of retrograde label in visual cortex…….36

Figure 5. Feedback arising from different extrastriate areas…….39

Figure 6. Proportion of feedback projections arising from supra- and infragranular layers in each area……....42

Figure 7. Cortical spreads of labeled cells in the supra- and infragranular layers within cortical areas 17, 18, 19, and 21……..…..…..45

Figure 8. Density map and receptive field locations of cells providing feedback to area 17 determined in the same cas…. ……..49

Figure 9. Cortical magnification factors in visual areas 18, 19, and 21……53

Figure 10. Visuotopic extents of cells providing feedback connections compared to the visuotopic extents of the cells at the injection site and of labeled cells within area 17……..….57

Figure 11. Measured visuotopic extents of labeled cells in areas 18, 19, 21 in a representative case shown in Fig. 8…….……..61

CHAPTER 3

Figure 1. Contour plots of the response magnitudes within the minimum response field of cells in ferret area 17…..…….……...80

Figure 2. Responses of area 17 neurons to an expanding mask stimulus..……83

Figure 3. Comparison of two measures of the classic receptive field…..…….……....86

Figure 4. Three types of summation responses to an optimal stimulus expanding in diameter…….…….90

Figure 5. Bar graphs showing the population distribution of peak summation diameters, asymptotic response and the suppression index.……...……93

Figure 6. Laminar distributions of minimum response fields, peak summation diameters and asymptotic response diameters…….…….…….96

Figure 7. Scatter plots of peak summation diameter and asymptotic response diameter compared to the minimum response field…….…..….100

Figure 8. Orientation tuning of the surround…….……..105

Figure 9. Comparison of retinotopic precision of cells monosynaptically linked to a single locus in area 17 to the summation properties of area 17 cells…….……108

CHAPTER 4

Figure 1. Photomicrographs showing anatomical characteristics of Suprasylvian cortex …….125

Figure 2. Photomicrographs showing areal bundaries and distainct lamination in parasagittal sections…….……129

Figure 3. Progression of receptive fields in Ssy cortex …….……..133

Figure 3. Progression of receptive fields in Ssy cortex in a second case……..….135

Figure 5. Progression of receptive fields in Ssy cortex in a third case……..…..137

Figure 6. Interpolated retinotopic maps in Ssy …….……..……140

Figure 7. Extent of visual field representation in Ssy…….……144

Figure 8. Reconstructions and photomicrographs of tangential sections showing retrogradely labeled cells in area 17 after CTb injections in two different cases made at different retinotopic locations in Ssy…….…….148

Figure 9. Relationship between receptive field size and eccentricity…….…….153

Figure 10. Relationship between cortical magnification factors (MF) along different axes of visual space……..…156

Figure 11. Relationship of cortical magnification factors (MF) to eccentricity…….159

CHAPTER 1: BACKGROUND

General organization of cortex

Visual cortex is divided into multiple anatomically and functionally distinct areas. Despite their differences, there are aspects common to all areas of cortex. All of cerebral cortex contains six laminae (running parallel to the pial surface of the brain) that differ in the cell types they contain, and which vary in thickness among the different areas. Closest to the cortical surface is the molecular layer (layer I), which is composed mostly of dendrites and axons of cells in deeper layers. The external granular layer (layer II) is composed of small granule cells, and is above the external pyramidal layer (layer III), which is primarily made up of pyramidal cells. These layers are referred to collectively as the supragranular layers. In area 17, the internal granular layer (layer IV) is comprised of inhibitory smooth stellate cells and excitatory spiny stellate cells, some of which form lateral projections (Levitt et al., 1996). In other non-visual areas of cortex layer IV contains larger pyramidal cells. The internal pyramidal layer (layer V) contains large pyramidal cells. The multiform layer (layer VI) borders the white matter, and contains various types of cells (Lund, 1973). Layers V and VI are referred to as the infragranular layers.

Within visual cortex each area contains a map of visual space (Daniel and Whitteridge, 1961; Allman and Kaas, 1971, 1971a,b, 1975, 1976; Palmer et al., 1978; Tusa et al., 1978, 1979; Van Essen and Zeki 1978; Tusa and Palmer, 1980; Gattass et al., 1981, 1988; Law et al., 1988; Manger et al., 2002a, 2002b, 2004). Retinotopic maps are described in visual cortex as the positions of receptive fields at different cortical locations in degrees of elevation (lines of constant elevation span horizontally across the visual

field), and degrees of azimuth (lines of constant azimuth span vertically across the visual field). They can also be described in terms of eccentricity and visual angle (Gattass and Gross, 1981; Van Essen et al., 1981; Maunsell and VanEssen, 1987; Gattas et al., 1988). Maps are formed by adjacent neurons having adjacent or overlapping receptive fields (RFs), the region of visual field over which a stimulus can directly elicit responses from a neuron (Hartline, 1940; Kuffler, 1953, Hubel and Wiesel, 1962, Barlow et al., 1967). RFs form columns, which were first described in somatosensory cortex by Mountcastle (1957), that process information from a specific region of the sensory area. Because columns run from pia to white matter maps are assumed to be consistent through the depth of cortex.

The representation of visual space can vary among visual areas. Area 17, also known as the primary visual area, visual area 1 (V1), or striate cortex contains a first order transformation of the visual field, which means that it has an orderly point-to-point representation on visual cortex; second order transformations are found in extrastriate areas, where there is often more than one representation of the regions of the visual field within an area, such as the horizontal and vertical meridians (Allman and Kaas, 1974b; Palmer et al., 1978). These meridians can also have multiple representations across visual cortex because they often form the borders between some visual areas (Allman and Kaas, 1971; Van Essen and Zeki, 1978; Tusa et al., 1978; Gattas et al., 1981, 1988; Manger et al., 2002a, 2002b, 2004).

In area 17, individual cells only respond strongly to a stimulus if it has the cell's preferred orientation, direction, spatial frequency, color, temporal frequency, and if the stimulus is presented in a preferred eye (Hubel and Wiesel 1962, 1968; Maffei and

Fiorentini, 1976; Movshon, 1974; Baker et al., 1998; Albright, 1984). Just as there are retinotopic maps in cortex, there are maps superimposed on each other based on the following functional properties: ocular dominance, orientation, spatial frequency and direction preference (Albright, 1984; Bartfeld and Grinvald, 1992; Obermayer and Blasdal, 1993; Weliky and Katz, 1994; Hubener et al., 1997; Rao et al., 1997; White et al., 2001). Cells that respond optimally to the same stimulus are often linked by long-range connections formed by large pyramidal cells (Gilbert and Wiesel, 1979; Rockland and Lund, 1982, 1983; Livingston and Hubel, 1984; Martin and Whitteridge, 1984; Bullier, et al., 1988; Yoshioka et al., 1996; Bosking et al., 1997). These connections create a cortical network that allows cells that are separated by several millimeters in cortex to communicate with one another. Functional interactions are known to occur between cells connected by intrinsic (within a single area) or corticocortical connections with receptive fields that respond to similar visual stimuli (Hubel et al., 1978; Gilbert and Wiesel, 1979; Rockland and Lund, 1982; Martin and Whitteridge, 1984; Engel et al., 1991; Nelson et al., 1992; reviewed in Weliky and Katz, 1994; Ts'o et al., 1996).

Distinct visual areas may be arranged into a hierarchy based on the laminar origins of connections (Rockland and Pandya, 1979, Van Essen and Maunsell, 1983; Felleman and Van Essen, 1991). Feedfoward and feedback connections, formed by pyramidal cells, reciprocally link these distinct areas (Symonds and Rosenquiest, 1984a,b; Matsubara et al, 1987; Salin et al., 1989; Salin et al., 1992; Einstein, 1996). Feedforward connections originate mainly in the supragranular layers, with fewer arising from the infragranular layers of lower order areas such as 17 and project to layer IV in higher order areas (Lund et al., 1993; Morley et al., 1997). Feedback connections

originate in the higher order areas, mainly from the infragranular layers, with fewer arising from the supragranular layers, and they project to lower order areas mainly outside of layer IV (Kuypers et al., 1965; Martinez-Millan and Hollander, 1975; Kaas and Lin, 1977; Spatz., 1977; Rockland and Pandya, 1979; Wong-Riley, 1979; Symonds and Rosenquist 1984a,b; Batardiere et al., 1988; Felleman and Van Essen, 1991; Shipp and Grant, 1991; Rockland and Van Hoesen, 1994; Salin and Bullier 1995; Morley et al., 1997). The retinotopic organization of each area also varies such that neurons at sequential levels respond to larger regions of visual space as one moves up in the hierarchy (Van Essen and Zeki 1978; Zeki, 1978; Gattass et al., 1981). The cortical magnification factor, which is defined as millimeters of cortex corresponding to 1° in visual field (Talbot and Marshall, 1941; Daniel and Whitteridge, 1961), decreases among areas, and with eccentricity, which is the distance from the fovea or *area centralis* in degrees. In contrast, receptive field size increases among cortical areas, and with eccentricity (Hubel and Wiesel, 1974; Gattass et al., 1981; Van Essen et al., 1984; Law et al., 1988; Pinon et al., 1998). Because of these variations both intrinsic and feedback connections are not strictly retinotopic and allow for signals from larger visuotopic regions to converge onto cells with smaller receptive fields in area 17, with the convergence through feedback connections being greater than that through intrinsic connections (Gilbert, 1992; Salin et al., 1989, 1992; Angelucci et al., 2002b).

Cortical connectivity and integration of visual information

Physiological characteristics of the neurons are presumed to result largely from their anatomical inputs, and the recruitment of neurons providing the inputs to a single neuron

is very specific (Hubel and Wiesel 1962; Gilbert and Wiesel, 1979; Eysel et al., 1988; Ferster, 1988; Hata et al. 1988; Bolz and Gilbert, 1989; Crook et al., 1991; Schwartz and Bolz, 1991; Worgotter and Eysel, 1991; Crook and Eysel, 1992; Shipp and Zeki, 2002). Neurons within area 17 summate information over large distances in visual space. These visual extents are often larger than the neuron's classic receptive field (CRF) or minimum response field (Zipser et al., 1996; Sceniak et al 2001; Cavanaugh et al., 2002; Levitt and Lund, 2002). It is also known that responses of neurons can be modulated by simultaneous presentation of surrounding stimuli that do not themselves evoke responses (Maffei and Fiorentini, 1976; Nelson and Frost, 1978; Gilbert and Wiesel, 1990; Li and Li, 1994; Allman et al., 1985; Sillito et al*.,* 1995; Zipser et al*.,* 1996; Levitt and Lund, 1997; Sengpiel et al*.,* 1997; Walker et al*.,* 1999, Jones et al., 2001). The modulatory surround effects can vary substantially based on the parameters of the surround relative to those in the receptive field, and like the receptive fields the surrounds are tuned for specific stimuli (Gilbert and Wiesel, 1990; Lund et al., 1995; Li and Li, 1994; Sillito et al., 1995; Levitt and Lund, 1997; Sengpiel et al., 1997; Sceniak et al., 1999). Similar to the CRF, these effects also depend the type of connection they form with that neuron, how the neuron integrates other distinct areas of visual space, and how strongly the surround is driven (Hirsch and Gilbert, 1991; DeAngelis et al., 1994; Li and Li, 1994; Levitt and Lund, 1997; Polat et al, 1998).

It is well established that intrinsic connections have a role in forming the response properties of area 17 neurons (Das and Gilbert; 1995, 1999; Kapadia et al., 1995; Gilbert et al., 1996; Stettler et al., 2002). However, monosynaptic connections in area 17 cannot account for the whole extent in visual space from which many cells in primate V1

summate information (Sceniak et al., 2001; Angelucci et al., 2002b; Cavanaugh et al., 2002; Levitt and Lund, 2002). The retinotopic precision of feedback connections to area 17 can account for the extent in visual space from which the modulatory surround effects can be elicited. These connections also relate to specific functional properties (Alonso et al., 1993a, b; Hupe et al., 1998). In extrastriate areas cells are responsive to more complex patterns, and can have higher contrast sensitivity (reviewed in Van Essen and Maunsel 1983; Levitt et al., 1994; Gegenfurtner et al., 1997). Therefore, in primates, feedback connections can account for both the tuning of surround effects as well as the retinotopic extent from which these effects arise. They are a plausible anatomical substrate for surround modulatory effects arising from more remote regions of the visual field. However, the extents of visual space from which neurons can summate information and the tuning properties of these modulatory surround effects have not been fully explored in other species.

One aim of this study is to establish if feedback connections are indeed a plausible anatomical circuit underlying summation fields in area 17 neurons. By making anatomical tracer injections into a restricted locus in area 17 of adult ferret (*Mustela putorius furo)*, we determine from which extrastriate areas and cortical laminae feedback connections to area 17 arise. We compare the spread of labeled cells in cortex of extrastriate areas to the representation of visual space within those extrastriate areas. We determine the amount of visual space converging onto receptive fields of area 17 neurons through feedback connections, and establish the extent in visual space from which some area 17 neurons integrate information. We then compare the summation fields of area 17 neurons to the visuotopic extents of cells providing feedback to area 17.

Although there could also be multisynaptic circuits providing input to these cells, this cannot be determined conclusively by this study. There is no clear limit to where multisynaptic connections would cease to influence a cell's response. That is why we limit this study to expanding the possible role of monosynaptic connections.

In studying the pattern of cortical connections of areas 17, 18 and 19, we consistently find a prominent reciprocal link with suprasylvian cortex (Ssy) (Cantone et al., 2002, 2005). Therefore, Ssy is of interest as this area may have a role in the integration of information throughout the visual field that results in long-range contextual effects previously described in area 17. Although Ssy has been identified (Innocenti et al., 2002; Manger et al., 2002a,b, 2004), the representation of the visual field in suprasylvian cortex is not yet described. Establishing the retinotopic organization of suprasylvian cortex can provide valuable information in establishing the functional relevance of connections arising from this area make in contributing to the functional properties of neurons in area 17.

Advantages in using ferret as model

The ferret is a popular model for cortical development because so much cortical development occurs postnatally (Jackson and Hickey, 1985). Studying the development and refinement of corticocortical circuits and that of the summation properties of area 17 receptive fields may provide functional implications of these connections. However, these characteristics of cortical neurons must first be established in the adult.

Another aim of this study is to establish the ferret as a viable model in which to further investigate the integration of information arising from remote regions of the visual

field, and to further investigate surround modulatory effects. Because of the general similarities between the ferret visual system those of cat and primate, there is an increased amount of interest in ferret as model for adult cortical processing, response properties, interactions of neurons, and their anatomical inputs (Chapman and Gödecke, 2002; Schwartz, 2003; Usrey et al., 2003, Alitto and Usrey, 2004; Ramsay and Meredith, 2004; Moore, et al., 2005). There are enough interspecies differences in retinotpic organization of extrastriare areas, and corticortical connectivity to make comparisons of the retinotopic precision of feedback connections, the characteristics of extrastriate areas, and the summation properties of neurons. Assesing these differences among species may aid in understanding the contribution of extrastriate areas to receptive field properties of area 17 neurons.

Ferrets are of interest for making these types of comparisons because the representation of visual space in extrastriate areas contains aspects not always seen in cat and primate. Unlike the representation of the visual field in area 17, which is gridlike and isotropic along both axes of visual space (Law et al., 1988) the representation of isoazimuth lines in exrastriate areas is irregular and more condesed than that of isoelevation lines (Manger et al., 2002a), resulting in an anistropic representation of the two axes of visual space in extrastriate areas that does not exist in area 17. We also find that the amount of visual space converging onto a restricted locus in areas 17 is larger in extent in degrees of azimuth as compared to the extent in degrees in elevation (Cantone et al., 2005). If a neuron in area 17 derives its receptive field properties from feedback conections as opposed to intrinsic connections then the summation properties of that cell may also differ along the two axes of visual space.

In addition to the difference in the representation in cortex of the visual axes, receptive fields themselves are larger in degrees of azimuth than in elevation in extrastriate areas (Manger et al., 2002a). These features may also reflect the anisotropic distribution of both photoreceptors and retinal ganglion cells. The density of both cell types is greater along the horizonatal axis as opposed to the vertical axis, resulting in a vertical streak (Calderone and Jacobs, 2003; Vitek et al., 1985). Although this would suggest that the MF in degrees of azimuth would be larger than MFs in elevation perhaps in extrastriate areas it can result in a larger retinotopic extent along the HM as opposed to the VM, which is reported in some extrastriate areas (Manger et al., 2002a, 2002b). Ganglion cell size and morphology does not change as much with distance from the area centralis (Henderson, 1985;Vitek et al., 1985). Similarly, in cortex RF size and MFs do not change as dramatically with eccentricity in extrastriate areas (Manger et al., 2002b; Cantone et al., 2005). In addition, both the retinal ganglion cells and lateral geniculate nucleus (LGN) cells are larger and have lower peak densities in ferret than in cat, reulssting in ferret area 17 cells being sensitive to lower spatial frequencies (Vitek et al., 1985; Baker et al., 1998).

The connections from LGN to cortex also vary in ferret from primate. In contrast to primate, areas 17 and 18 receive the direct input from LGN (Baker et al., 1998; Cantone et al., 2002). However, the geniculate input to areas 17 and 18 varies in the laminar origin and in soma size, suggesting that parallel not serial processing is occurring among cortical areas (Baker et al., 1998). This is suggestive of a weaker hierarchial arrangement of cortical areas relative to that described in primate (Rockland and Pandya, 1979, Van Essen and Maunsell, 1983; Felleman and Van Essen, 1991). In addition to

predicting some of the cortical organization in ferret, differences in the input arising from the retina and LGN relative to other species may also provide useful information as to what information an animal needs to extract from its visual enviroment can shape its cortical processing.

Relevance to understanding cortical processing

Information obtained from of this study can provide new insight concerning the physiological processing of the visual field and functional roles of various areas of visual cortex. Connectional data may suggest functional differences among extrastraite areas. We also investigate the retinotopic organization of Ssy, as it may be the case that higher areas sacrifice retinotopic precision for other functional properties. This study also may provide useful information about the interactions among the various cortical areas through corticocortical connections. Feedback is an established corticocortical circuit but its exact function is still not known. This study specifically addresses the type retinotopic information extrastriate areas contain and what information connections arising from these areas provide to their target neurons through feedback connections. Results from this study can also contribute to further investigation of the contribution ~~role~~ of feedback to RF properties in ferret.

These studies also address more general questions pertaining to dynamic changes in RF properties and the way in which visual cortex processes stimuli in the natural world. They can also provide information about the general connectivity of sensory cortex, and how it governs higher visual and possibly cognitive processing. Knowing how the individual anatomical circuits integrate information throughout the cortex is essential to an understanding of how the brain functions.

CHAPTER 2: FEEDBACK CONNECTIONS TO FERRET STRIATE CORTEX: DIRECT EVIDENCE FOR VISUOTOPIC CONVERGENCE OF FEEDBACK INPUTS. (Cantone G, Xiao J, Mcfarlane N, Levitt J, 2005. Journal of Comparative Neurology. 487:312-31. Reprinted by permission of Wiley-Liss, Inc.)

2.1 INTRODUCTION

Previous physiological studies show various effects of feedback on receptive field (RF) response properties (Alonso et al., 1993 a,b; Hupé et al., 1998, 2001a, b; Martinez-Conde et al., 1999; Wang et al., 2000). Bullier et al. (2001) and Angelucci and Bullier (2003) suggest one role of feedback is the selective modification of responses of area 17 neurons to stimuli within the classic receptive field (CRF) when paired with stimuli placed in the surround (Maffei and Fiorentini, 1976; Nelson and Frost, 1978; Gilbert and Wiesel, 1990; Li and Li, 1994; Allman et al., 1985; Sillito et al., 1995; Zipser et al., 1996; Levitt and Lund, 1997; Sengpiel et al., 1997; Walker et al., 1999). Other studies suggest intrinsic connections are sufficient to produce these center-surround interactions (Stettler et al., 2002). However, monosynaptic connections in area 17 cannot account for the whole extent in visual space from which some cells summate information (Sceniak et al., 2001; Angelucci et al., 2002b; Cavanaugh et al., 2002; Levitt and Lund, 2002). Because they link cells that respond to non-overlapping areas of visual space that are still centered on the same retinotopic location as their target neurons, feedback connections provide an anatomical substrate that can account for the largest spatial extent of the non-classical receptive field from which modulatory surround effects can arise (Angelucci et al., 2002 a,b).

Our specific aim in this study is to establish if these same topographic rules govern feedback connections in ferret (*Mustela putorius furo*). We are extending these studies to ferret, because, unlike cat and primate the majority of extrastriate cortex is exposed on the lateral surface. Therefore, these areas are more easily accessible for both anatomical and electrophysiological examination of visual topography than extrastriate areas of more extensively studied species.

Although Rockland (1985) and Ruthazer and Stryker (1996) report that connections arise from several extrastriate areas in the adult ferret, these connections are not described in any detail. By injecting the neuronal tracer CTb into cortical area 17 we quantify the proportion of feedback arising from a given cortical area and layer. We also determine if feedback connections provide for the convergence of extensive regions of visual space onto more restricted regions in area 17. We accomplish this by converting the spread of labeled cells in cortex into a span of visual field. Then we compare the aggregate receptive field of the labeled region in each extrastriate area with that of the injection site and that of intrinsic connections. We directly measure the visuotopic extents of labeled fields in cases in which we made both CTb injections and physiological recordings; we then compare the aggregate receptive field (ARF) of the labeled region in each extrastriate area with that of the injection site. Our data show that cortical feedback in the ferret can indeed potentially provide for the extent of visual space needed for modulatory surround effects. This work is described in full in Cantone et al. (2005).

2.2 MATERIALS AND METHODS

Anatomical tracer injections

Twelve adult ferrets (*Mustela putorius furo*) (0.6-1.2 kg) were used for this study. All underwent anatomical injection experiments. Terminal electrophysiological mapping experiments (see below) were also performed on 6 of the tracer-injected animals prior to being sacrificed; two of these cases yielded both CTb labeling and mapping data. All procedures conformed to National Institutes of Health guidelines. Prior to all surgeries animals were premedicated with IM injections of dexamethasone (0.5 mg/kg) to prevent cerebral edema and atropine (0.04 mg/kg), and preanesthetized with IM injections of ketamine (25 mg/kg) plus xylazine (2 mg/kg). For recovery surgeries a mask or an endotracheal tube coated with a topical anesthetic was inserted in order to artificially ventilate the animals with isoflurane (0.5-2.5%), in a 50:50 mixture of N_20 and 0_2. The EKG rate was stabilized and blood oxygenation was maintained at a level near 100% throughout the procedure by adjusting the isoflurane level. Rectal temperature was maintained near 37º C with a thermostatically-controlled heating pad.

The animal's head was fixed in a stereotaxic apparatus. Lidocaine HCl (2%) was injected into the scalp prior to incisions. During a sterile surgery the scalp was retracted, and a craniotomy and durotomy were performed on one or both hemispheres. Using glass micropipettes either iontophoretic (tip diameter 10-15 μm) or pressure injections (tip diameter 15-40 μm) of 1% Cholera toxin B subunit (CTb, low salt; List Biologic, Campbell, CA) were made into primary visual cortex (Fig. 1A). For iontophoretic injections, CTb was reconstituted in 0.1 M potassium phosphate buffer (PB pH 6.0), and delivered with 2 μA positive current passed for 10 minutes with a 7 sec. on-off cycle. For pressure injections, CTb was reconstituted in dH_20 or 0.1 M PB (pH 6.0) and a total volume of ~30 nl was delivered with a Picospritzer II (Parker Hannifin Corp.). All

injections were made at two depths to ensure that the injection site spanned both the upper and lower layers of the cortex. The micropipette was left in place for at least 10 minutes after each injection to prevent leakage of tracer along the pipette track. The craniotomies were then covered with gelfoam and the scalp closed. All ferrets were recovered from the anesthesia, and allowed to survive for 7-9 days. Following this period, animals were sacrificed with an overdose of sodium pentobarbital either immediately or following the terminal recording session.

Electrophysiological recording

In 6 animals that underwent both tracer injections and electrophysiological mapping experiments, the retinotopic locations of single- and multiunit receptive fields around both the injection site in area 17 and at cortical locations potentially containing retrogradely labeled cells in areas 18, 19, and 21 were established; retinotopic locations of receptive fields at the injection site were recorded prior to the injection as well as being remapped more extensively in the terminal recording session. Ferrets were premedicated and anesthetized as described above. For terminal recording sessions the trachea was cannulated to respire the animal. The femoral veins were cannulated so drugs could be administered intravenously in a solution of Normosol-R (Abbot Laboratories, IL). The animals were ventilated with a 50:50 mixture of N_2O and 0_2. EKG, pulse, blood oxygenation, and rectal temperature were continuously monitored and maintained within normal limits. The peak expired CO_2 was maintained between 4-5%. After making a craniotomy and durotomy, a chamber was placed over the exposed cortex and filled with saline. After the surgery the animal was paralyzed with vecuronium bromide (0.1

mg/kg/hr, i.v.) to minimize eye movements. Isoflurane (0.5-1.5%) was used to anesthetize animals throughout the recordings. High levels of isoflurane seemed to suppress the responsiveness of cortical neurons, and therefore may have decreased apparent RF size. However, since cortical magnification factors (MFs) were calculated from positions of RF centers, our assessments were unaffected by anesthesia. In one case propofol (12-25 mg/kg/hr, i.v.) was also used as an anesthetic. No obvious difference was seen in mapping results.

Accommodation was paralyzed with atropine sulfate (1.0%), and nictitating membranes were retracted with phenylephrine HCl (2.5%). Corneas were protected with zero power, rigid gas permeable lenses. The optic disks were projected with a reversible ophthalmoscope onto the tangent screen, marked on paper sheets, and their position checked throughout the experiment. The ferret's *area centralis* was estimated to lie 11º inferior and 31º medial to the optic disk (Henderson, 1985; Vitek et al*.,* 1985). Recordings were made 250 μm-1000 μm apart with insulated tungsten microelectrodes (Frederick Haer & Co., ME). The size and location of minimum response fields were plotted in azimuth and elevation relative to the *area centralis*. This was done by hand using light or dark oriented lines. Electrolytic lesions were made at recording sites of interest by passing 4 μA anodal current for 4-5 seconds.

Histological processing and identification of visual cortical areas

All animals were transcardially perfused with a saline rinse solution, followed by 4% paraformaldehyde (10 cases) or 2% paraformaldehyde solution (2 cases). After a 30 minute period of initial fixation, 10% sucrose was added to the respective perfusion

solutions in all cases. Brains were removed from the skull, and the posterior portion of the brain was blocked. In the cases fixed in 2% paraformaldehyde, the posterior portions of both hemispheres were flattened by removing the underlying white matter, and making relieving cuts at the caudal pole of the cortex. In 7 cases the cortex was partially flattened without making relieving cuts. Flattened and partially flattened cortexes were placed between two slides using spacers, and postfixed in 4% paraformaldehyde containing 30% sucrose, which was used as a cryoprotectant. Fixation solutions were made with 0.02 M PBS (pH 7.4). Frozen sections were cut at 40 μm. Three unflattened cortexes, which were processed for CTb, were cut parasagittally. All others were cut tangentially to the pial surface of cortex.

The sections were separated into numbered series. One or two series were processed to reveal the CTb label using a modified version of the protocol described by Angelucci et al. (1996). The tracer was developed using the Vector Laboratories ABC kit (Burlingame, CA) and either a Vector VIP kit or DAB as the chromogen. The tissue was then mounted onto slides, dehydrated, and cleared in toluene if developed with a VIP kit (Lanciego et al*.,* 1998) or xylene if developed with DAB, and coverslipped using Permount. The remaining series were further divided so that alternate sections were processed for cytochrome oxidase (CO) (modified method of Wong-Riley, 1979), myelin using the method described by Gallyas (1979), or Nissl substance. Figure 1B shows these stains reveal areal and laminar boundaries as previously described by Innocenti et al. (2002). It is worth noting that areal boundaries were often quite irregular, often meandering dramatically as inFig.8A below rather than forming straight contours as the composite Figures 1A and 2A suggest.

Every 3rd tangential section or every 6th parasagittal section containing CTb label was examined under brightfield microscopy at 100X magnification. Section outlines were traced and retrogradely labeled cells were plotted using the Neurolucida tracing and reconstruction program (MicroBrightField, Inc.). The resulting tracings were superimposed onto adjacent CO, myelin, and Nissl stained sections. Vascular landmarks were used for local alignment so the CTb labeled cells could be assigned to a cortical area and layer.

Since a number of measures within each area would be affected by the mis-assignment of labeled cells, correct determination of laminar and areal boundaries was crucial to our analysis. Anatomical features were tracked through serial sections for assignment of labeled cells to cortical laminae or areas since the histological features of laminar transitions could potentially be mistaken for areal transitions (particularly in tangentially sectioned material). Errors concerning assignment of labeled cells were most likely made in the cortical reconstructions using the tangential sections. As confirmation, parasagittal sections in which the laminar boundaries are very clear and could not be mistaken for areal boundaries were also used to reconstruct cortex. Statistical differences between data we obtain from tangential sections and parasagittal sections were not seen. Therefore, any errors in assigning cells to areas or layers were minimal.

Figure 1. Multiple visual areas in ferret cortex. (A) Lateral view of ferret brain depicting typical CTb injection location (arrow) relative to the sulcal pattern and areal boundaries described by Innocenti et al. (2002) and Manger et al. (2002 a,b). Numbers indicate cortical areas. Scale = 4 mm. Digital montages of parasagittal sections show anatomical areal (dashed lines) and laminar boundaries in areas 17, 18, 19, 21, and Ssy evident after staining for cytochrome oxidase (B) and myelin (C). Artifacts have been removed from photomicrographs. Scale = 1 mm. PPr/PPc = Posterior Parietal areas rostral/caudal; Ssy = Suprasylvian area; LT = lateral temporal areas; LS = lateral sulcus; SsyS=suprasylvian sulcus; WM = white matter; A = anterior; D = dorsal.

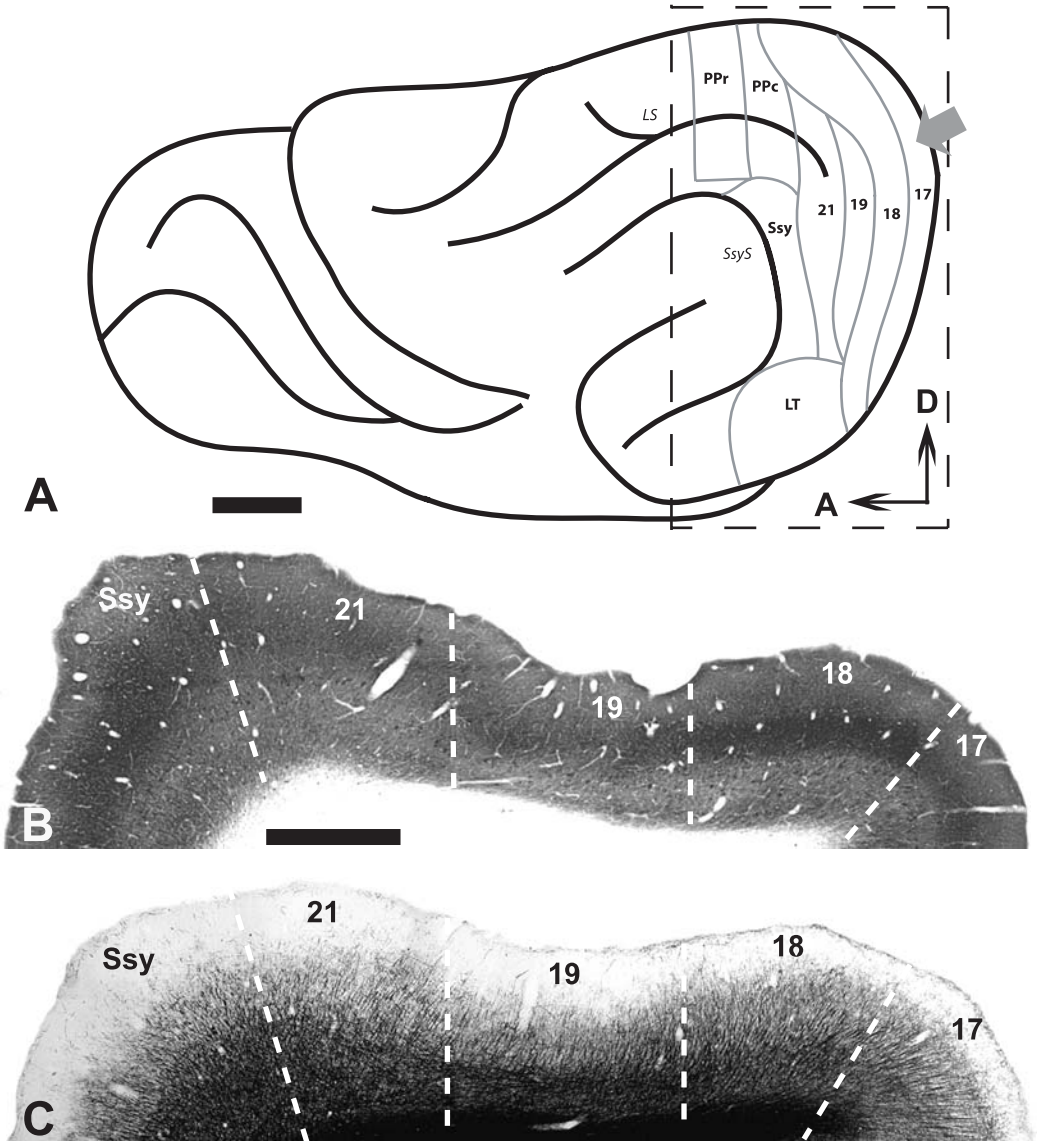
PPr
PPc
LS
21
19
18
17
Ssy
SsyS
LT
D
A
A
Ssy
21
19
18
17
B
21
Ssy
19
18
17
C

Cell counts and cell densities

The proportion of labeled cells located in each extrastriate area was calculated by dividing the number of cells in a given extrastriate area by the total number of labeled cells in outside of area 17. The proportion of labeled cells located in the different layers of each area was determined by dividing the number of labeled cells in the supra- or infragranular layers of a given area by the total number of labeled cells found within that area.

Three-dimensional plots of cell density were generated from serial reconstruction of sections containing CTb label. Tracings of sections were aligned using lateral and suprsylvian sulci patterns, radial blood vessels, lesions. CTb labeled cells were counted and binned within each section. In sections cut tangentially to the pial surface, counting bins were defined by first determining the areas of concentric circles centered on the injection core differing in radius by 125 μm. The area of a smaller circle was then subtracted from that of the next consecutive larger circle, and each counting bin was set to $1/60^{th}$ of the area of the resulting annulus. Counting bins used for parasagittal sections were 200 μm by 200 μm in area. A drawing of a grid of bins was aligned onto serial reconstructions, and then superimposed on each traced section, which were corrected for shrinkage. Both types of counting bins were close to the size of the clusters of labeled cells in area 17, and produced a reasonable resolution of the clustered pattern of cell label in the cell density plots (see below). A sample volume of stacked counting bins was calculated by multiplying the area of the bins in each section by the section thickness (40 μm) and by the number of sections used in the reconstruction. Using this volume, the density of cells within each series of stacked bins was calculated and contour maps of cell

density were generated with custom-written routines in Matlab (Mathworks, Inc).

To determine the peak densities within each extrastriate area, the volume of stacked counting bins was calculated by multiplying the area of the bins in each section by the average section thickness within each extrastriate area, and by the number of sections used in the reconstruction. Multiple measurements of section thickness were taken separately in each extrastriate area at locations containing large amounts of labeled cells. For this analysis all measurements used to calculate the sample volumes were taken before correcting for shrinkage. In 6 animals used for electrophysiological mapping experiments a shrinkage correction was applied case-by-case. An average shrinkage correction of 17% along the x- and y-axes due to CTb processing was calculated from lesions made in these 6 animals, and was applied to all tissues processed for CTb.

Cortical magnification factors

The retinotopy in ferret extrastriate cortex has been reported to vary among areas (Manger et al*.,* 2002a). Due to this variability, and because cortical magnification factors (MFs) were not explicitly addressed by Manger et al. (2002a), retinotopic maps were derived for areas 17, 18, 19, and 21 (n=6). MFs are examined in detail in our study. Within each extrastriate area, MFs were determined separately for visual axes representing azimuth and elevation by calculating the difference in degrees of azimuth and elevation of the receptive field (RF) centers recorded at adjacent penetration sites. RF centers less than 3° apart in azimuth or elevation were considered to lie at the same azimuth or elevation respectively; we estimate this to be the accuracy with which we could define RF centers. The distance in cortex (millimeters) between adjacent

penetration sites was divided by the distance in visual space (degrees) between the centers of the corresponding receptive fields. MFs were calculated using the following equation from Daniel and Whitteridge (1961):

MF = millimeters in cortex/degrees of visual space (1)

Only adjacent penetration sites whose RFs were separated by at least 3° (and therefore considered not to lie along lines of isoazimuth or isoelevation) were used to calculate MFs.

In some cases, due to the necessarily limited sampling of cortex, no adjacent recording sites in area 17 had RF centers separated by at least 3º. Thus, a modified criterion was used to calculate the MFs in area 17. Our mapping agreed with previous studies showing that in area 17 isoelevation lines run parallel to each other approximately along the rostrocaudal axis, while isoazimuth lines run perpendicular to isoelevation lines, roughly parallel to each other (Law et al., 1988; Manger et al*.,* 2002a). This grid-like visual field representation allowed for continuous isoazimuth or isoelevation lines to be drawn based on our recordings. Then MFs were calculated using penetration sites that fell along a line perpendicular to these contours.

Unlike area 17, a grid-like map was not formed by the representations of isoazimuth lines and isoelevation lines in extrastriate areas (Manger et al*.,* 2002a). Isoazimuth lines could form closed contours, often running parallel to isoelevation contours, so that one could move large distances in cortex and not move in the visual field. Therefore MFs can vary considerably along a single isoelevation line as well as

along a single isoazimuth line. Because of these irregularities in the retinotopic maps, a simple correlation between MF and eccentricity in extrastriate areas was not found. MFs in mm/deg. of elevation were grouped within 4 azimuth ranges based on the mean eccentricity of the RF centers: 0-10°, 11-20°, 21-30°, and >31° for each area. Because penetrations were made in a restricted region of cortex where labeled cells were most likely to be found, RFs in extreme upper or lower visual fields were not recorded. This resulted in the MFs in mm/deg. of azimuth within each area being grouped within 3 elevation ranges: 0-¯10°, ¯11-¯20°, ¯21-¯30°. MFs within each cortical area were compared using finer binning: across 10° ranges of azimuth or elevation based on which was used to calculate the MF. MFs within these bins were then compared across ranges each spanning 5° of the orthogonal axis of visual space.

Determining cortical spread of retrogradely labeled cells

It was first necessary to define the axes along which we measured the spread in cortex of labeled cells; these did not correspond simply to axes such as rostrocaudal. In cases in which we could not directly compare RF maps with label patterns, we used the following method to relate the pattern of cell label to the retinotopic organization of each area. These relationships were established by comparing the spread of retrogradely labeled cells directly to physiological recordings made in the same animals (n=2), by comparing the pattern of label resulting from injections made in area 17 with our own and previously published retinotopic maps in ferret cortex (Manger et al*.,* 2002a), and are consistent with previous findings in primate (Angelucci et al*.,* 2002b). Despite some interanimal variation in the pattern of retinotopic maps, maps were consistent enough

among animals (Manger et al., 2002a) to determine these relationships. The summary map shown in figure 2 was derived by aligning retinotopic maps of six cases using the patterns of Lateral and Suprasylvian Sulci and anatomical areal boundaries determined by using CO and myelin stained sections for comparison. The retinotopic locations corresponding to a given location in cortex were averaged to generate the map.

For each field of labeled cells in areas 17, 18, 19, and 21, 2 axes of label spread were established relative to representations of both isoazimuth and isoelevation contours on the cortical surface. Although assignment of these axes was somewhat subjective, we are reassured that the assignments are accurate because of the criteria described above, particularly since the pattern of retrogradely labeled cells reflected the retinotopic organization in cortex (See results for detailed description). Because the representations of azimuth and elevation could be quite different (Manger et al., 2002a), different axes were determined for each. We inferred that the orientation of one axis of the spread of both intrinsic and feedback label *within* an individual cortical area generally ran along a continuous isoazimuth contour. Thus, there would be little change in the degree of azimuth at which cells' RFs along this axis were located. As noted above, isoazimuth lines in extrastriate cortex were not necessarily perpendicular to isoelevation lines. The axis of the overall spread of retrograde label was inferred to run *across* all cortical areas along a continuous isoelevation contour (Fig. 2A). Thus, along this axis there would be little change in the degree of elevation at which cells' RFs were located. We assumed the axes of a labeled field perpendicular to the axes described above spanned isoazimuth or isoelevation contours, respectively. Within a labeled field, the RFs of cells along one perpendicular axis would differ in azimuth or elevation; cells located at the ends of this

axis would have the most widely separated RFs. Thus, the axes spanning isoazimuth or isoelevation contours represented the maximum retinotopic separation, rather than maximum cortical separation. *Within* a given cortical area the length of the axis of a field of label spanning isoazimuth (Fig. 2B) or isoelevation (Fig. 2C) contours was converted to a visuotopic extent in degrees of azimuth or elevation respectively. The length of the axis representing the maximum retinotopic separation in each area (determined separately for supra- and infragranular layers) was defined as the distance between the most widely separated counting bins at which cell density had fallen to 5% of the peak labeled cell density. In one partially flattened case the axis of intrinsic connections in area 17 spanning isoazimuth lines could not be measured because area 17 extends around the caudal pole of cortex; this resulted in area 17 running roughly perpendicular to the lateral surface of the flattened brain. Therefore, this axis of label in area 17 was determined by counting the number of sections containing labeled cells and multiplying that by the thickness of each section which was corrected for shrinkage (40 μm). The diameter of the injection core was measured in each case using Neurolucida.

Figure 2. Relationship of the pattern of labeled cells to retinotopic organization in areas 17, 18, 19 and 21. (A) Density map of retrogradely labeled cells in visual cortex obtained from a representative case in which a CTb injection was made into area 17 without electrophysiological recording. Superimposed on the cell density map is a summary retinotopic map of 6 cases in which only recordings were made. Solid and dashed black lines represent isoazimuth and isoelevation contours, respectively. Small numbers superimposed on these lines indicate the eccentricity in azimuth or elevation. The vertical meridian (VM) corresponds to the 17/18 and 19/21 borders. Gray lines represent other areal borders. Large numbers indicate cortical areas. Black circle represents injection core; surrounding gray region represents an annular area (radius 500 μm) in which cells were not counted due to uniformly high density of label. Scale = 1 mm. Cell density plots of fields of labeled cells within the supragranular (B,D) and infragranular (C,E) layers of area 19. Black lines (B, C) represent the axis of a labeled field inferred to run along an isoazimuth line within 19. Dashed lines (D, E) represent the axis of label inferred to run along the segment of an isoelevation line that falls within 19. Gray lines represent the axis of a field of labeled cells spanning isoazimuth (B, C) or isoelevation lines (D, E) used to calculate a corresponding visuotopic extent in degrees of azimuth or elevation, respectively. The cortical spreads used to calculate corresponding visuotopic extents in azimuth and elevation were determined from the same density plots but were perpendicular to different axes. All contour plots exclude cell densities less than 5% of the peak labeled cell density within supra- or infragranular layers. Scale = 1 mm.

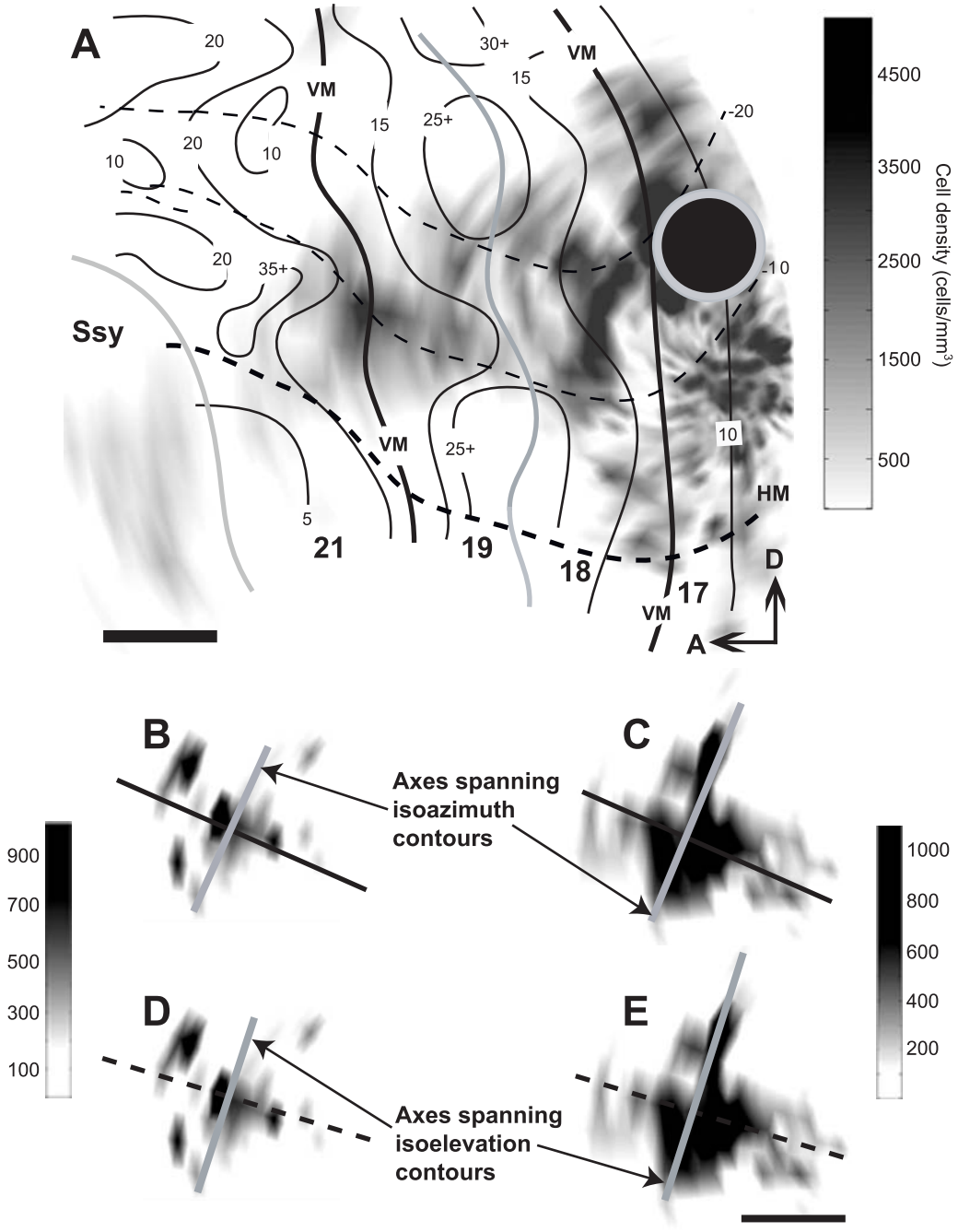
A
20
VM
30+
VM
15
15
25+
-20
20
10
10
20
35+
-10
Ssy
VM
25+
10
HM
5
21
19
18
17
VM
D
A
4500
3500
2500
1500
500
Cell density (cells/mm3)
B
C
Axes spanning
isoazimuth
contours
900
700
500
300
100
1000
800
600
400
200
D
E
Axes spanning
isoelevation
contours

Determining retinotopic extents of retrogradely labeled cells

In two cases (one of which was incompletely mapped) the density map of labeled cells in areas 18, 19, and 21 was aligned to the physiological maps recorded in the same animal using the electrolytic lesions made during the recording session. In these cases the visuotopic extents corresponding to the cortical spreads of label were derived directly from the measured retinotopic maps in each area. In cases in which no recordings were made, we related the spread of labeled cells in the various cortical areas to the MFs derived from separate cases in which only retinotopic maps were determined. Based on our recordings in area 17, the retinotopic location of all injection sites was estimated to be in the lower visual field, within the central 20°. Therefore, the average MFs within 20° of azimuth and elevation were used to convert the distance in cortical space into a distance in visual space. The spread of a labeled field in cortex (D_{mm}) was defined as the length of the axis of a labeled field inferred to span isoazimuth or isoelevation lines. (D_{mm}) was converted into a distance in degrees of visual space (D°) in both azimuth and in elevation using the equation:

$$D° = D_{mm} / MF_{\ mm/deg.} \qquad (2)$$

Then the visuotopic extents or aggregate receptive fields (ARFs) were determined using a modified version of the equation from Dow et al. (1981):

$$ARF^{o} = D° + mRF \qquad (3)$$

where (mRF) is average RF size, determined for each cortical area, in degrees of azimuth or elevation within the central 20°. The ARF is defined as the combined RFs of all the cells in a labeled field. In area 17 the mRF at the injection site's eccentricity was used to calculate the ARFs of the injections. Ratios of the ARFs of labeled cells within extrastriate areas to the ARFs of cells at the injection core and to the ARFs of cells linked by intrinsic connections were then calculated. Angelucci et al. (2002b) give a more detailed description of these methods.

RF scatter down a column of cortex could not be directly measured in animals in which we calculated the ARF. Scatter was previously estimated to approximate the average size of the RFs at a given eccentricity (Hubel and Wiesel, 1974). Based on our limited measurements of scatter in ferret extrastriate cortex and findings in other species (Dow et al., 1981; Sherk et al., 1992), it has been suggested that average RF size is an overestimation of scatter. Because we wanted conservative estimates of ARFs, scatter was not included.

Statistical analyses were performed using Matlab Statistical Toolbox (Mathworks Inc.), and NCSS version '01 (Kaysvill, UT). Non-parametric Wilcoxon Rank-Sum tests were used to compare MFs in mm/deg. of elevation to MFs in mm/degree of azimuth within each cortical area in each range of eccentricity. Comparisons of MFs were made within areas across ranges of eccentricity, and across areas within ranges of eccentricity using Kruskal-Wallis tests, followed by multiple-comparison z-value tests. These same tests were used to compare the MFs, pooled over all eccentricities, across areas and to compare peak cell densities across areas. Kruskal-Wallis tests were followed by Tukey-

Kramer multiple comparison tests to compare cell percentages. Photomicrographs were adjusted for brightness, contrast and sharpness, and artifacts were removed using Adobe Photoshop (Adobe Systems Inc.)

2.3 RESULTS

Characteristics of retrograde label in extrastriate cortex

We defined an injection core as the uniform, densely labeled region of CTb. After shrinkage correction, they ranged between 600-900 μm in diameter. All injection sites were located at the caudal pole of brain, were confined to area 17, and spanned all layers of cortex without intruding on the white matter (Fig. 3A). We confirmed this by comparing tracings of the injection core with adjacent tissue sections stained for CO, myelin, and Nissl substance, and locating the anatomical border between areas 17 and 18 based on descriptions by Rockland (1985) and Innocenti et al. (2002).

We analyzed 6 hemispheres from 5 animals. Following CTb injections, neurons having axon terminals at the injection locus were retrogradely labeled with CTb (Fig. 3). After full serial reconstruction we found no obvious differences in the distribution of labeled cells between layers 2 and 3, or layers 5 and 6. Therefore, we pooled the labeled cells into supra- and infragranular layers, respectively. In addition to the extensive label in area 17, substantial numbers of retrogradely labeled cells were located in extrastriate areas 18, 19, 21, and Suprasylvian cortex (Ssy), while lateral temporal areas (LT), rostral posterior parietal (PPr), and caudal posterior parietal (PPc) areas contained very few labeled cells. The majority of labeled cells were located in the infragranular layers. The label was densest at the anatomical borders between areas 17 and 18, and between areas

19 and 21, while label in SSy was not associated with the areal border. In two cases sparse labeled cells were located in two anatomically distinct but physiologically undefined areas. Based on their locations they are possibly equivalent to the splenial visual area (Kalia and Whitteridge, 1972) and the anterolateral lateral suprasylvian visual area (Palmer et al*.,* 1978) described in cat. The orthogradely labeled neuronal terminals found in extrastriate areas show that each area makes reciprocal connections with area 17 (Fig. 3B-D). Detailed analysis of orthogradely labeled of connections will be the subject of a separate study.

Figure 3. Brightfield photomicrographs of parasagittal brain sections showing labeling in cortex after a CTb injection in area 17. (A) Area 17 injection site. (B-D) Retrogradely labeled cells and orthogradely labeled processes in extrastriate areas. Black and gray arrowheads indicate anatomical boundaries between areas. IV = layer 4, A = anterior, D = dorsal, Scale = 400 μm (A), Scale = 200 μm in (B-D).

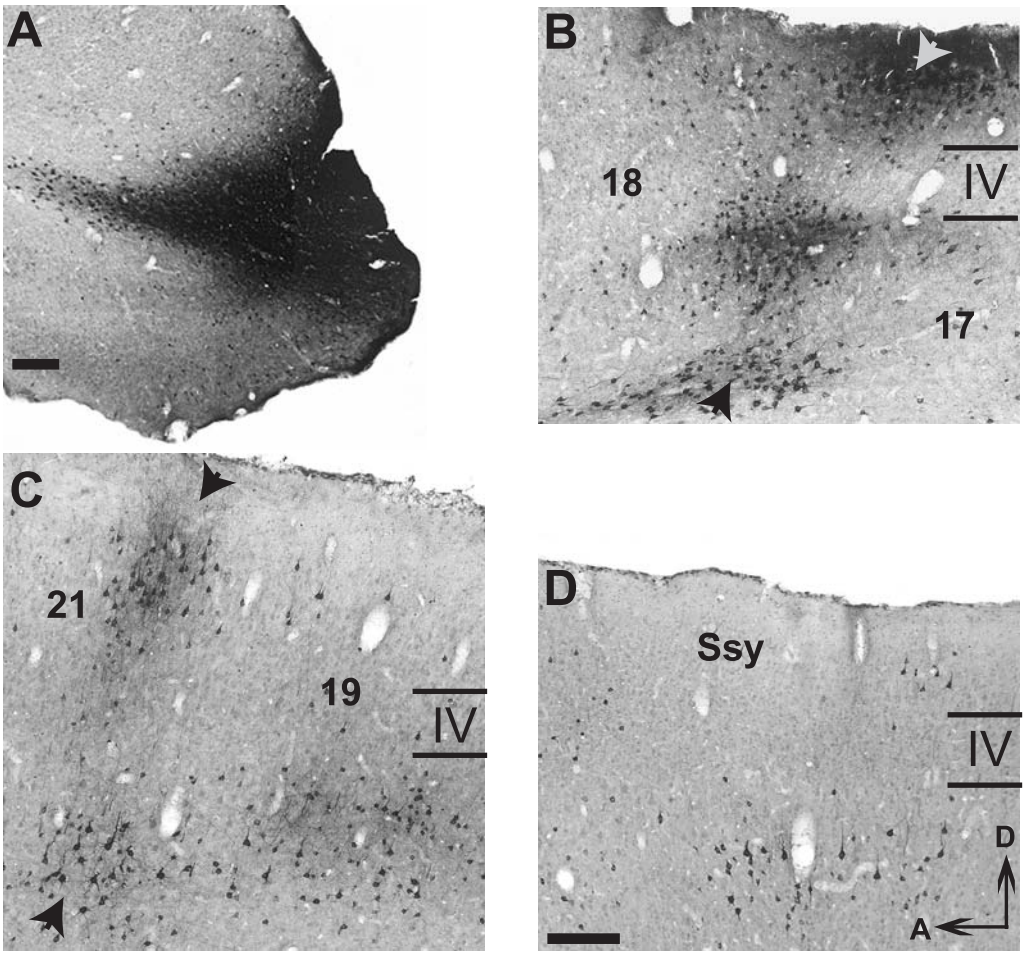
A
B
18
IV
17
C
21
19
IV
D
Ssy
IV
D
A

We observed a restricted spread of label across areas 17, 18, 19, 21, and Ssy extending roughly along the rostro-caudal axis to the suprasylvian sulcus. Serial reconstructions showed two typical patterns of label (Fig. 4). The borders between areas 17/18 and between 19/21 both correspond to the representation of the vertical meridian (Manger et al., 2002a). Since we made our injections at locations in area 17 that respond to central fields, the concentration of label at these anatomical borders suggests that monosynaptic interareal feedback connections are topographic. Our preliminary data (Cantone et al., 2003) suggest this also to be true for connections arising from Ssy. Each cortical area containing labeled cells contains a representation of the visual field. The different patterns of label in each case mirror different aspects of the retinotopic organization of these extrastriate areas previously described by Manger et al. (2002a). In Figure 4A the label formed one continuous band across areas 17, 18 19, and 21. This reflects isoazimuth lines running along the same axis as isoelevation lines. In Figure 4B the label forms a ring, reflecting isoazimuth lines running parallel to isoelevation lines at some points and perpendicular to them at others.

Figure 4. Serial reconstructions of retrograde label in visual cortex. Black dots represent retrogradely labeled cells. Note the distinct labeling pattern resulting from 2 different cases (A,B) in which CTb was injected into area 17 (A is the same injection case as shown in Figure 2). The sparse labeling anterior to 21 and dorsal to Ssy is located in areas PPr and PPc. The SsyS is drawn more anterior than it normally lies in cortex to show the full extent of the label in Ssy, some of which lies within the sulcus. Scale = 2 mm. Other conventions are as in Figures 1 and 2.

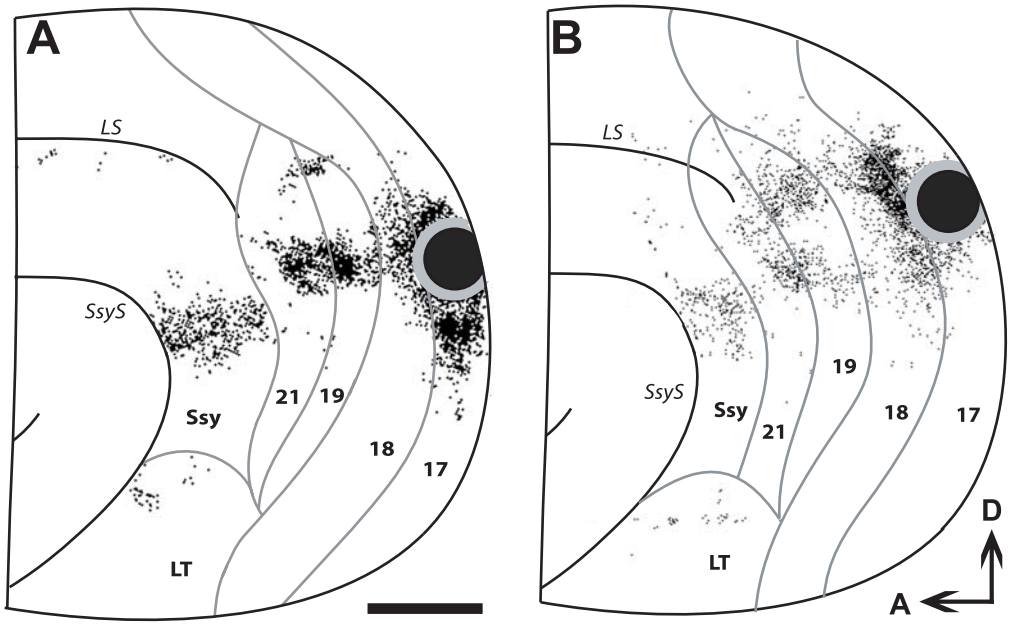
A
LS
SsyS
Ssy
21
19
18
17
LT
B
LS
SsyS
Ssy
21
19
18
17
LT
D
A

We compared the proportions of cells within each extrastriate area providing feedback to area 17, and found that the amount of feedback connections arising from each extrastriate area differs significantly (Kruskal-Wallis, $p<0.001$). Area 18 provides the greatest proportion of the total number of cells providing feedback to area 17 (mean 45.5%). Areas 19, 21, and Ssy each provide about the same amount; areal means range between 15.3%-20.7%. The proportion of labeled cells found within each of the areas 18, 19, 21 and Ssy is significantly different from that in LT, PPr, and PPc. PPr, PPc, and LT each provide less than 1% of the total amount of feedback; areal means range between 0.3%-0.9% (Fig. 5A). In 4 injection cases we also normalize counts for the different sizes of cortical areas 18, 19, 21, and Ssy; we then find no significant differences among areas in the proportions of feedback cells arising from each area (Fig. 5B). This suggests the difference in the proportion of total feedback to area 17 arising from each extrastriate area can largely be attributed to the size of the area.

Figure 5. Feedback arising from different extrastriate areas. (A) The proportion of feedback projections arising from areas 18, 19, 21 and Ssy. (B) The proportion of feedback projections arising from 18, 19, 21 and Ssy after normalizing for the size of each cortical area. (C) The peak densities of labeled cells within the cortical areas providing substantial amounts of feedback to area 17. Values represent means of 6 cases ± s.e.m. (*) indicates significant difference ($p<0.01$) from area 18. (+) indicates significant difference ($p<0.01$) from areas 18, 19, 21, and Ssy.

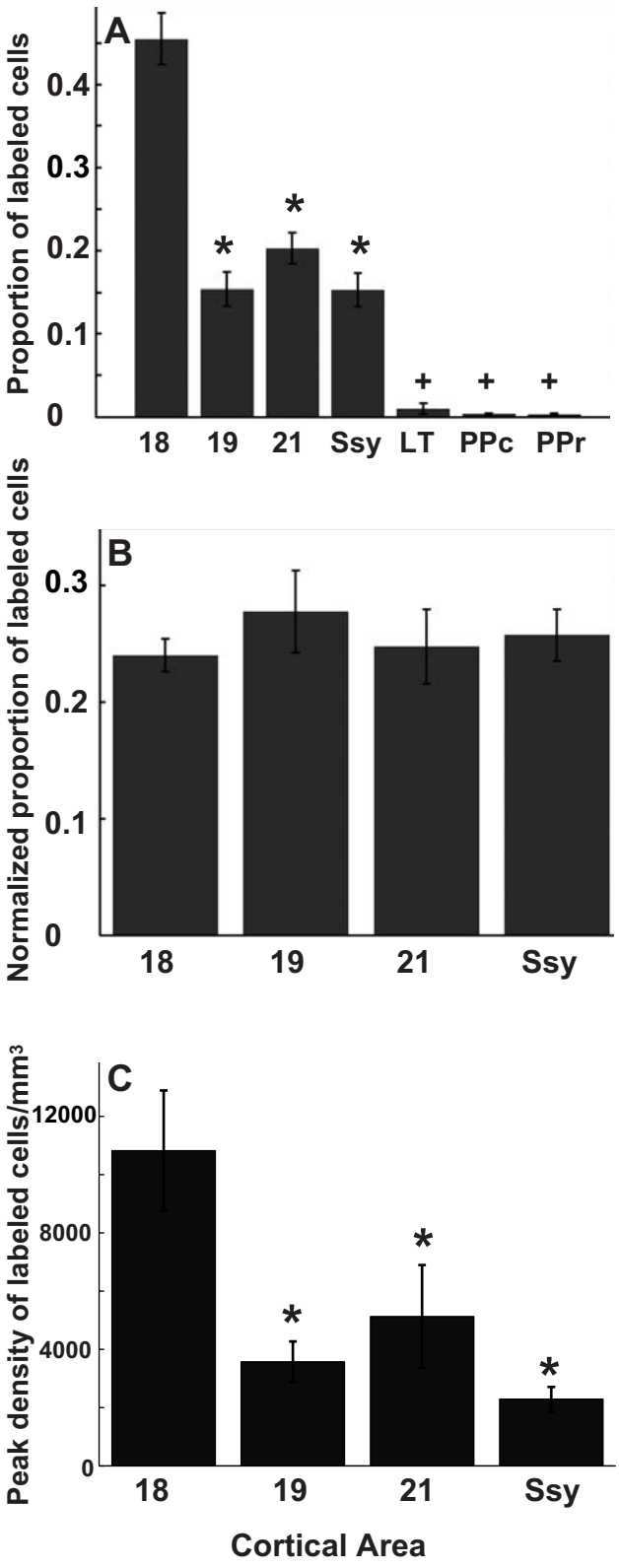
A
Proportion of labeled cells
0.4
0.3
0.2
0.1
0
*
*
*
+
+
+
18
19
21
Ssy
LT
PPc
PPr
B
Normalized proportion of labeled cells
0.3
0.2
0.1
0
18
19
21
Ssy
C
Peak density of labeled cells/mm³
12000
8000
4000
0
*
*
*
18
19
21
Ssy
Cortical Area

To further quantify the distribution of connections arising from areas providing prominent feedback to 17, we compared the peak densities of labeled cells across these areas. The peak density within a cortical area was defined as highest density within one of the reconstructed series of stacked counting bins. Thus despite the similarities among areas seen in Figure 5B, area 18 has a statistically greater *peak* density of cells providing feedback connections to area 17 than areas 19, 21, or Ssy (Kruskal-Wallis, $p<0.01$) (Fig. 5C). In all areas, the peak densities of labeled cells can be as much as three times larger in the infragranular layers than the supragranular layers.

Since the densities of labeled cells vary among layers, we wanted to determine the laminar contribution of feedback connections. We compared the amount of labeled cells located in the infragranular layers versus the supragranular layers. Within each area there is a significantly larger proportion of feedback connections arising from the infragranular layers (means range between 68.2%-81.6%) than from the supragranular layers (means range between 18.6-29.9%) (Kruskal-Wallis, $p<0.0001$) (Fig. 6).

Figure 6. Proportion of feedback projections arising from supra- and infragranular layers in each area. (*) indicates significant ($p<0.01$) difference between supra- and infragranular layers in each area. (+) indicates significant difference in supragranular cell percentage from those in areas 18, 19, 21 and Ssy. Black bars = supragranular layers, White bars = infragranular layers. Values represent means ± s.e.m.

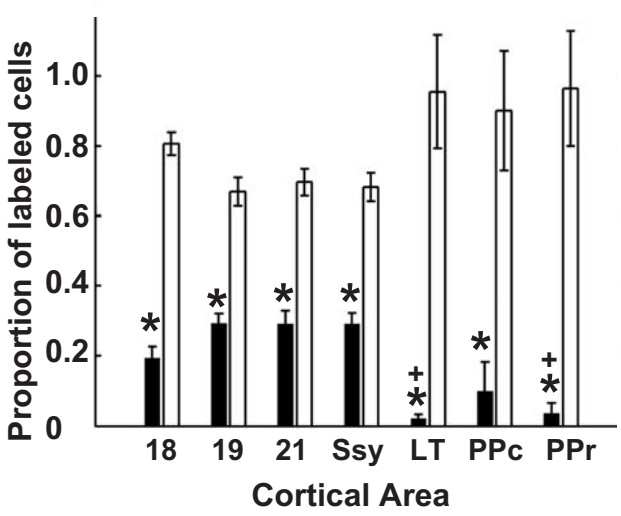
Proportion of labeled cells
1.0
0.8
0.6
0.4
0.2
0
18
19
21
Ssy
LT
PPc
PPr
Cortical Area

We found two groups differing significantly in the proportion of cells located in the supragranular layers (Kruskal-Wallis, $p<0.001$). Areas 18, 19, 21, and SSy each contain more labeled cells in the supragranular layers, than do LT, PPr and PPc. Areas 18, 19, 21, and Ssy each differ significantly from LT and PPr. Due to the small number of labeled cells in PPc, the proportion of supragranular cells in PPc is not significantly different from the percentages in the supragranular layers of any area. There is no significant difference among areas in the proportion of labeled cells located in the infragranular layers.

The large differences in the proportion of labeled cells between the layers could result in larger cortical spreads of labeled fields within the infragranular layers. We therefore compared the cortical spreads of labeled fields in supra- and infragranular layers in areas 17, 18, 19 and 21. Because in most cases the spread of label was anisotropic, we compared 2 axes of labeled fields within each area as described above in the methods (Fig. 2). Figures 7A and C show the spread of labeled cells within each area along the axes *spanning* isoazimuth and isoelevation lines, respectively. Figures 7B and D show the spread of labeled cells within each area along the axes running *along* isoazimuth and isoelevation lines, respectively. There is no significant difference between the cortical spread between the supra- and infragranular layers for either of the axes measured.

Figure 7. Cortical spreads of labeled cells in the supra- and infragranular layers within cortical areas 17, 18, 19, and 21. The length of the axes spanning (A) and running along (B) isoazimuth lines. The length of the axes spanning (C) and running along (D) isoelevation lines. Same conventions as in figure 6.

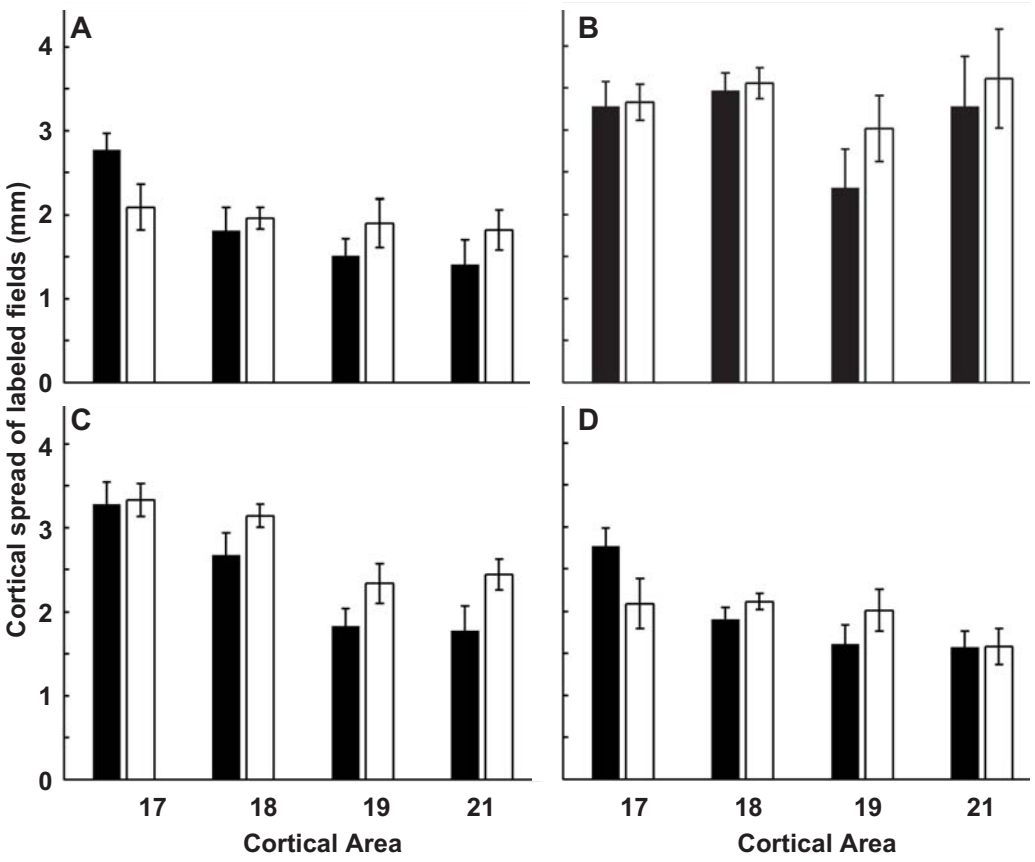
A
B
C
D
Cortical spread of labeled fields (mm)
0
1
2
3
4
17
18
19
21
Cortical Area
Cortical Area

Unlike other cortical areas providing prominent feedback to area 17, the cell label was diffuse in Ssy. It was impossible to relate the pattern of label to the retinotopic organization because in Ssy the retinotopy can be coarse and irregular (Cantone et al., 2003). We simply measured the long and short axes of the labeled fields within Ssy to compare the cortical spreads in the supra- and infragranular layers. As with other areas the cortical spreads are the same in the supra- and infragranular layers (mean long axis: upper layers = 3.2±0.8 mm, lower layers = 3.6±0.4 mm, mean short axis: upper layers = 1.8±0.5 mm, lower layers= 2.8±0.7 mm). Feedback connections from all areas converge onto the injection cores in area 17 whose mean diameter is 0.8±0.04 mm.

Direct evidence for retinotopic convergence of feedback connections

We determined if feedback connections arising from these areas allow for the convergence of larger visuotopic regions onto smaller visuotopic regions in area 17. We did this by explicitly comparing the cortical spreads and pattern of retrogradely labeled cells to the retinotopic maps in visual cortex by making physiological recordings across visual cortex in the same animals in which we made CTb injections in area 17. We made numerous closely spaced electrode penetrations throughout the region of extrastriate cortex likely to contain cells retrogradely labeled following area 17 tracer injections. We show in Figure 8 results from the most completely mapped case. Figure 8A shows the distribution of labeled cell density overlaid by the positions of electrode penetrations; coordinates of corresponding receptive field locations at each recording site are indicated. The pattern of label reflects the retinotopic organization of the lower visual fields in these extrastriate areas, and is located at similar retinotopic locations as the injection site. RFs

at the edge of the injection core spanned from –12° to –17° in elevation, and from 2° to 11° in azimuth in the contralateral hemifield (Fig. 8B). Large numbers of labeled cells were located near the transitions between areas 17/18 and 19/21 (Fig. 8A), which correspond to representations of the vertical meridian (Manger et al*.,* 2002a). In contrast, the number of labeled cells decreased as one approached the transitions between areas 18/19 and areas 21/Ssy, which correspond to the representation of more peripheral regions of the visual field (Manger et al*.,* 2002a). Similar patterns of label were present in all our injection cases, two of which are shown in Figure 4. Our data also show that the locations where there were high densities of labeled cells were not restricted to similar retinotopic locations as our injection sites.

Figure 8A shows directly that cortical locations containing cells directly projecting to the injection locus can have RFs at locations in visual space up to 30° away from RFs of cells at the injection site. Figure 8B-D shows RFs of cells at selected cortical locations containing retrogradely labeled cells; each panel compares the receptive fields mapped in a different extrastriate area with those mapped in area 17. Receptive fields of cells in all cortical areas providing intrinsic or feedback connections were located in the same visual hemifield as the RFs at the injection site, and occupied a larger extent of visual space than the receptive fields located at the injection site in area 17. ARFs of cortical loci in all areas providing feedback to area 17 appear to cover a greater distance in visual space in azimuth than in elevation (Fig. 8B-D). The other case in which we recorded receptive fields at labeled locations throughout cortex, though incompletely mapped, was consistent with this case in showing clearly that feedback connections link cells that respond to widely separated regions of visual space.

Figure 8. Density map and receptive field locations of cells providing feedback to area 17 determined in the same case. (A) The density of retrogradely labeled cells found in cortex following an injection of CTB into area 17 (black area). Asterisks represent penetration sites in cortex. The numbers in white circles are the penetration sites whose RFs are shown in panels B, C, D. Numbers above each site represent the retinotopic location (azimuth, elevation) of the corresponding RF centers. LS = lateral sulcus. Gray dotted lines represent areal borders. Large numbers indicate cortical areas. Cell densities less than 5% of the peak density of cells within each area are excluded. Scale = 1 mm. The receptive fields of cells located at the edges of a labeled field in areas (B) 18 (orange), (C) 19 (green), or (D) 21 (blue) are compared in each panel to the RFs located at the injection site (dark yellow) and at the edges of intrinsic connectional fields (pale yellow). For clarity only RFs in each area that were most distant from those at the injection site are shown. The small numbers represent the penetration numbers shown in (A).

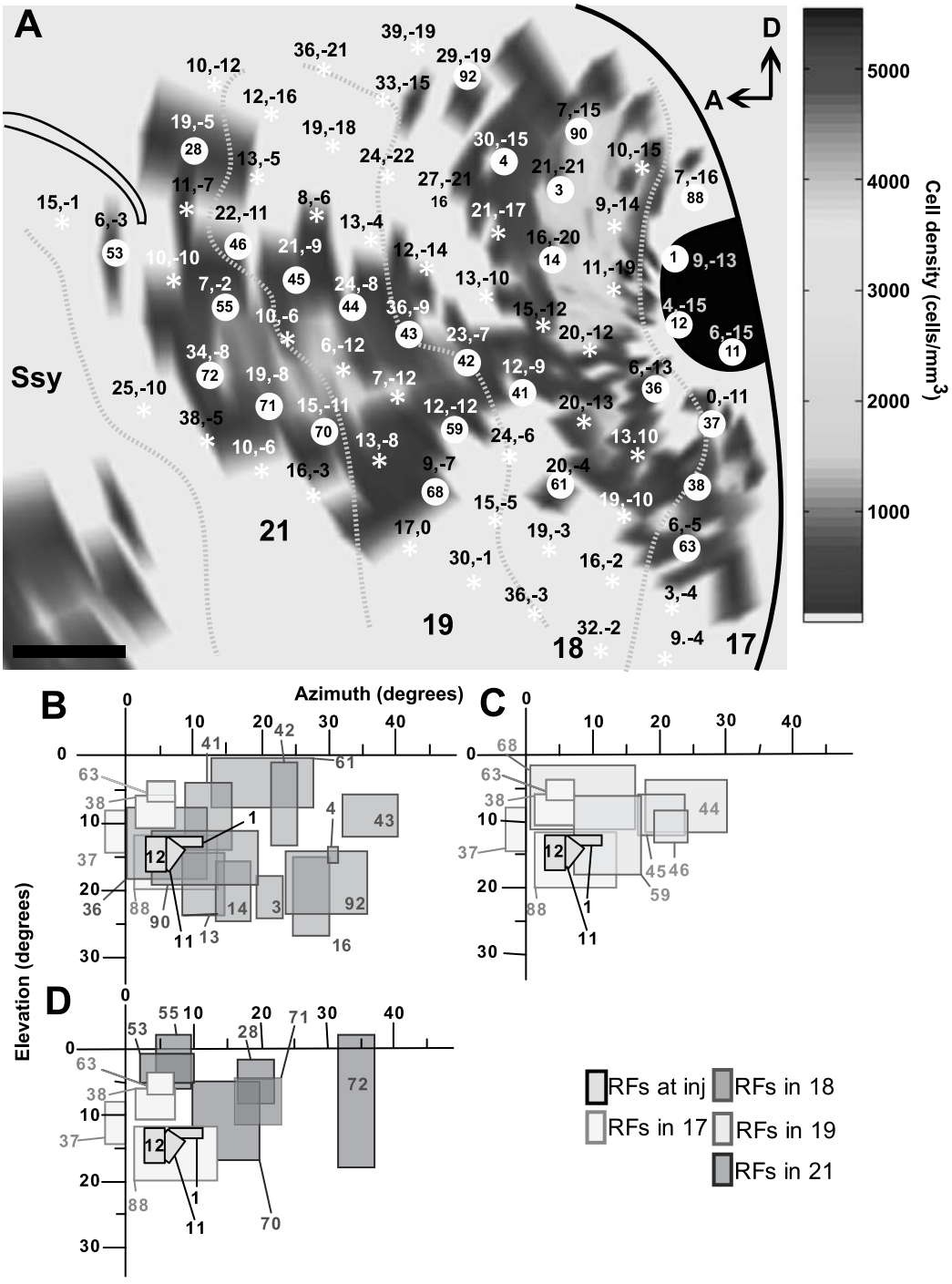
A
D
A
Ssy
21
19
18
17
Cell density (cells/mm3)
5000
4000
3000
2000
1000
B
C
D
Azimuth (degrees)
Elevation (degrees)
RFs at inj
RFs in 17
RFs in 18
RFs in 19
RFs in 21

Cortical magnification factors in extrastriate cortex

We calculated the cortical magnification factors (MFs) within areas 18, 19, and 21 This was a necessary step in determining if the same retinotopic convergence of feedback connections is seen in the cases lacking electrophysiological mapping data. Manger et al. (2002a) previously described the retinotopic organization of these extrastriate areas, but did not explicitly report on MFs. As the main focus of this study was not to remap these areas, we report only MFs here. We found few consistent MF differences with eccentricity or among areas. No previous mapping studies report any variation in MFs across cortical laminae in any cortical area (e.g. Allman and Kaas, 1971; Van Essen and Zeki, 1978; Tusa et al., 1979; Tusa and Palmer, 1980; Law et al., 1988; Manger et al., 2002a). We therefore made the common assumption that MFs are similar through the depth of the cortex. Data from one typical case show no correlation between MFs in mm/deg. of elevation and of azimuth within the representation of lower visual fields in areas 18, 19, and 21 (Fig. 9A). If MFs measured in azimuth and elevation both decrease with increasing eccentricity, these measures will be positively correlated, and will therefore fall along the diagonal in Figure 9A. The lack of any significant correlation indicates that there is no consistent relationship between the spacing of isoazimuth and isoelevation contours. Most of the MFs fall to the left of the line of identity indicating that isoelevation contours are generally spaced further apart than isoazimuth contours. In cases in which 2 cortical loci have receptive fields that differ in azimuth or elevation but not both, it was not possible to calculate a MF along the axis of visual space along which receptive field position did not change. Therefore, we plotted such unpaired MFs in Figure 9A outside the axes. The data from this one case show MFs along both axes in

visual space in all 3 areas cover the same range, with no apparent difference in mean values among areas (mean MF in mm/deg. azimuth: 18=0.08, 19=0.07, 21=0.07; mean MF in mm/deg. elevation: 18=0.12, 19=0.12, 21=0.11).

Using data from 6 cases in which we made extensive electrophysiological recordings, we also assessed the relationship between cortical magnification factors and eccentricity among areas. We found that isoelevation lines within the central 30° of elevation, and isoazimuth lines at all eccentricities, were essentially equally spaced regardless of eccentricity (consistent with Manger et al., 2002a). Thus, comparing MFs across eccentricity we find the average MFs do not differ greatly. However, MFs across isoelevation lines were generally greater than those across isoazimuth lines, but this holds only in areas 18 and 19 within the central 20°. Comparing values in Figure 9B with those in Figure 9C for each area within a given range, only MFs in mm/deg. of elevation within azimuth ranges 0°-10 ° and 11°-20° in areas 18 and 19 were significantly greater than the MFs in mm/deg. of azimuth at elevation ranges of 0°-10° and 11°-20° (Rank-Sum, $p<0.001$). There were no significant differences among areas in MFs in mm/deg. of azimuth (Fig. 9B). There was only one significant difference among areas in MFs in mm/deg. of elevation; those within the azimuth range of 11°-20° were significantly larger in area 18 than in area 21 (Kruskal-Wallis, $p<0.032$ (Fig. 9C). This difference is most likely the result of the condensing of isoelevation lines in area 21 due to a split representation of the horizontal meridian, which is reported by Manger et al. (2002a) and is present in 3 of 6 cases in which we made recordings.

Figure 9. Cortical magnification factors in visual areas 18, 19, and 21. (A) The relationship between MFs in mm/deg. of elevation and azimuth is shown for one case. Data points without a corresponding MF along the opposing axis of visual space were plotted outside the range of MFs, indicated by dotted lines. The symbols outside the box indicate the mean MF for each area. (B) MFs in mm/deg. of azimuth compared across 3 elevation ranges. (C) MFs in mm/deg. of elevation compared across 4 azimuth ranges. Ranges are indicated on the abscissa. Numbers at the top of the figure indicate cortical areas. In each box plot solid horizontal lines indicate the lower quartile, median, and upper quartile values. The dotted lines extend to the most extreme data points whose values fall within 1.5 times the inter-quartile range. (+) indicates outlying data points. (*) indicates significant differences among areas within each range. (^) indicates significant differences between MFs in mm/deg. of elevation and azimuth within a given area.

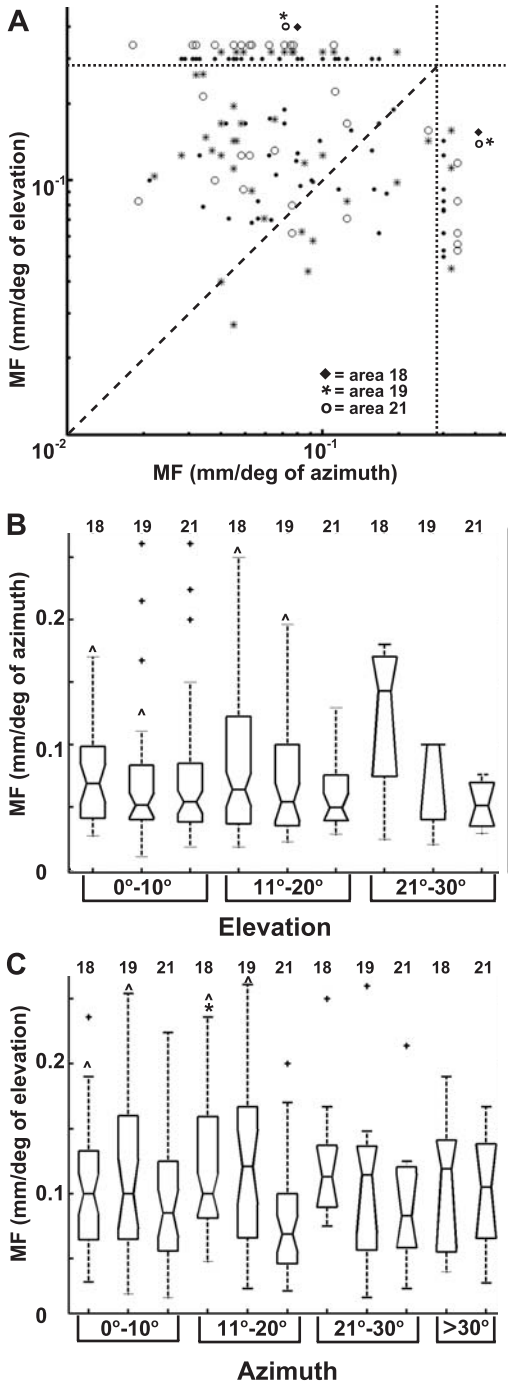
A
MF (mm/deg of elevation)
10-1
10-2
10-1
MF (mm/deg of azimuth)
◆ = area 18
* = area 19
o = area 21
B
18 19 21 18 19 21 18 19 21
MF (mm/deg of azimuth)
0.2
0.1
0
0°-10°
11°-20°
21°-30°
Elevation
C
18 19 21 18 19 21 18 19 21 18 21
MF (mm/deg of elevation)
0.2
0.1
0
0°-10°
11°-20°
21°-30°
>30°
Azimuth

Calculation of visuotopic extents corresponding to the cortical spreads of labeled fields

We also determined the amount of visual space converging onto area 17 through feedback connections in the 6 cases for which we have only anatomical data using an inferential method that relates the pattern of label of our injection cases to the MFs derived from our recording cases. We found the condensing of isoelevation lines and the anisotropic representation of isoazimuth lines in extrastriate areas described in Manager et al. (2002a) result in lower MFs in extrastriate areas as compared to those of area 17 (Kruskal-Wallis, $p<0.001$). Therefore, labeled cells in each of these areas can potentially respond to larger regions of visual space than cells at the injection site or the labeled region within area 17. For cortical locations whose RF azimuths were less than 20° (pooled across all elevations), the average MFs in mm/deg. are: area 17= 0.200±0.018, area 18= 0.078±0.004, area 19= 0.071±0.005, and area 21=0.068±0.004. Likewise, for cortical locations whose RF elevations were less than 20° (pooled across all azimuths) the average MFs in mm/deg. of elevation are: area 17= 0.207±0.026, area 18= 0.109±0.004, area 19= 0.114±0.007 and area 21=0.086±0.006. We use these MFs to convert a distance in cortical space (D_{mm}) into an extent in visual space (aggregate receptive field). The approximate diameter of the aggregate receptive field (ARF) of labeled cells at the area 17 injection core was 10°, of area 17 intrinsic connections was 21°, of area 18 was 34°, of area 19 is 30° and of area 21 is 33° (see Table 1). We do not calculate visuotopic extents of label in Ssy. The average MF in Ssy is much lower than the MF in area 17 (Cantone et al., 2003). Based on the overall cortical spreads of label we find in Ssy, it is likely that Ssy cells providing feedback connections also respond to larger regions of visual space than their area 17 targets.

To determine the amount of visual space converging onto area 17 through feedback connections we compared the extents of aggregate receptive fields (ARFs) of labeled cells within the supra- and infragranular layers of areas 18, 19, and 21 to the extents of ARFs of cells at the injection site or linked by intrinsic connections within area 17 (Fig. 10). These calculated ratios compare ARFs that were derived using the length of the axis of a labeled field inferred to span isoazimuth or isoelevation lines. The extent in azimuth of the ARFs of labeled extrastriate neurons can be as much as 4 times larger than that of their target neurons in area 17, and up to twice as large as that of cells in area 17 linked by intrinsic connections (Fig. 10A). The extent in elevation of extrastriate ARFs can be as much as 3.5 times larger than the ARFs of their target neurons, and as much as 1.5 times larger than the ARFs of the cells in area 17 linked by intrinsic connections (Fig. 10B). There is little difference in the extent of visuotopic space converging onto the target site in area 17 through feedback arising from the supragranular layers compared to that arising from the infragranular layers. This is despite the fact that there are many more labeled cells found in the infragranular layers.

Figure 10. Visuotopic extents of cells providing feedback connections compared to the visuotopic extents of the cells at the injection site and of labeled cells within area 17. Ratios for both upper and lower layers are shown. (A) Calculated ARF extent in azimuth of labeled cells in areas 18, 19, and 21 divided by the ARF of cells at the area 17 injection site, or by the ARF of cells in area 17 linked by intrinsic connections. (B) Calculated ARF extent in elevation of labeled cells in areas 18, 19, and 21 divided by the ARF of cells at the area 17 injection site, or by the ARF of cells in area 17 linked by intrinsic connections. Black bars = Ratio of the ARF of labeled cells in supragranular layers of extrastriate area to the ARF of area 17 cells linked by intrinsic connections. Dark gray bars = Ratio of the ARF of labeled cells in infragranular layers of extrastriate area to the ARF of area 17 cells linked by intrinsic connections. Light gray bars = Ratio of the ARF of labeled cells in supragranular layers of extrastriate area to the ARF of cells at the area 17 injection site. White bars = Ratio of the ARF of labeled cells in infragranular layers of extrastriate area to the ARF of cells at the area 17 injection site. Values represent means ± s.e.m.

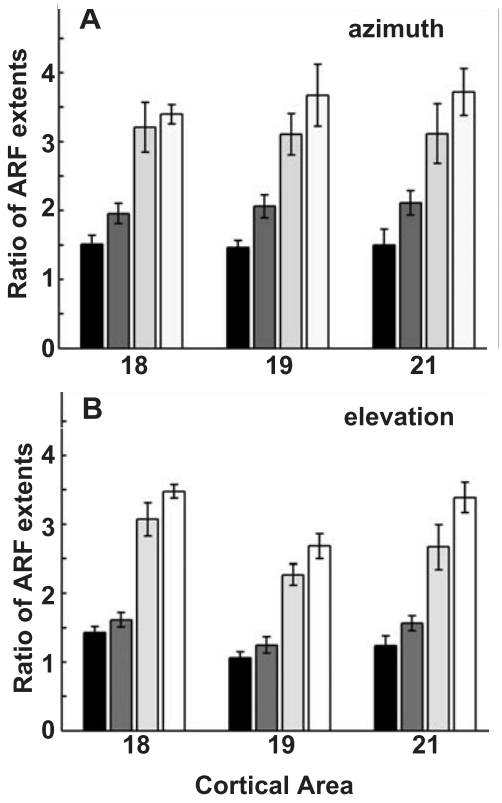
A
azimuth
Ratio of ARF extents
0
1
2
3
4
18
19
21
B
elevation
Ratio of ARF extents
0
1
2
3
4
18
19
21
Cortical Area

TABLE 1. Aggregate receptive field extents (ARFs) of injection cores and labeled fields

Case	17 inj.	17 intr.	18	19	21
ARFs in deg. of azimuth					
avg 1 calculated	10.8 ±1.2				
supra		20.9±1.0	25.4±2.8	21.8±2.0	24.6±3.8
infra		17.5±1.4	26.7±1.3	25.2±2.8	29.4±3.0
172 calculated	10.9	19.9	33.9	31.8	39.7
172 measured	9	17	41	29	34
ARFs in deg. of elevation					
avg 1 calculated	10.1±0.2				
supra		23.4±1.4	33.2±2.7	24.6±2.0	28.9±3.7
infra		23.5±1.0	37.6±1.4	29.9±2.2	36.6±2.4
172 calculated	10.9	21.9	33.4	20.2	25.7
172 measured	7	17	27	16	21

1 avg, Average of ARFs for 6 cases ± s.e.m. in which retinopic organization of cortex is not mapped

Table 1 shows the average calculated aggregate receptive field extents (ARFs) corresponding to the injection sites and labeled fields within the supra- and infragranular layers of areas 17, 18, 19, and 21 for the 6 cases for which we have no recording data. It also shows the calculated and measured ARFs for a representative case in which we have

both anatomical and physiological mapping data (case shown inFig.8). Like the cortical spreads, the ARFs of labeled fields within each area do not vary significantly between upper and lower layers. Our calculated ARFs are reasonable estimates of the measured data we obtain from this single case. However, the calculated ARFs in elevation are slight overestimates of the retinotopic extents relative to the measured extents in this single case.

Using data from the case shown in Figure 8, we calculated the convergence of visuotopic extents of labeled fields from extrastriate areas onto area 17 and compared them to the ratios we directly measured. By comparing these values we could assess the accuracy of the method we used to calculate ratios of retinotopic extents in injection cases in which the cortical retinotopic organization is not known. The calculated ratios of ARF extents in both azimuth and elevation for each area agree with the measured ratios (Fig. 11). This indicates that our estimates of the convergence of visual space through feedback connections onto smaller regions in areas 17 are reasonably accurate. In area 18, where there is the largest discrepancy between the measured and calculated data, the calculated ratios are underestimates. The measured ratios match not only the calculated ratios in the single case shown here, but they also match the mean calculated ratios for the 6 other cases in which no recordings were made (shown in Figure 8). Since both area 17 and extrastriate ARFs are overestimates, the calculated ratios closely match the directly measured values.

Figure 11. Measured visuotopic extents of labeled cells in areas 18, 19, 21 in a representative case shown inFig.8. (A) Compares the ARFs in deg. of azimuth (B) Compares the ARFs in degrees of elevation. Balck bars = calculated ratio of ARFs of labeled cells in extrastriate areas to ARF of labeled cells in area 17. Dark gray bars = measured ratio of ARF labeled cells in extrastriate areas to ARFs of labeled cells in area 17. Light gray bars = calculated ratio of ARFs of labeled cells in extrastriate areas to ARF of injection core. White bars = measured ratio of ARF labeled cells in extrastriate areas to ARFs of injection core. Arrows indicate the calculated mean of the ratios of ARFs of cells in supra- and infragranular layers in each area to labeled cells in area 17 and injection core for 6 cases shown in Figure 8.

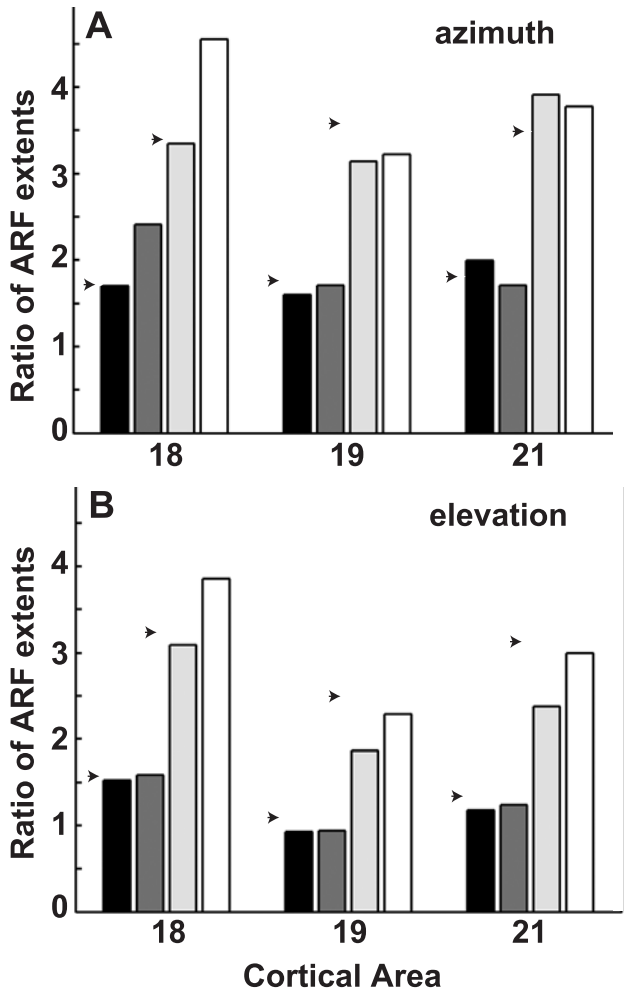
A
azimuth
Ratio of ARF extents
0
1
2
3
4
18
19
21
B
elevation
Ratio of ARF extents
0
1
2
3
4
18
19
21
Cortical Area

2.4 DISCUSSION

Summary

Strong feedback connections arise from the 4 cortical areas rostral to area 17 known to receive input from area 17 and to contain a representation of the visual field: areas 18, 19, 21 and Suprasylvian cortex (Ssy). We find fewer projections from the posterior parietal areas PPr and PPc, and lateral temporal areas (LT). In all areas examined, feedback originates largely from the infragranular layers, with smaller contributions arising from the supragranular layers. Many feedback connections from ferret extrastriate cortex to area 17 link cells with non-overlapping receptive fields, confirming that these circuits allow for the convergence of signals from large retinotopic extents onto cells in ferret area 17.

Methodological considerations

For most of our cases we use an inferential method to quantify the convergence of larger regions of visual space restricted locus in area 17. In this method, the axis of the labeled field inferred to span isoazimuth or isoelevation lines within each area provides a conservative estimate of cortical and visuotopic extent of label. One can directly prove convergence by making paired tracer injections at different locations in a given extrastriate area, and looking for overlap of orthograde terminals in area 17 (Shipp and Grant, 1991). If distinguishable tracers are used, one has to contend with unequal sensitivity of the two tracers. A more fundamental issue is that divergent locations in ferret extrastriate cortex may have overlapping receptive fields, so a demonstration in this way of *anatomical* convergence does not necessarily imply *retinotopic* convergence. We

therefore chose to directly measure the visuotopic extent of feedback connections using electrophysiological mapping, which confirms the accuracy of our inferential estimates.

There are some limitations in our calculated method. Our calculated ARF extents in elevation are larger than the measured extents in our representative case. These overestimates in ARF extents in elevation are largest in areas 19 and 21. It is in these areas that the representations of elevation can vary the most (Manger et al*.,* 2002a, personal data). Therefore, the mean MF we used to calculate retinotopic extents of labeled cells in these areas may be slightly smaller than the actual MFs. Without directly mapping the regions where there are labeled cells in each animal, the assignment of the axis of labeled cells running along either isoazimuth or isoelevation contours is somewhat subjective. This can result in some uncertainty about the length of the axis used to calculate the visuotopic extents. Both the possible underestimation of MFs and the overestimation of cortical spreads can account for the differences between our calculated and measured data. However any misestimates are slight given that the difference between our calculated results and our measured results is small.

It is also possible that the visuotopic extents of label we measure by directly recording RFs are underestimates due to sampling. The spacing of our penetration sites may not be fine enough to reveal RFs more remote from those at the injection site. In addition we may not have recorded in the extreme margins of the field of cell label. These locations in cortex potentially can respond to more remote regions of visual space.

Factors governing the distribution of feedback connections and their functional relevance

The size of the area contributes significantly to the average strength of the connections

originating from the area (Hilgetag and Grant, 2000). The proportion of feedback connections from each area in ferret cortex supports this idea. However area 18 has the greatest peak density of feedback cells of any extrastriate area. This cannot be attributed solely to the size of the cortical area. Scannell et al. (1995) suggest that within the visual system of the cat a better predictor of the connectivity is the hierarchical organization of cortical areas. Since our data do not support a strict hierarchy among areas, other aspects of neuronal function may be more important in governing cortical connectivity in ferret (Einstein, 1996). Physiological studies in cat report synchronized firing between neurons in different cortical areas with overlapping receptive fields and similar orientation preferences (Engel et al., 1991; Nelson et al., 1992). We have shown that feedback cells are not restricted to similar retinotopic regions as their targets. This suggests that corticocortical connections may be governed by other functional attributes of cells despite retinotopic mismatch. Previous studies show neurons in extrastriate cortex strictly retinotopically linked with their targets in area 17 can drive responses. In contrast, connections linking non-overlapping areas of visual space may mediate modulation of evoked responses (Bullier et al., 1988).

Connectional strength may be an indication of the functional influence each area has over the response properties of neurons in area 17. Our data suggest that area 18 can have the strongest influence on area 17 neurons as compared to areas 19, 21, and Ssy, with areas PPr, PPc, and LT having only minor influences. However, the percentage or density of projections provided by each area does not necessarily reflect the functional influence connections from each area may have over neuronal responses. For example the effect of each individual synapse may be important in shaping neuronal responses, or

each cortical area may have distinct functional properties that shape RFs (Hupé et al., 1998, 2001a) regardless of the number of connections. Thus, although there is little difference in the number or density of feedback cells among areas 19, 21, and Ssy, connections from each of these areas can well have very different effects on area 17 neurons.

The functional purpose of more feedback arising from the infragranular layers is uncertain. The supra- and infragranular layers differ in morphological cell types, functional properties, intrinsic and extrinsic connectivity, and their affects on neuronal responses (Lund, 1973, 1988; Rockland and Pandya, 1979; Bullier et al., 1988; Lagae et al., 1989; Nowak et al., 1995). The laminar origin and termination of projections from extrastriate areas to area 17 may also depend on the area from which they arise, indicating that feedback forms precise circuits among cortical areas (Batardière et al. 1998; Henry et al., 1991). Therefore, projections arising from different layers would presumably provide different types of input and possibly have different roles in shaping RF properties of their targets. Physiological studies in cat show that inactivating layer V cells in area 18 affects response magnitude and selectivity to stimulus velocity and orientation in layer V cells of area 17. In contrast, inactivating area 18 cells in layers II/III affects response magnitude only, without changing the selectivity of neuronal responses of area 17 cells in layers II/III (Alonso et al., 1993; Martinez-Conde et al., 1999).

Comparisons to cat and primate

Our finding of convergence of visual signals from retinotopically divergent

locations onto area 17 cells is broadly in agreement with previous results in monkey (Angelucci et al., 2002b), and expands on findings in cat that were limited to projections from area 18 (Salin et al., 1992) This suggests that cortical feedback in ferret obeys similar rules as in these other species. However, there are some differences among ferret and these other species. There appears to be a difference in the topographic extents of feedback arising from supra- and infragranular layers in primate and cat (Barbas, 1995; Barone et al., 1995; Batardière et al., 1998; Angelucci et al., 2002a), whereas we find no such difference. This is true despite the larger number of feedback projections arising from the lower layers. Another major difference between the primate and the ferret is that all ferret extrastriate visual areas appear to provide roughly the same visuotopic extent of feedback to area 17 (based on a limited number of recording cases). This is consistent with our data and those of Manger et al. (2002a) on retinotopic organization of ferret extrastriate cortex showing that unlike other species, cortical magnification factors (MFs) vary little with eccentricity or among areas. Although receptive field sizes do vary among areas, this is most pronounced at more peripheral receptive field locations than the ones we studied.

Our data addressing retinotopy reveal further interspecies differences. There is a less obvious hierarchical organization of ferret visual areas. In macaque, at sequential hierarchical levels neurons respond to larger regions of visual space (at any eccentricity), and cortical magnification factors (MFs) decrease. Unlike the findings in macaque, but in agreement with Manger et al. (2002a), we find little difference in MFs among extrastriate areas, or in RF sizes within the central 20° of visual space. Overall, our data suggest only subtle differences in the extent of visual space to which cells in each extrastriate area

providing feedback connections respond. However, whether cells in different extrastriate areas providing feedback to area 17 have ARFs of differing extent (or provide signals of a qualitatively different nature) remains an important question for further study.

Our anatomical data do not support a strictly hierarchical arrangement among areas 18, 19, and 21 either. Felleman and Van Essen (1991) base their hierarchical organization of visual areas in cortex on the laminar distribution of connections among different cortical areas in primate. There is a negative correlation between the amount of feedback projections from the supragranular layers and the distance from area 17 in the hierarchy (Batardière et al., 1998; Barone et al., 2002). If one applies this criterion to our anatomical findings, areas 18, 19, 21, and Ssy may be considered to be on one level of visual processing, while areas PPr, PPc, and LT fall within another level of processing. This agrees with other evidence in cat showing the laminar organization of corticocortical projections is not strictly correlated with the hierarchy (Symonds and Rosenquist, 1984a).

We can compare the connectivity of area 17 in ferret to that of area 17 in cat to further demonstrate similarities between species. Based on the retinotopic organization, Law et al. (1988) report that area 17 in ferret is homologous to area 17 in the cat. The corticocortical connections of area 17 described here support this. Our restricted injections into the central representation of area 17 reveal reciprocal connections to areas 18, 19, 21, and Ssy, with weaker connections from PPr, PPc, and LT. Similar injections into cat area 17 show major connections to areas 18, 19, 21a PMLS, and 20a, with weaker connections arising from PLLS, AMLS, and 21b, (Symonds and Rosenquist, 1984b). Manger et al. (2002a, 2004) do suggest areas 18, 19, and 21 in ferret are homologous with areas 18, 19, and 21a and 21b and temporal area 20a of cat,

respectively. Based on our unpublished data, Ssy in ferret shows some similarities with the lateral suprasylvian areas (Palmer et al., 1978), which include PMLS. If these comparisons are accurate, areas providing strong feedback in cat also provide strong feedback to area 17 in ferret. The one dissimilarity between cat and ferret is area 17's connectivity with temporal area 20a. Although the connections between 17 and temporal areas are consistent in ferret they are not as strong as those reported in cat.

Because ferrets are not as closely related to primates as to cats it is difficult to determine if there are homologous cortical areas in ferret and primates. However, there are general similarities between species in connectivity of area 17. In monkey, areas V2, V3, V4, and MT provide prominent feedback to area 17. There are also weaker feedback connections from temporal and parietal areas (Felleman and Van Essen, 1991; Rockland and Van Hoesen, 1994). Similarly, in ferret, there are 4 areas providing prominent feedback to area 17, with weaker projections arising from both temporal and parietal areas.

The role of feedback in modulatory surround effects

It is currently of widespread interest to determine which anatomical circuits underlie the nonclassical modulatory receptive field surround. As in the cat and primate, our data from ferret indicate that both intrinsic connections within area 17 and feedback connections from extrastriate cortex link cells that respond to non-overlapping regions of visual space, although feedback circuits link cells with more widely separated receptive fields. Both circuits could thus potentially have a role in mediating center surround interactions in area 17. Stettler et al. (2002) suggest intrinsic connections are more likely

to mediate the integration of oriented contours, one manifestation of the modulatory surround. Their study in macaque reports that though both intrinsic and feedback connections link cells with non-overlapping receptive fields, intrinsic connections are denser and show greater patchiness (suggesting an association with orientation columns). The argument why cortical feedback circuits are more likely to underlie the nonclassical modulatory surround has been developed more fully elsewhere (Angelucci et al., 2002a,b; Cavanaugh et al., 2002; Angelucci and Bullier, 2003). In brief, we have shown that feedback projections to ferret area 17 are in fact quite dense, as they are in macaque. Furthermore, the extent of visual space to which cells linked by horizontal connections respond is not as large as that of cells linked by feedback connections from other extrastriate areas. By recording visual responses at cortical locations of cells furnishing feedback projections to a target site in area 17, we have provided direct evidence of the broader convergence of feedback signals to area 17. Our data are thus consistent with those of Angelucci et al. (2002b) suggesting that horizontal connections are indeed responsible for the spatial summation of visual signals of area 17 neurons over a limited visuotopic extent, whereas feedback connections may be the anatomical substrate mediating modulatory surround effects originating from more remote regions of visual space.

CHAPTER 3: EXTENT OF SUMMATION FIELDS OF NEURONS IN FERRET STRIATE CORTEX

3.1 INTRODUCTION:

It is well documented that neuronal responses in area 17 may be modulated over a larger spatial extent than the minimum response field (Zipser et al., 1996; Sceniak et al 2001; Cavanaugh et al., 2002; Levitt and Lund, 2002), and that physiological characteristics of the neurons are known to result from their afferent inputs (Hubel and Wiesel 1962; Gilbert and Wiesel, 1979; Eysel et al., 1988; Ferster, 1988; Hata et al. 1988; Bolz and Gilbert, 1989; Crook et al., 1991; Schwartz and Bolz, 1991; Worgotter and Eysel, 1991; Crook and Eysel, 1992; Shipp and Zeki, 2002). Therefore, it is important to determine the extent in the visual field from which neurons can pool visual signals to understand the anatomical substrates underlying the summation properties of receptive fields.

Our specific aim in this study is to establish the extent of integration of information arising from remote regions of the visual field of neurons in area 17 of ferret (*Mustela putorius furo*). We are examining these issues in ferret because it has been suggested that investigating the interactions between visual signals within the center or spanning different regions of the center and surround may provide more insight to RF center-surround interactions (Chisum and Fitzpatrick, 2004). Since ferret area 17 cells have large receptive fields (Law et al., 1988; Manger et al, 2002a; Cantone et al., 2005) they may be useful for investigating these issues. Because we have so carefully documented the anatomical characteristics of feedback to area 17 in this species,

examining the summation fields of cells allows us to propose a role for these connections.

In electrophysiological experiments using adult ferrets, we determine the extent of visual space over which responses of area 17 neurons can be elicited or modulated. We classify the sizes of the minimum response field, determine the extent of visual space over which cells can summate information and determine modulatory effects caused by stimuli placed in the surround. We then relate these extents to known measures of cortical connectivity and retinotopic maps. These comparisons aid in determining whether the extent of the nonclassical modulatory surround field of neurons in striate cortex derives from circuits within area 17 or from extrinsic inputs such as cortical feedback. We find that responses of cells can be modulated from more extensive regions than the MRF. As in the primate, the extent of the nonclassical surround for a substantial proportion of cells cannot be accounted for by the monosynaptic spread of intrinsic connections within area 17, suggesting a role for cortical feedback (Angelucci et al*.,* 2002; Cavanaugh et al*.,* 2002).

3.2 MATERIALS AND METHODS

Surgical procedures

Nine adult female ferrets (~0.6-0.8 kg) were used in this study. All general surgical procedures and preparation for these experiments are described in the previous chapter. Only the procedures specific to this set of experiments are described here. Three animals were anesthetized throughout the recordings with 0.5-1.5% isoflurane. The remaining 6 were anesthetized with propofol (10-24mg/kg/hr, i.v.).

Recording methods and receptive field analysis

These methods have been adapted from Levitt and Lund, (2002). Penetrations were made into the caudal pole of cortex obliquely to the pial surface, at an angle that resulted in the longest track. This allowed us to sample from all cortical layers. Recordings were made using glass coated tungsten microelectrodes (tip 5μm) (Merrill and Ainsworth, 1972). Single unit responses were fed into an audiomonitor and were initially isolated manually. RFs were hand plotted using bars of light. The dominant eye was determined, and only that eye was used for quantitative testing. Achromatic sinusoidal or square wave drifting grating stimuli (mean luminance 30 cd/m2) were displayed on a SONY GDM-F500 television monitor driven by a CRS VSG board. The maximum size stimulus that filled the square display aperture was then centered on the RF manually using a front-silver mirror. The viewing distance ranged among cases from 42 to 48 cm.

Characterization of receptive field

All computer-generated stimuli were presented in several randomized block trials presented for 2-4 seconds each. Each block was repeated between 3 and 10 times depending on the variability of the responses. The spontaneous firing rate was determined within each block trial by presenting a uniform gray field that had the same mean luminance of the other stimuli. Responses were recorded and computed into averaged histograms that were synchronized to each temporal cycle of the stimulus. These histograms were Fourier transformed to calculate the mean firing rate (DC response) and the response at the fundamental stimulus frequency (F1 response). If the maximum F1

response was greater than the maximum DC response, then the F1 responses were used for the further analyses. Otherwise, the DC responses were used. Cells were defined as simple if F1/DC>1, otherwise they were classified as complex.

The optimal orientation and direction were first determined by using full field drifting sinusoidal grating. Using the preferred orientation, the optimal spatial frequency was determined. Then with the optimal spatial frequency the preferred drift rate was established. Using a stimulus with these optimal parameters the contrast response function was obtained. For most experiments the contrast was fixed at 75% of the maximum stimulus contrast. These optimal parameters were used for all subsequent stimuli. We first measured the minimum response field (MRF) by placing small patches of a drifting grating at varying positions on the display screen. The size of the patches was the same across trials for each individual cell. Among cells the sizes varied between 1.66°, 3.33°, and 6.66°. In all cases the smallest patch that would elicit a response from the cell was used to measure the MRF. This measure also ensured that the stimulus was centered on the RF. The area in degrees squared of visual space over which responses could be elicted was calculated by interpolating across the locations in the visual field at which the stimulus evoked a response. The MRF diameter was defined as the square root of the area of the MRF. Once the stimulus was centered on the RF, a second measure of the classic receptive field was made. A full screen, optimal drifting grating was presented with a mask that blanked out the RF center. The mask was a uniform field with the same mean luminance as that of the grating. This mask was expanded uniformly along both axes of visual space to the limit of the screen display. The spatial summation properties of each cell were then established by first centering the drifting stimulus on the RF, then

uniformly increasing the stimulus aperture to the limits of the display screen. The centering of the stimulus was checked throughout the experiment.

After the summation extents were established, the orientation tuning of the surround was determined in a sample of cells. A full screen stimulus with a mask set at the size of the peak summation diameter was presented randomly within each block of trials. Cells that had responses larger than spontaneous activity to this stimulus were not included in this analysis. A drifting grating set at the peak summation diameter was held constant at the cell's preferred orientation while changing the orientation and direction of surround stimulus.

Data analysis

For all cells in this study, orientation-tuning curves were fit to the data and the half bandwidth and preferred orientation were obtained from these fits, using Gaussian function. The preferred orientations of the cells were determined using these fits. All spatial summation data (this excludes the surround data) were fit with the following function, which has been shown to accurately describe these types of summation data (Rodieck, 1965; DeAngelis et al., 1994; Sceniak et al., 2001; Cavanaugh et al., 2002; Levitt and Lund, 2002):

$$Y=A+B\int e^{-(2(x-C)/D)^2}dx-E\int e^{-(2(x-F)/G)^2}dx \qquad (1)$$

This function represents the difference of the integral of an excitatory Gaussian sensitivity function and an inhibitory Gaussian sensitivity function. A is the response

offset, B and E are the relative magnitudes of the excitatory and inhibitory influences, D and G represent the space constants of the excitatory and inhibitory mechanisms. C and F represent the x coordinates of the space constants of each Gaussian. For each cell parameters were extracted from fitting the data with this function. These inclued the peak summation diameter (defined as the stimulus diameter at which responses were the largest if the responses decreased to larger stimuli or 95% of the largest response if they did not), the asymptotic response diameter (defined as the stimulus diameter at which responses had fallen to 5% of the difference between the peak response diameter and the largest stimulus diameter measured), and the suppression index (defined as 1-[asymptotic response/peak response]). The responses of cells to the expanding mask stimulus were also fit with equation 1 with the excitatory Gaussian set to zero. The asymptotic mask diameter was defined using the same criterion as the asymptotic response diameter.

The orientation index [(response at an orientation 90° less than the orientation at the peak response + response at an orientation 90° more the orientation at peak response)/ 2 (peak response)], the direction index (the response at 180° from peak response /peak response), and the circular variance were all calculated from the raw data. The circular variance, an index that provides another description of the orientation tuning, was calculated using the formula used by Ringach et al., (2002):

$$CV = 1 - \frac{\sum_k R_k e^{i2\theta_k}}{\sum_k R_k} \qquad (2)$$

Where R_k is the mean spike rate in response to drifting grating at θ_k which ranged from 0°

to 360°. This index expresses the angles as radians, and averages the responses for the 2 directions of motions at each orientation. A CV= 0 indicates strong tuning while a CV =1 indicates weak tuning. The circular variance was also calculated for the surround stimulus. For these calculations R_k was equal to the response of center + surround stumulus at θ_k – the response to the center stimulus alone at θ_k.

Histology and track reconstruction

After recording sessions, 3 or 4 electrolytic lesions were made at sites of interest along the electrode track using anodal current (10μA for 10-15 seconds). The lesions were unequally spaced (0.5mm-2 mm) to aid in the track reconstruction. Animals were then sacrificed with an overdose of sodium pentobarbital (i.v.), and transcardially perfused with normal saline followed by 4% paraformaldehyde or 10% formalin. The brain was removed and post fixed and sunk in a 4% paraformaldehyde or 10% formalin with 30% sucrose used as a cryoprotectant. The brains were blocked and frozen coronal sections were cut at 40 μm. Alternate sections were stained for cytochrome oxidase or cresylviolet to reveal tracks and laminar boundaries, and to ensure that all the recordings were restricted to area 17. The sections containing lesions were traced using a camera lucida. Tracks were reconstructed by aligning tracings of section using lesions, blood vessels and section outlines. Recording sites were placed along the reconstructed tracks relative to the lesions. Each site was assigned to a cortical layer, and if possible relative cortical depth was determined for each recording site by dividing the depth of the recording site by the thickness of cortex at the recording site location.

Functions were fit to the data, correlation analyses were performed, and graphs

were generated in Matlab (Mathworks, Inc, Natick, MA). Any laminar differences of the parameters described above were determined using Kruskal-Wallis non-parametric one-way analysis of variance, followed by multiple comparison z-value tests. These tests were performed in NCSS version 97 (Kaysville, UT).

3.3 RESULTS:

Classic receptive fields

There were 103 units included in this study, with an equal sampling from all cortical layers. Sixty four percent were simple cells and 36% were complex. All except 10 units were within 20° of the *area centralis*. The parameters we examined did not differ between complex and simple cells nor did they obviously vary with eccentricity. Law et al. (1988) and Manger et al. (2002) also report a wide range of RF sizes within the central 20°of of visual space. Therefore, we pooled the data over cell types and eccentricities. We defined the classic receptive field (CRF) as the region of visual field within which responses could be elicited from an optimal grating stimulus. Our first measured of the CRF is the minimum response field (MRF). We placed small patches of grating at varying locations on the display screen. All cells included in this analysis (n=101) had responses exceeding the spontaneous discharge plus 1 standard deviation of the spontaneous discharge of the DC response. If there was no spontaneous discharge or the F1 response was greater then responses had to exceed 10% of the peak response. Although there are some cells that responded to the smallest stimulus grating (1.66°) the responses tended to be weak, and many cells would only respond to larger stimuli. We found cells that have a single discrete hot spot of maximum activation (Fig. 1A) among

all size MRFs. In both average size MRFs (Fig. 1B) and very large MRFs extending up to 33° (Fig. 1C,D) we found more than a single region of high activation. Large RFs with multiple sub regions of peak activity have been also reported in layer IV (Usrey et al., 2003).

Figure 1. Contour plots of the response magnitudes within the minimum response field (MRF) of cells in ferret area 17. (A) Example of small discrete field with a single region of peak activity (B-D) Show representative cases of MRFs containing multiple regions of high activity.

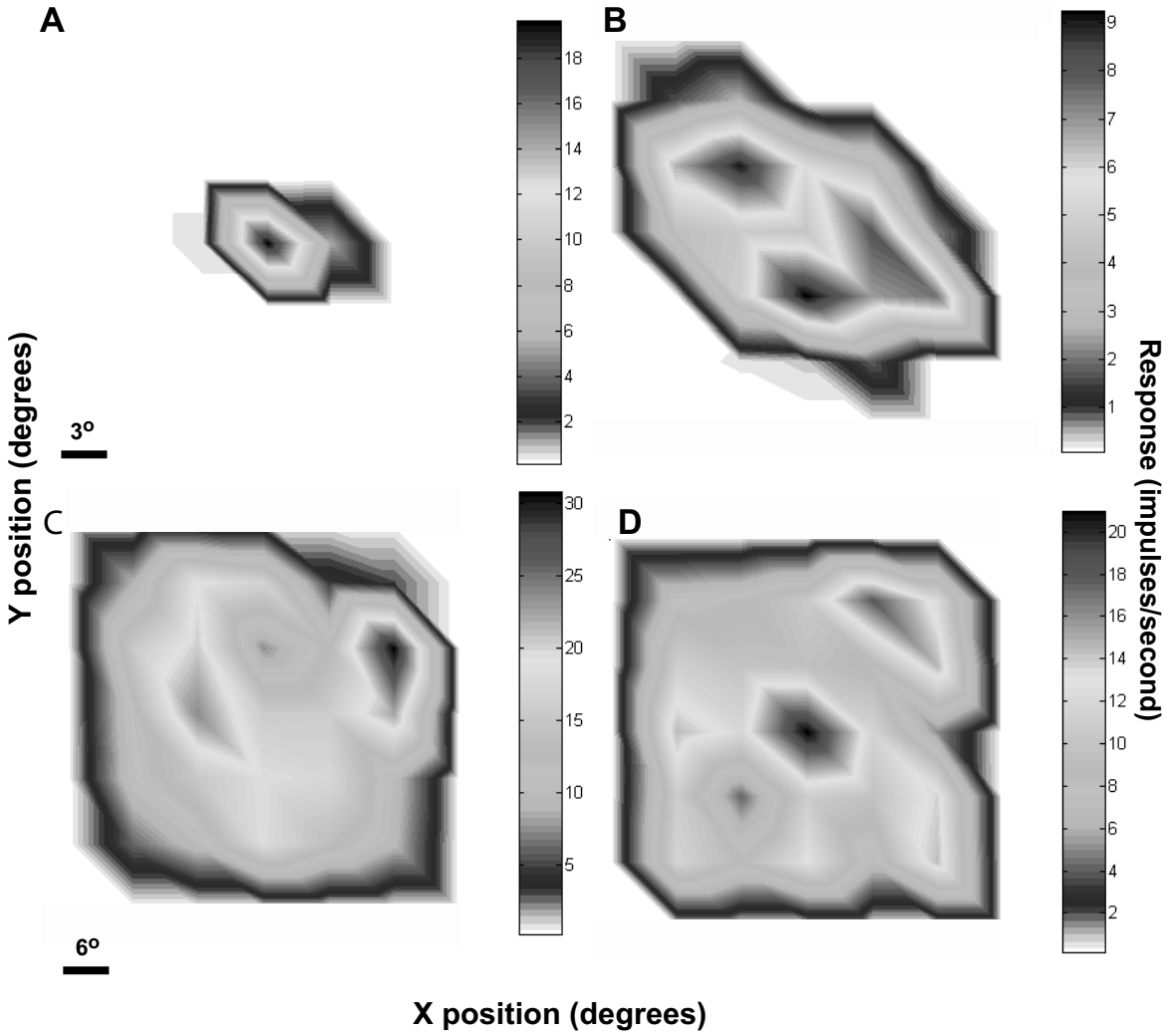
A
B
C
D
3°
6°
Y position (degrees)
X position (degrees)
Response (impulses/second)

To make a second measure of the CRF, we presented a full screen stimulus, ranging up to 33°-35° depending on the screen distance, of an optimal drifting grating. This stimulus elicits a strong response from the neuron. By increasing the diameter of a mask (a blank central region within the stimulus) over the center of the receptive field, the responses decrease until the entire receptive field was covered and no response was elicited. We defined the asymptotic mask diameter (AMD) as the diameter of the mask at which the neuron no longer responds above baseline. Figure 2 shows the responses of 2 representative cells to an increasing central mask. In figure 2A the diameter of the both measures of the CRF are about the same. Figure 2B shows a case in which the AMD is twice as much as the MRF diameter.

Figure 2. Responses of area 17 neurons to an expanding mask stimulus. (A) Case in which the response of the cell asymptotes when the mask is the same diameter as the MRF. (B) A case in which the RF diameter is larger when measured using the expanding mask stimulus. Solid lines indicate the best-fit function of the difference of an excitatory Gaussian function (set to 0) and an inhibitory Gaussian function. Error bars s.e.m.

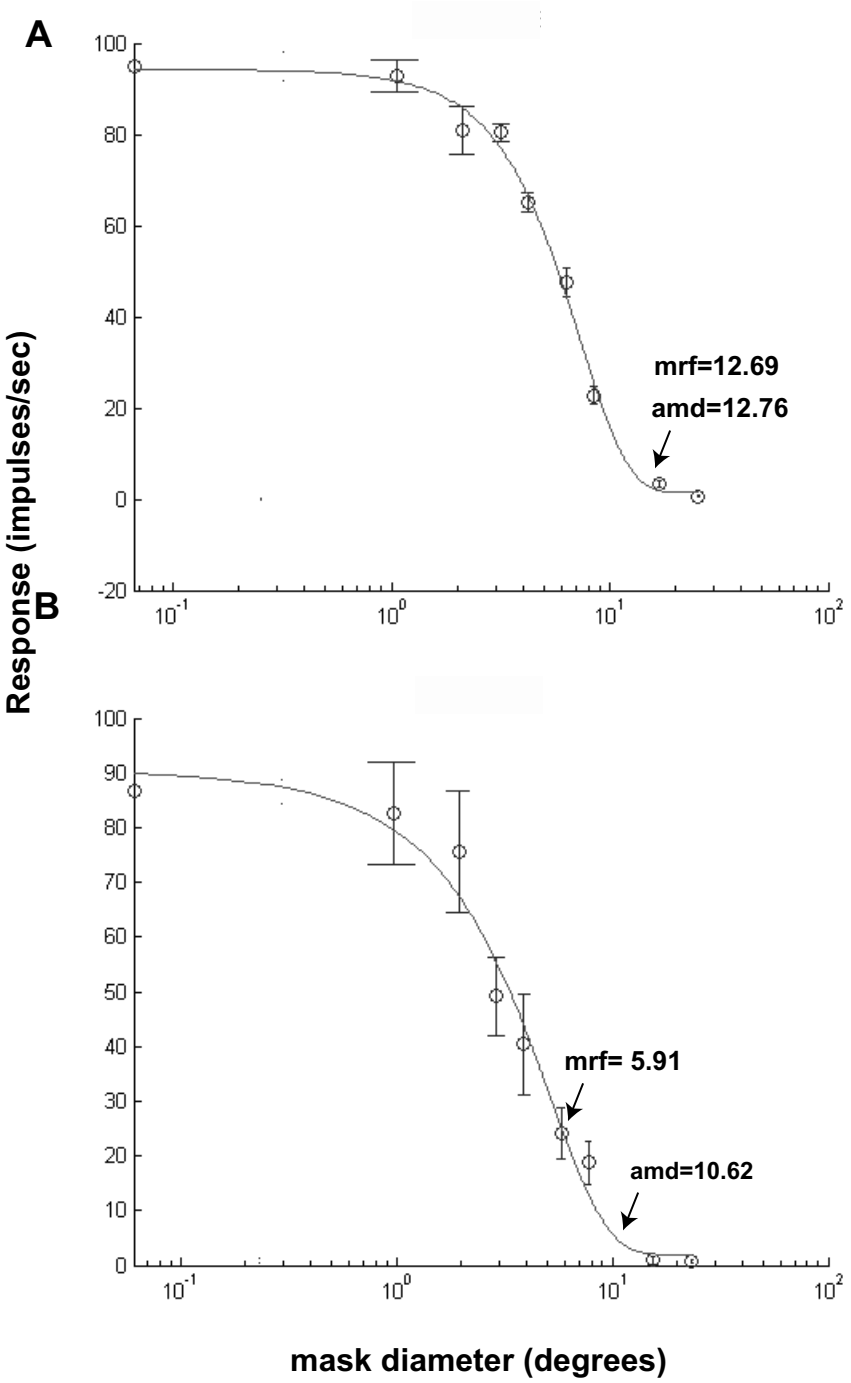
A
B
Response (impulses/sec)
mrf=12.69
amd=12.76
mrf= 5.91
amd=10.62
mask diameter (degrees)

The scatter plot in Figure 3 compares the MRF diameters and AMDs of cells. As expected there is a highly significant correlation of these 2 measures of the CRF (r^2=0.8, p<<0.001), indicated by the majority of points falling along or within 1° (dashed lines) of the central diagonal (solid line). Points falling below this line represent cells whose responses fall to baseline over a smaller region of visual space than the extent of the MRF. Responses of this type are consistent with cells whose responses drop considerably if the central hot spot is occluded (Levitt and Lund, 2002). Points falling above the dashed line represent cells whose responses fall to baseline over a larger region than the MRF, similar to the case in figure 2B. We have found that many area 17 cells in of ferret do not respond optimally to smaller stimuli, and in both cat and primate it is shown that responses to stimuli tend to decrease as one moves from the central hot spot (Movshon et al., 1978a, b, Levitt and Lund, 2002). Therefore, small gratings placed at the edges of the CRF may not stimulate this type of cells enough to elicit a response. However, the larger border formed with the full screen stimulus containing the mask may be enough to elicit a response. Since stimuli placed in the surround do not cause the cell to respond, the asymptotic mask diameter gives a more accurate extent of the CRF for these types of cells. More likely this differnece is because of the release from inhibition that would be evoked by a stimulus in the center of the RF, thus enhancing reponses to stimuli along the borders.

Figure 3. Comparison of two measures of the classic receptive field. Scatter plot shows the asymptotic mask diameters (AMD) are very similar to minimum response field (MRF) diameters. The bar graph along the x-axis (above) shows the population distribution of the MRFs. The bar graph along the y-axis (side) shows the population distribution of the AMD. Arrows indicate the population mean. Arrowheads indicate the median. Dashed lines indicate a boundary of a 1° difference in the 2 measures.

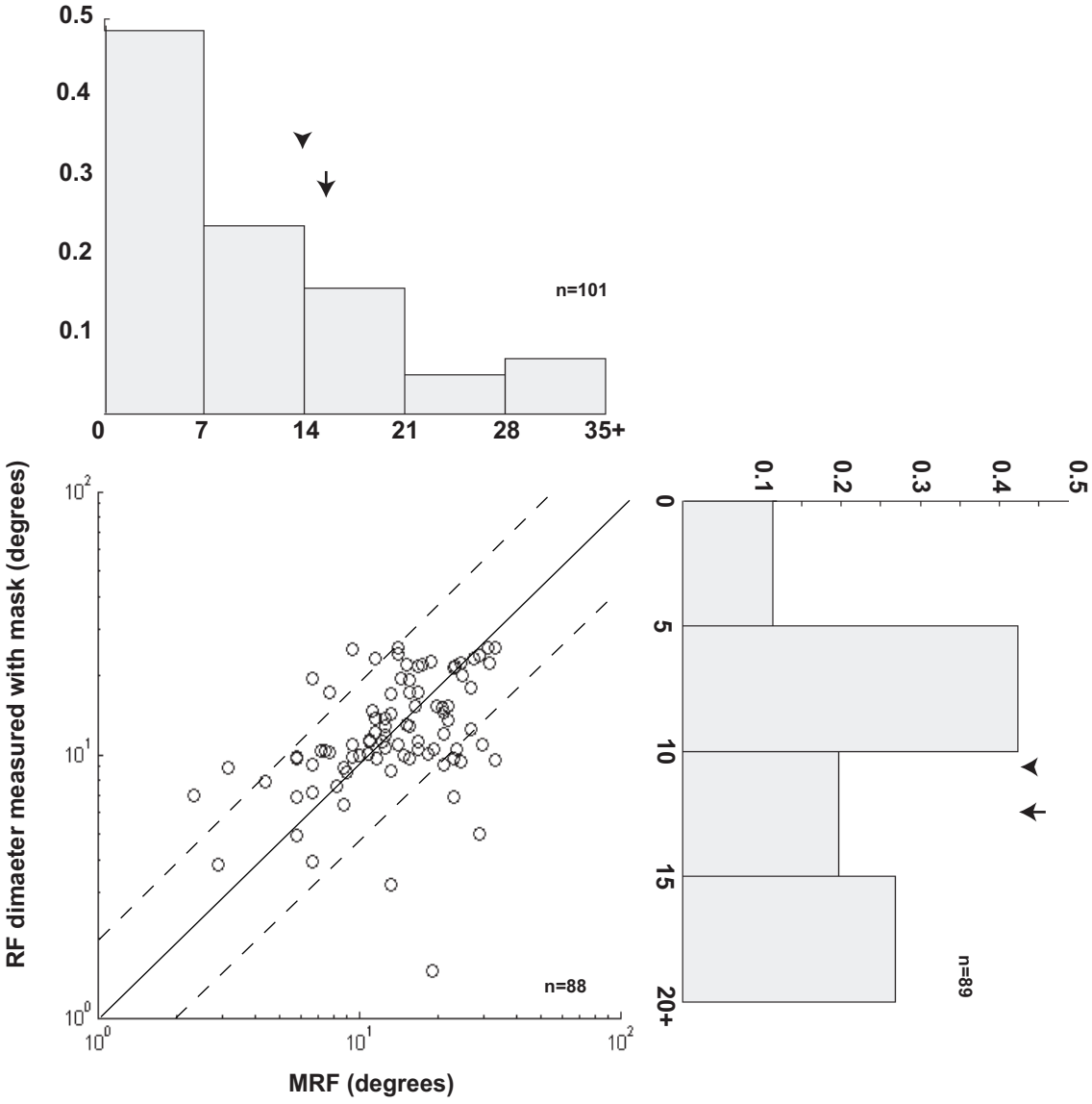
0.5
0.4
0.3
0.2
0.1
n=101
0
7
14
21
28
35+
RF dimaeter measured with mask (degrees)
10^2
10^1
10^0
n=88
10^0
10^1
10^2
MRF (degrees)
0.1
0.2
0.3
0.4
0.5
0
5
10
15
20+
n=89

The bar graph above the scatter plot shows the population distribution of the MRF diameter. They ranged from 1.7° to 33.2°, (mean= 15.3° ±0.8°, median=14.1). There is no difference in the mean MRF of simple cells (15.7±1) and that of complex cells (15.3°± 1.6). Since, the largest extent of visual space covered by the stimuli used to measure the MRF is 33.3° it is possible that some cells have larger MRFs than we could measure. However only 3 of these cells have responses that do not asymptote when tested using the expanding mask method. This indicates that most of our MRFs measures are not underestimates. The population distribution of the AMDs is shown along the right axis (mean= 13.2°±0.6, median = 11.3°). The population means being so similar also suggests that our measure of the CRF is accurate.

Spatial summation properties

Once we determined visual extents of the MRF we systematically quantified the extents of the visual field over which neurons in area 17 can integrate information. With the optimal stimulus grating centered on the receptive field, we expanded the stimulus until it filled the display screen (~35°). Figure 4 shows responses of three representative cells, each responding differently to a stimulus with an increasing diameter. The response of the cell in panel A increased to the full spatial limit of our stimulus. This suggests that this cell continued to summate information from regions of the visual field beyond 35°. This cell also had a large MRF (31.4°). The response of the cell in panel B peaked and then asymptoted at a stimulus diameter of 13.5°, indicating it did not summate information much beyond its MRF (9°). In contrast, the cell's response in panel C peaked when the stimulus is 8.8° in diameter, decreased and then asymptoted at a

stimulus diameter of 30.6°. These cells are similar to what Hubel and Wiesel (1968) described as endstopped. Presumably this cell integrated information over an extent that was more than twice the size of its MRF (12.7°) (Fig. 4C). These types of responses are similar to those reported in primate and cat, except the extents in visual space over which responses can be elicited or modulated are much larger than the other species, even for RFs at similar eccentricities (Li and Li., 1994; Sengpiel et al., 1997; Levitt and Lund, 2002).

Figure 4. Three types of summation responses to an optimal stimulus expanding in diameter. (A) Responses continue to increase with the increasing stimulus diameter possibly beyond the largest stimulus presented. (B) Responses peak then asymptote at the same stimulus diameter. (C) Cell in which responses peak then decrease as stimulus diameter increases. Other conventions same as figure 2 except excitatory Gaussian function is not set to 0.

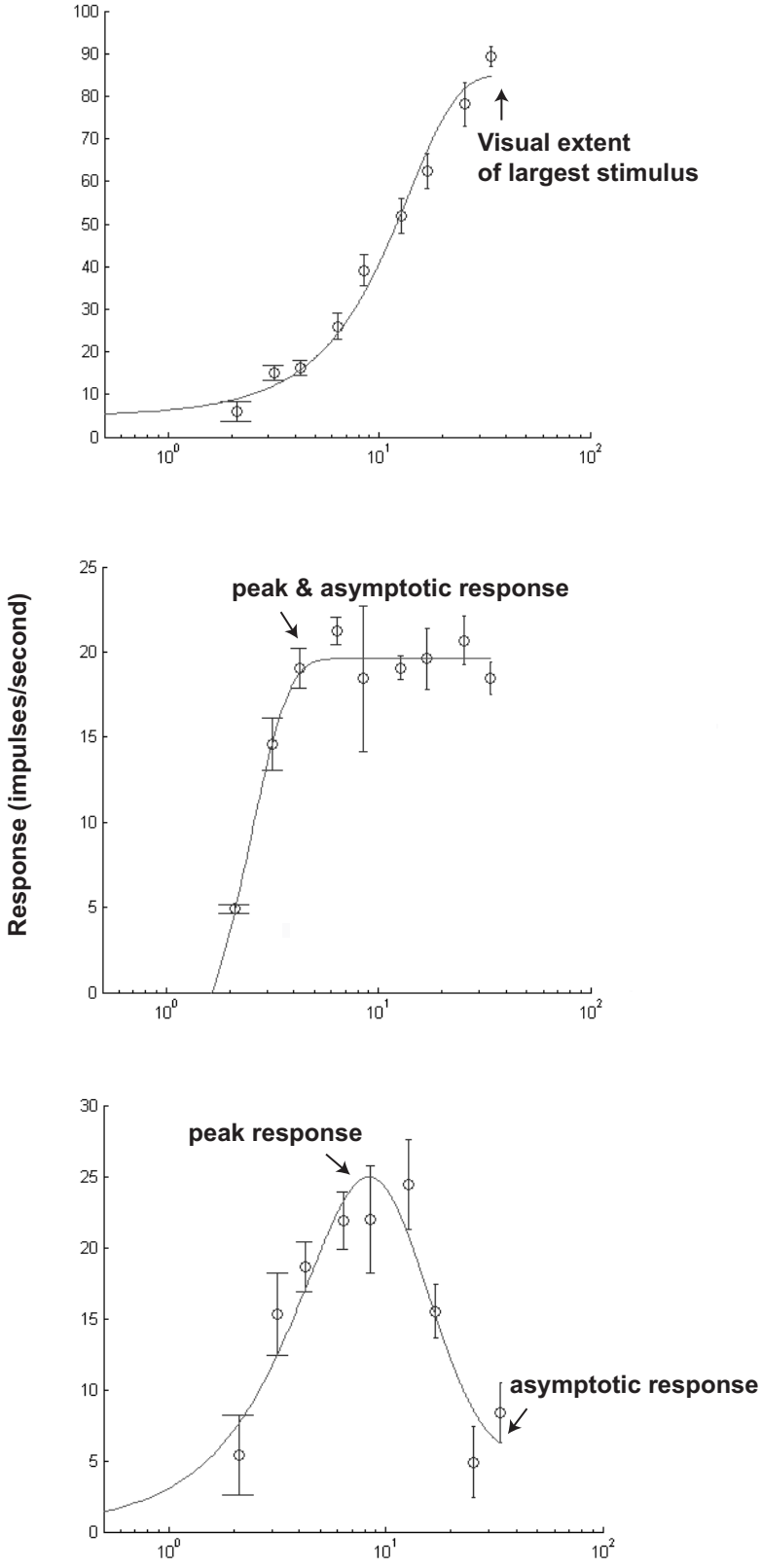
Visual extent
of largest stimulus
peak & asymptotic response
Response (impulses/second)
peak response
asymptotic response

We fit the data using the best fitting difference of integrals of two Gaussians (solid lines) and derive the peak response diameter (PRD), and the asymptotic response diameter (ARD). This is the dimension of the stimulus at which we considered the responses to have stabilized, and therefore to be the maximal spatial extent of integration of that cell. We also determined a suppression index (SI), which describes how strongly the surround suppresses the response of a cell. Figure 5A shows the population distribution of the PRD (range= 3.7°- >35.5°, mean = 25°±1.0, median=27.9°). Figure 5B shows the ARD (range=5.2°- >35.5° mean = 30.5°±0.8°, median=33.9°) (Fig 5B). Not only are there cells that summate visual information up to 35° in visual space, 28.4% of the cells have responses that do not asymptote. These cells may continue to summate beyond this extent. Therefore the mean PRD and ARD may be underestimates of the actual population means.

The average SI is equal to 0.09±0.02 (Fig. 5C). There appears to be rather fewer surround endstopped cells found in area 17 of ferret than has been reported in cat and primate. Sixty percent of cells have a SI = 0, indicating that they have no surround suppression when the center and surround stimulus match. The mean SI is much lower than that reported in primate (0.6, 0.4, 0.3)(Sceniak et al., 2001; Cavanaugh et al., 2002; Levitt and Lund, 2002).

Figure 5. Bar graphs showing the population distribution of peak summation diameters (A), asymptotic response diameters (B), and the suppression index (C). Conventions same as in figure 3.

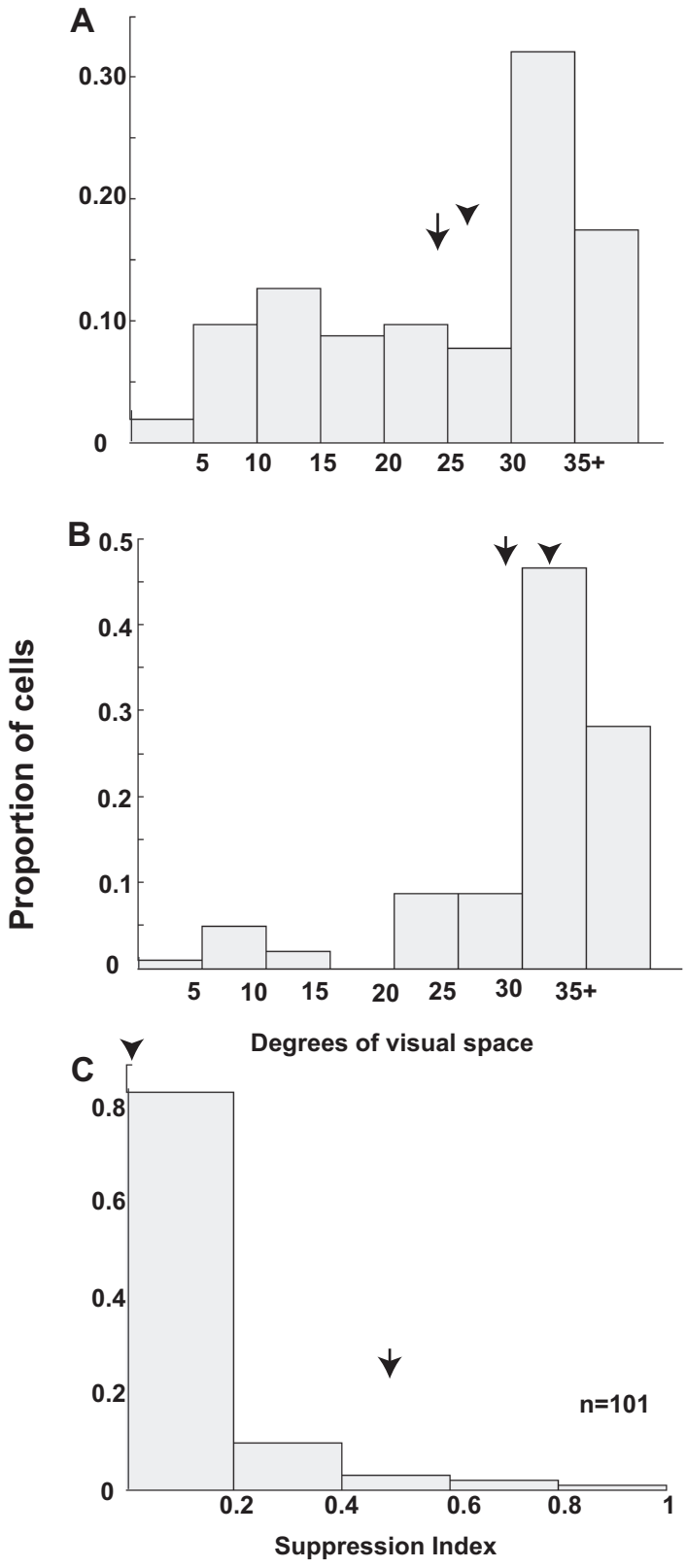
A
0.30
0.20
0.10
0
5
10
15
20
25
30
35+
B
0.5
0.4
0.3
0.2
0.1
0
5
10
15
20
25
30
35+
Proportion of cells
Degrees of visual space
C
0.8
0.6
0.4
0.2
0
n=101
0.2
0.4
0.6
0.8
1
Suppression Index

Comparisons across cortical layers

Cortical layers receive varying afferent inputs that may result in different size summation fields (Lund, 1988; Bolz and Gilbert, 1989). Therefore, we examined if any of the summation properties of cells in area 17 of ferret varyz among layers. Although we were able to assign most cells to a cortical layer (n=97), because of the trajectory of the track we could only determine a relative depth for a subset of 60 cells. Only these cells were included in comparisons made in Figure 6. We found MRF diameters (A), peak summation diameters (B) and asymptotic response diameters were equally distributed across a lamina. There as a slight trend for layers V and VI to contain more cells with smaller PRDs and ARDs than layer II/III (fig. 6B,C). Cells whose responses did not stabilize were included in these comparisons (filled circles). However, we found no significant differences in the sizes of MRFs, PRDs or ARDs when we compared these diameters across lamina using a one-way analysis of variance (n=94). Our data differ from primate. Levitt and Lund (2002) do not report any significant differences of summation field sizes across layers. However, they do report a trend that larger fields are located in the lower layers, while Sceniak et al. (2001) found significantly larger surrounds in the deeper layers.

Figure 6. Laminar distributions of minimum response fields (A) peak summation diameters (B), and asymptotic response diameter (C). Dashed lines indicate the relative depth of each cortical layer averaged over six cases. Cortical layers are indicated by numbers to right of graph. In B and C closed circles indicate cells whose responses did not asymptote. Open circles represent cells whose responses asymptoted or had a SI<0.3. Crosses indicate enstopped cells with a SI>=0.3.

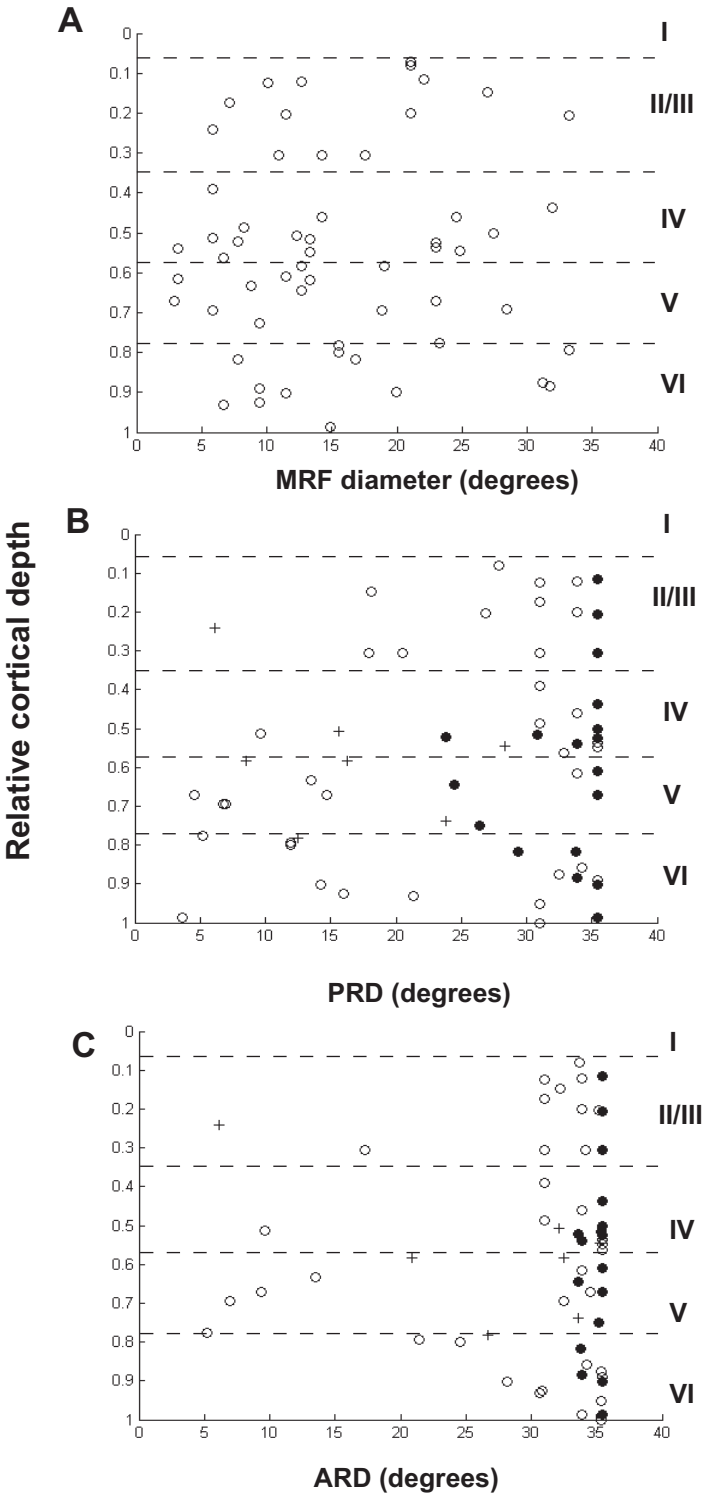
A
I
II/III
IV
V
VI
MRF diameter (degrees)
B
Relative cortical depth
I
II/III
IV
V
VI
PRD (degrees)
C
I
II/III
IV
V
VI
ARD (degrees)

Comparison of summation properties to MRF

To establish if cells summate beyond their MRF, we directly compared the PRD and the ARD measurements to the MRF diameter (Figure 7A, B respectively). Cells whose responses did not asymptote are plotted above the dashed line. There are cells whose PRDs were similar to their MRFs indicated by a large number of points falling near the central diagonal, within the dashed lines in Figure 7A. However, these measures are not significantly correlated and 72% of cells have PRDs that are at least 20% larger than the MRF. This is indicated by the greater number of points in Figure 7A falling above the diagonal compared to the number falling below. This agrees with our findings that on average PRDs are significantly larger than MRFs ($p<0.001$). This indicates that for a majority of cells their responses are facilitated when the surround orientation matches preferred orientation of the cell. This contrasts with the finding in primate where the PRDs were equal or slightly smaller than MRFs (Levitt and Lund, 2002).

DeAngelis et al. (1992) argues that this facilitation is simply subthreshold excitation elicted from more remote regions of the visual field, which is apparent because suprathreshold responses are evoked by the center stimulus. This subthrehold excitation would not be revealed by the method used to measure MRF because the stimulus patch is moved off the center of the RF to different locations across the display screen, as opposed to expanding the stimulus centered o the RF. This makes the MRF a conservative estimate of the classic receptive field (CRF), and may explain why the MRF is smaller than the PRD.

It is unlikely that this trend is due to underestimation of the MRF. Of the 2 measures of the classic receptive field, the MRFs were on average larger than the

asymptotic mask diameters, indicating that the MRFs were slight over estimates of the CRFs. Furthermore, there are 13 cells whose PRDs could be larger than 35° of visual space. If this is the case it would only enhance the trend. The excitatory space constant described by the Gaussian sensitivity function (mean=23.1º± 1.1°) is very similar to the peak summation diameter for most cells. The mean inhibitory space constant is equal to the excitatory, indicating that the spread of the inhibitory influences match that of the excitatory

We also find that the ARD for 94% of cells is larger than the MRF (Fig. 7B). Several ARDs are at least 3 times the size of the MRF. These findings show that ferret area 17 cells can summate information and have surrounds significantly larger than their MRFs ($p<0.001$). This indicates that the actual summation field over which visual inputs are recruited for a large portion of our cells (28.4 %) is beyond 35° of visual space.

Figure 7. Scatter plots of peak summation diameter (A) and asymptotic response diameter (B) compared to the minimum response field. Both the peak response and asymptotic diameters tend to be larger than minimum response field. Points outside of the dotted lines indicate cells that have response diameters that did not stabilize at 35°.

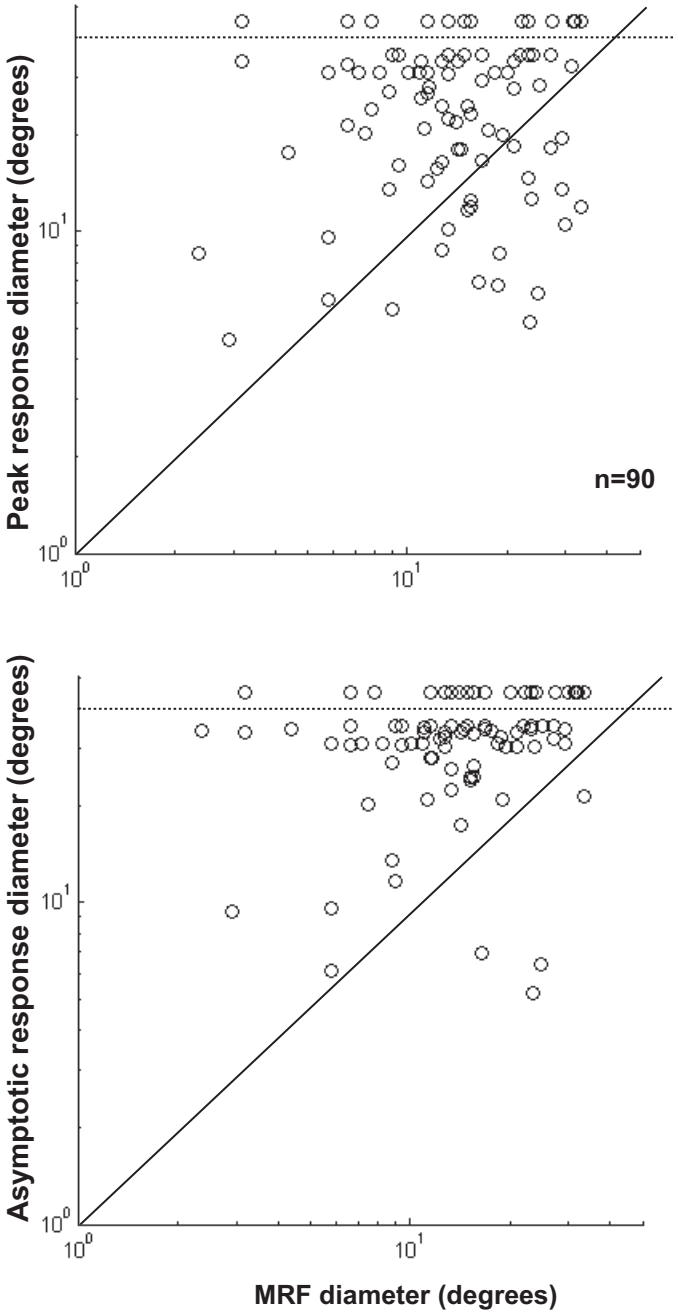
Peak response diameter (degrees)
n=90
Asymptotic response diameter (degrees)
MRF diameter (degrees)

S*urround tuning*

Since we have established that extensive modulatory regions outside the MRF exist in cells in area 17 of ferret, we examined the properties of response modulation elicited from the surround. Only 10 cells have a SI =0.3 (the mean SI found in primate, Levitt and Lund 2002; Cavanaugh et al., 2002). Therefore, there were very few cells whose responses decrease from the peak response when the orientation of the center stimulus and surround stimulus match. All of these cells were located in layers II/III or V. Each cell has a MRF and ARD similar to the population mean. Seven out of ten of these cells have PRDs smaller than MRF. Cells such as these are described in cat by Gilbert (1977) as special complex cells, and were noted in primate by Levitt and Lund (2002).

We were able to test if the surrounds of ferret cells are tuned to orientations other than the cells preferred orientation in a subset of cells (n=28). Only cells that didn't show a response above the spontaneous activity when presented with the surround alone were included in these analyses. In all cases the surround stimulus abutted the center stimulus. Holding the center stimulus constant, we varied the orientation of the surround stimulus. We found both suppressive or facilitatory effects of the surround on the responses of the center alone are weakly tuned for orientation (Fig. 8). In this sub-sample of cells the mean MRF =13.1°±1.6°, which is very close the mean of the MRF of all the cells in this study. Eleven showed surround suppression when the center and surround stimulus matched, although only 2 had an SI larger than 0.3.

Figure 8A is a case showing typical modulatory surround effects of area 17 cells in ferret. This cell's had a small MRF (5.6°), was orientation selective (OI=0), and somewhat direction selective (DI=0.5). When a grating with an orientation 30°and 60°

away from the cell's preferred orientation of 180°, the cell's response fell to about 50% of its response to the center stimulus alone. There did seem to be a directional component since the suppression around the 180° is not symmetrical. Since this cell did show some modulation at every orientation the circular variance (CV) of the surround was relatively high (0.8). This indicates the surround was not strongly tuned. The surround also slightly enhanced the response of the cell relative to the center stimulus alone at 330°, 150° away from the preferred orientation of center. However this effect was very small. Figure 8B shows a case in which the stimulus in the surround oriented at 0°, 120° away from the cell's preferred orientation of 240°, increased the cell's response to the center alone by 20%. This cell had an average size MRF (12.6°), was also strongly selective for orientation (OI=0) and somewhat tuned for direction (DI=0.6). There was less of a directional component since relatively strong facilitation also occured when the surround stimulus is at 120°. As in the other case the surround was weakly tuned for orientaion (CV= 0.8). Each case show similarities to cat; the largest suppression occured at an orientation that flanks the cell's preferred orientation (Fig. 8A), and the presence of a surround enhanced responses at the cell's non-preferred orientation (Fig. 8B) (Sillito et al., 1995; Sengpiel et al., 1997).

The orientation tuning of the surround was not very strong in any of the individual cells examined. The CVs range from 0.6-1.0, and the mean CV is 0.8±0.2. The lack of surround tuning was also seen across the popoulation. There was also no relationship between the difference in orientation between the center and the surround stimulus and strength of modulation arising from the surround (Fig. 8C). Responses of cells could be modulated by very small changes in orientation between the center and surround as well

as very large changes, as opposed to strong inhibition occurring when the orientation of center surround match or strong facilitaion occurring when the surround orientation is orthogonal to the center.

Figure 8. Orientation tuning of the surround. Representative cases of cells' responses to an optimal drifting stimulus placed over the minimum response field paired with a drifting grating placed in the surround. The orientation of the center stimulus was held constant while the orientation of the surround stimulus varied. The cells' preferred orientation is centered along the x-axis indicated by arrow. The solid line indicates the cell's response to the center stimulus alone. Bottom trace represents the cell's response to the surround stimulus only. (A) The strongest surround modulation inhibits the cell's response. (B) The strongest surround modulation facilitates the cell's response to the center alone. C) The difference in responses of cells to the center stumulus and to the center+surround stimulus relative to the difference in orientation between the center stimulus and the orientation of the surround. Filled circles represent the cells whose strongest modulatory surround effect is facilitation of the response to the center alone. Open circles represent cells whose strongest surround modulatory effect is inhibition of the response to the center alone. Error bars = s.e.m.

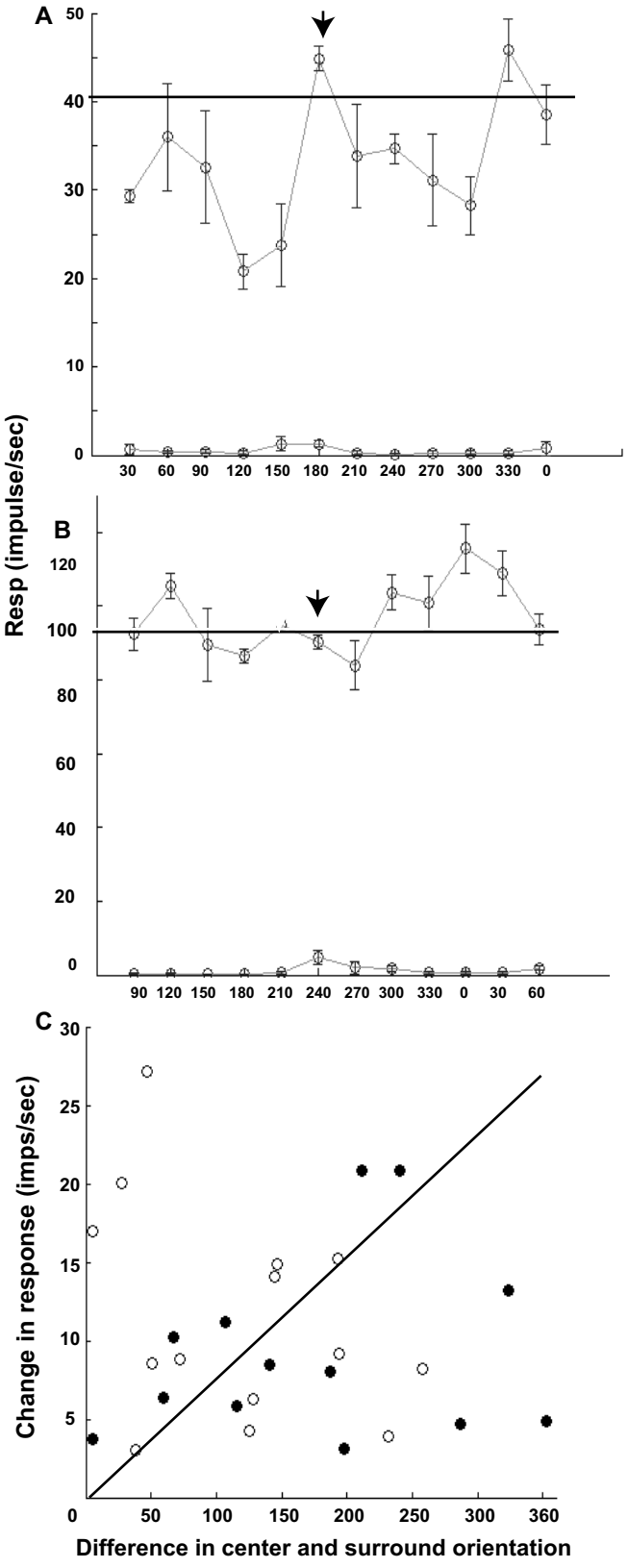
A
B
C
Resp (impulse/sec)
Change in response (imps/sec)
Difference in center and surround orientation
30 60 90 120 150 180 210 240 270 300 330 0
90 120 150 180 210 240 270 300 330 0 30 60
0 50 100 150 200 250 300 360

Comparison to anatomical data

One of the goals of this study was to establish which anatomical substrates could possibly underlie the summation fields extending beyond the classic receptive fields of area 17 neurons. We determined the extent of visual space that converges onto an extent in space the size of an average MRF of a cell in area 17 through intrinsic or feedback connections (Fig. 9A). The ARFs are values taken from anatomical studies in which restricted injections of the neuronal tracer Cholera Toxin Beta subunit (CTb) were made into locations area 17 that respond to central fields (Cantone et al., 2005). The ratio of the ARFs of intrinsic connection shows that twice the amount of visual space is converging onto a single locus in area 17 through intrinsic connections. This amount of convergence is enough to account for the average peak response diameters and the amount of visual space over which area 17 neurons can integrate information average. Therefore, for the majority of the cells we tested these intrinsic connections can account for extent from which surround modulation arises in ferret area 17 cells. For the other subset of cells that summate information beyond 35° of visual space, feedback connections may be able to account for the summation properties. Almost 4 times the amount of visual space is converging onto the ARF of a restricted locus in area 17 through feedback connections. However, the actual extent of their summation fields remains unknown based on this study.

Figure 9. Comparison of retinotopic precision of cells monosynaptically linked to a single locus in area 17 to the summation properties of area 17 cells. Ratios of the ARFs of cells providing intrinsic connections and cells in extrastriate areas providing feedback connections to a restricted locus in area 17 with an ARF equal to the average MRF. Arrows indicate the ratios comparing the ARD and PRD to the MRF.

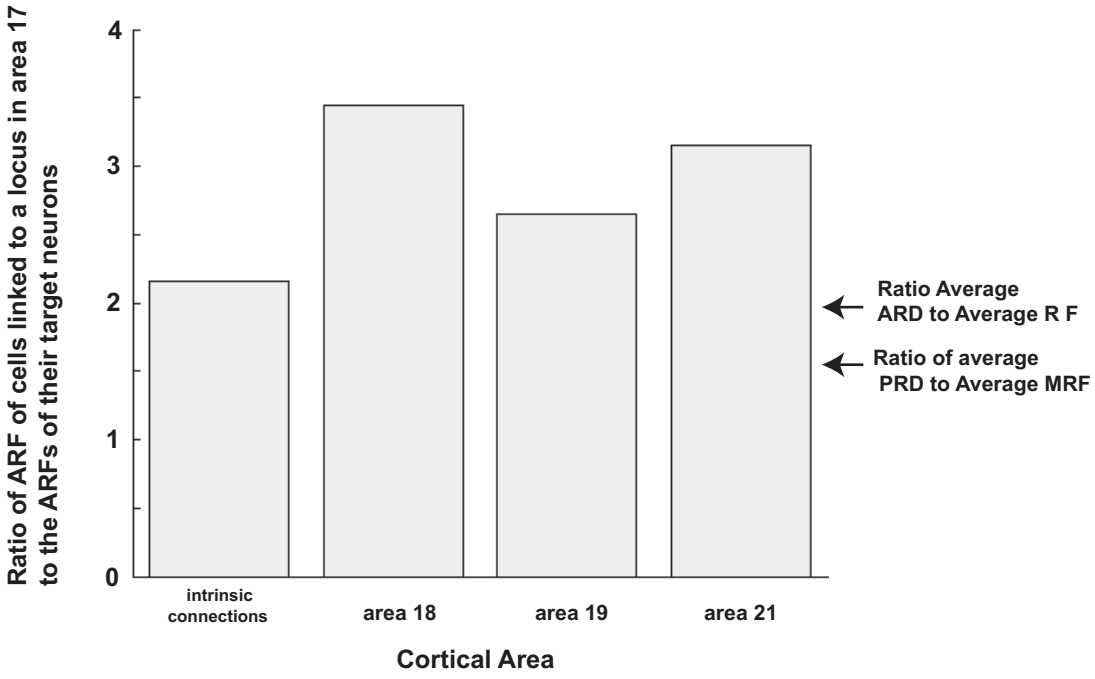
Ratio of ARF of cells linked to a locus in area 17
to the ARFs of their target neurons
4
3
2
1
0
intrinsic
connections
area 18
area 19
area 21
Cortical Area
Ratio Average
ARD to Average R F
Ratio of average
PRD to Average MRF

3.4 DISCUSSION

Summary

Using high contrast drifting grating stimuli we find that the minimum response fields (MRF) of cells, most within the central 20° of visual space, vary greatly in size (1.66° to >33° in diameter). Many MRFs have more than one locus of peak activity. A majority of these cells have summation fields considerably larger than their MRF. MRFs, peak response diameter (PRD) and asymptotic response diameters (ARD), or summation field of all sizes can be found across all cortical layers. We find the effect of the surround on the cells' responses to stimuli within the classic receptive field can be facilitatory and inhibitory. The modulatory surrounds are not strongly tuned for orientation. Neurons in area 17 derive their summation fields from both intrinsic and feedback connections.

Methodological considerations

The summation fields can span large extents in visual space, with 28.4 % of cells showing responses that do not stabilize at the maximum stimulus diameter of 35°. Because of this limitation of our measurements the actual full extent of the visual field to which some area 17 cells are influenced remains unclear. Approximately one third (10 out of 28) of the cells that did not stabilize showed some suppression in response to an increasing stimulus diameter. We find that the excitatory space constant we derived is much larger than what the above studies report in primate. We also find that the mean inhibitory space constant is equal to the excitatory space constant. Since we find both space constants to be equal and weak surround inhibition, it is probable that the inhibitory space constant is not constrained in the fit by the data. This could result from not being

able to measure the full summation field of all cells. This can also explain the low suppression indexes. If ferret is similar to primate in that inhibitory influences arise from a greater region of visual space than the excitatory regions (Sceniak et al., 2001; Cavanaugh et al., 2002; Levitt and Lund, 2002), then it is likely that we are not seeing any endstopped cells because of the limited stimulus size. The responses of cells could continue to be influenced by inhibitory inputs from more remote regions of the visual fields that would continue to decrease, and thus, increasing the suppression index.

It may also be the cases that propofol, the anesthesia used, could be extinguishing the inhibitory input to the cell. Ramoa et al. (1988) report inactivation of GABAergic inhibition in cat results in an increase in receptive field size from 10° to 30° of arc. The lack of inhibitory influence could account for both the large receptive field size and the lack of suppression. Propofol is commonly used in studies of this type in cat (Samonds et al., 2003), one of which specifically looks at inhibitory influences involved in surround suppression (Brown et al., 2003). It is unlikely at propofol can abolish inhibitory influences to that extent in ferret. In addition we do find cells that show suppression. Therefore, inhibitory influences exist, just not in many cells.

We must also consider the accuracy with which the difference of Gaussian (DOG) model describes our data. It assumes that both the excitatory and inhibitory influences decrease uniformly with distance from the center. We find that for some cells in our sample this not true because they do not have a single central point of peak excitation with responses falling uniformly from the center. Anderson et al. (2001) found that the excitatory membrane currents decreased with distance while inhibitory increased, with

neither decreasing uniformly with distance from the center. In cat, Bringuier et al. (1999) also reports that the field of depolarization, and hyperpolarization were patchy and 'subfields' were separated from the center of minimum discharge field. They also report that the underlying excitatory influences on a cell arise from a wider extent in the visual field than the inhibitory influences, which is in agreement with Das and Gilbert (1995). As suggested by Sengpiel et al. (1997), the latter studies would predict that the large patch gratings would elicit a facilitatory surround effect when the diameter a uniform optimal patch of grating is increased. We do find this for the majority of our sample. The PRDs are larger than the MRFs, indicating excitatory influences are elicited from the surround. Therefore, despite the differences among the possible underlying influences forming the summation fields of cells, the DOG model does provide a description of our data that is predicted by other studies.

Minimum response fields

The most salient feature of the MRFs in area 17 of the ferret is their size. They are much larger than what is reported in both monkey and cat (DeAngelis et al., 1992; Li and Li, 1994; Sengpial et al., 1997; Sceniak et al., 2001; Cavanaugh et al., 2002). This could be because MRF were pooled over larger eccentricities. However, the MRFs of a peripheral calcarine sample still spanned less than 10° of visual space (Levitt and Lund, 2002). Because large RFs are common and easily accessible, ferret is a good model in which to expand the types of studies that examine center- surround interactions. In this study and previous ones, the center is defined as extent in visual space from which responses can be elicited relative to single receptive field center, and the surround lies

outside of that boundary (Sceniak et al, 2001, Levitt and Lund, 2002, Angelucci et al., 2002b, Bair et al., 2003). Chisum and Fitzpatrick (2004) suggest that because the underlying circuitry of these interactions is continuous, the center surround regions should not be considered discrete regions of the visual field. They argue that studying the interactions of different regions within the center or with stimuli that span the center and surround may provide information that is more applicable to understanding how the visual system processes natural scenes. The RFs of more extensively studied species are often too small to look at these types of interactions (Chisum and Fitzpatrick, 2004). The larger RFs in ferret do not have this limitation.

In addition to being larger, many MRFs have the sub regions of high activity separated from the center of the MRF by regions of lower activity. These differences in underlying excitatory or inhibitory influences reflect subthreshold depolarization and hyperpolarization reported in other species (Anderson et al., 2001, Bringuier et al., 1999). In ferret, integration of these influences can be seen in suprathreshold responses. This allows for investigation of interactions of different sub-fields within the center of the RF using the spike activity, which represents the response properties of neurons that cannot always be predicted by membrane potentials

Modulatory surround tuning

In ferret, facilitation is most often seen when the surround stimulus is presented with a similar orientation to the cell's preferred orientation. This facilitation has been well documented in other species (Maffei and Fiorentini, 1976; Nelson and Frost, 1985; Li and Li, 1994; Polat and Norcia, 1996; reviewed in Fitzpatrick, 2000). Sengpial et al.

(1997) found no facilitatory effects from the surround. They attributeted their findings to the fact that included the region encompassed by the PRD as part of the RF field. We use the same parameter when testing for influences from the surround and do find facilitatory effects. Because stimuli placed in this region alone don't elicit responses on their own, we consider them surround effects.

The orientation tuning of surrounds of individual cells in ferret does differ slightly from other species. Gilbert and Wiesel (1990) report more suppressive effects when the center and surround orientations match. However, they also report that in general the orientation tuning of the surround is broad. Our findings differ greatly from studies in primate. The surrounds of individual cells are highly tuned for orientation, with most of the facilitatory effects are seen when the orientation of the center and surround stimulus don't match, and suppression when the two stimuli do match (Knierim and Van Essen, 1992; Sillito et al., 1995; Levitt and Lund, 1997). Our data suggest that the most common surround effect described in other species, inhibition when the center and surround stimulus match in orientation, is not as common in ferret. Many cells in our sample have responses that asymptote without decreasing when the center stimulus diameter is increased beyond the MRF. However we find that many responses of cells are not modulated by stimuli placed in the surround if they match the center stimulus; rather surround inhibition can occur when the surround stimulus is at varying orientations relative to that of the center stimulus. Therefore, surround inhibition may be as common in ferret but just not as obvious since it is not manifesting itself as in other species. Therefore, different types of investigation maybe need to fully understand these effects in this species, or as suggested above our stimlus was not laege enough to reveal the ful

extent of surround inhibition.

Laminar differences

In ferret there is no evidence that the receptive field sizes or summation field sizes differ significantly across the cortical laminae. One would expect to find some differences in layer 6, since receptive fields of neurons in layer 6 have been found to summate more extensively than cells in the other layers (Sceniak et al., 2001, Bolz and Gilbert, 1989). The horizontal connections, described in anatomical tracer studies in ferret, form a patchy spread similar to cat and primate. It is more extensive in upper layers than in layer 4 or lower layers 5 and 6 (Lund, 1973; Gilbert and Wiesel, 1979; Rockland et al., 1982; Rockland and Lund, 1982; Rockland, 1985; reviewed in Lamme et al., 1998). So there would be some size differences in summation properties between upper and lower layers expected if intrinsic connections underlie surround effects. We may expect to see larger peak summation diameters or asymptotic diameters in the upper layers, compared to those in layer 4, 5 and 6. However, we find that known differences in connectivity between layers are not reflected in summation properties of area 17 cells.

Possible anatomical substrates of summation

There is a subset of cells for which feedback connections arising from extrastriate areas are more likely anatomical substrate because intrinsic connections cannot account for there summation field (Angelucci et al., 2002b, Sceniak et al., 2001; Cavanaugh, 2002). To determine the surround properties of these cells more studies must be done. As

with other studies intrinsic connections do appear to be a plausible underling circuit for most of our sample (for review see Chisum and Fitzpatrick, 2004). Long-range horizontal connections arising from pyramidal cells that are recruited in the facilitatory surround effects link cells along a colinear axis in the map of visual space and link neurons with similar orientation preferences (Gilbert and Wiesel, 1989; Malach et al., 1993; Fitzpatrick, 1996, Bosking et al., 1997). Therefore, these are most likely underlying the response properties of cells that have peak summation diameters larger than the MRF. Although these same connections are also associated with inhibitory surround effects, pyramidal cell connections are excitatory; therefore they are believed to recruit either local or long range GABAergic cells in order to produce inhibitory surround effects (Maguire et al., 1991; Hirsch and Gilbert, 1991; Lund et al., 1995).

Our physiological data do not reflect the general properties of underlying intrinsic connectivity reported in ferret. The intrinsic anatomical connections and functional properties reported in cat and primate such as columnar organization, orientation and other functional maps, horizontal connections that mediate both excitatory and inhibitory synaptic interactions between orientation columns and across large extents in cortex are present in ferret (Rockland, 1985,Weliky et al., 1995; Tucker and Katz, 2003, Roerig and Chen, 2002; White et al., 2001; Chen et al., 2005). Therefore, one would expect the surround effect should be tuned for orientations. All the cells for which we have surround data have a summation field for which the extent in visual space to which cells linked by intrinsic connections can account. However, since these surrounds lack strong tuning there seems be no obvious pattern of recruitment of cells with a particular orientation preferences through horizontal connections.

There are small differences between ferret, cat and primate that may account for this lack of tuning. The patchy or lattice spread is similar between cat and ferret, but lack a bilaminar distribution in layers II-III and 4B, and have a simpler geometric patchy formation than what is found in primate (Rockland, 1985, Rockland and Lund, 1983). Physiological studies report the magnitude of orientation preference is much lower in ferret compared to that in cat, and that there is greater overlap between orientation domains (Rao et al., 1997). Therefore, because ferret cortex lacks these features, intrinsic connections may not capable of producing well tuned modulation arising from the surround.

Input from the Lateral geniculate nucleus (LGN) also seems to have an indirect role in surround modulation in both cat and ferret (Hirsch, 1995; Ozeki et al., 2004). Ozeki et al. (2004) report that surround stimuli used for area 17 neurons suppress the LGN input to cortex in cat. Thus, the surround inhibition may be because of a lack of excitatory thalamic inputs. Hirsch (1995) also reports that integration of afferent input from cortical cells and from the thalamus can produce strong and non-linear inhibitionwhich may result in surround inhibition. It is unlikely, however, that the LGN inputs are directly influencing the surrounds because inputs in ferret are strictly retinotopic and cannot account for the summation fields of area 17 neurons (Cantone et al., 2001; 2002).

The pattern of feedback projections seems to be governed by the orientation preference of the cells from which they arise (Shmuel et al., 2005). However, Stettler et al. (2002) argue that the feedback connections in primate are too diffuse, and do not terminate in clusters associated with orientation columns in area 17

(Gilbert and Wiesel, 1979). Therefore, they cannot account for the tuning properties of surround effects. The lack of surround tuning in ferret could be a result of feedback connection having a role in the surround effects of cells with smaller summation fields. Although it is possible that these surround effects may be tuned for other functional properties, these findings also imply that both types of connections may be retinotopically based and can only provide input to a cell that would extend the area of the summation zone. Thus, the integration of visual space through both intrinsic and feedback connections in ferret cortex may be necessary for more global top-down influences as opposed to specific contextual effects.

CHAPTER 4: RETINOTOPIC ORGANIZATION OF FERRET SUPRASYLVIAN CORTEX. (This manuscript is under final revisions for resubmission to Visual Neuroscience)

4.1 INTRODUCTION

Several visually responsive areas in ferret (*Mustela putorius furo)* cortex are known to be retinotopically organized. These areas differ in the extent of visual space represented, the amount of cortex devoted to the representation of different locations of the visual field, and in the irregularities and coarseness of the representation (Law et al., 1988; Manger et al., 2002a,b, 2004). These differences in topography may reflect functional differences among areas, and affect the influence a given area has over response properties of cells in other brain regions to which it connects. Assessing retinotopy is the first step in assessing functional roles of each area. Suprasylvian cortex in ferret (Ssy) is a visually responsive extrastriate area (Innocenti et al., 2002; Manger et al., 2002a) that is not yet fully described.

Electrophysiological studies suggest that receptive fields are larger in Ssy than in area 17 (White et al., 2002; Manger et al., 2002a). It is therefore possible that cells in Ssy providing feedback connections convey signals from larger regions of visual space than their target neurons in lower areas, as reported for extrastriate areas of cat, monkey, and ferret (Salin et al., 1992; Angelucci et al., 2002; Cantone et al., 2005). However, the retinotopic organization of Ssy must be established to confirm the retinotopic precision of feedback connections from this area.

Here we use electrophysiological mapping to define the representation of the

visual field in Suprasylvian cortex as a comparison to that in striate and other extrastriate areas of ferret cortex. We also use injections made into Ssy of the neuronal tracer Cholera Toxin b subunit to confirm this representation by examining the relationship of connections to the retinotopy of area 17. Portions of this work have appeared previously in abstract form (Cantone et al., 2003).

4.2 MATERIALS AND METHODS

Nine adult female ferrets (*Mustela putorius furo*) (0.56-0.95 kg) were studied. All underwent terminal electrophysiological mapping experiments. Two of these animals also underwent anatomical injection experiments. All procedures conformed to National Institutes of Health guidelines. Methods for general surgical procedures, electrophysiological recording experiments, general histology and anatomical tracer injections are the same as described in Chapter 2. Only methods that are specific to these experiments are described here. CTb injections were made into Ssy.

Electrophysiological recording

Penetrations were separated by 250-1100 μm. The size and location of single and multiunit minimum response fields were plotted in azimuth and elevation relative to the *area centralis.* This was done by hand using light or dark oriented lines. At the end of the recording session electrolytic lesions were made by passing 4 μA anodal current for 5-10 seconds. Animals were then euthanized with an i.v. overdose of sodium pentobarbital.

Reconstruction of retrogradely labeled cells

Outlines of tangential sections containing CTb label were traced, and retrogradely labeled cells were plotted using the Neurolucida tracing and reconstruction program (MicroBrightField, Inc.). Injection cores were defined as uniformly dense regions of CTb label. The tracings of CTb labeling were superimposed onto adjacent CO and myelin stained sections to determine if CTb injection cores were restricted to Ssy, and if CTb labeled cells were located in area 17. Radial blood vessels, lesions and sulcal patterns were used for alignment. We referred to previously published retinotopic maps of area 17 (Law et al., 1988; Manger et al., 2002a) to determine the retinotopic location of the retrogradely labeled cells in area 17.

Reconstruction of recording sites in Ssy

Since all of our recordings and the injections were made on the exposed surface of Ssy, tangential sections provided a better view and simplified the reconstruction of the maps. Partially flattened tangential CO and myelin stained sections were traced using Neurolucida. Tracings of serial sections were aligned using lesions, and then CO and myelin stained sections were overlaid. The areal borders of Ssy were outlined using anatomical features revealed by both stains. To determine the areal extent of Ssy, the area within the traced outline was directly measured using NeuroExplorer (MicroBrightField, Inc.). Lesions were used to calculated shrinkage corrections that were applied on a case-by-case basis (average shrinkage = 8 %). Individual maps were constructed by plotting recording sites onto traced serial reconstructions at anterior-posterior and mediolateral coordinates relative to the positions of the lesions. The retinotopic location of each receptive field in azimuth and elevation was determined, and was assigned to the

corresponding penetration sites.

Calculating cortical magnification factors

Within Ssy, magnification factors (MFs) were determined separately for visual axes representing azimuth and elevation by calculating the difference in degrees of azimuth and elevation of the receptive field (RF) centers recorded at adjacent penetration sites. The coordinates of the midpoint between these pairs of RFs were used to compare MFs with eccentricity in azimuth and elevation. RF centers less than 3° apart in azimuth or elevation were considered to lie at the same azimuth or elevation respectively; we estimate this to be the accuracy with which we could define RF centers. The distance in cortex (millimeters) between adjacent penetration sites was divided by the distance in visual space (degrees) between the centers of the corresponding receptive fields. MFs were calculated using the following equation from Daniel and Whitteridge (1961):

MF = millimeters in cortex/degrees of visual space (1)

Our main interest was to obtain complete maps across the entire Ssy. Given the extent of the area, laminar differences in MF were difficult to assess. Although we did not systematically investigate receptive field scatter down a cortical column, we did not observe any obvious change in RF position at different depths.

Interpolation of retinotopic maps

Because of the coarse retinotopic organization in Ssy we could not generate maps

using lines of best fit between receptive field locations at adjacent recording sites as described in Allman and Kaas (1971). Therefore we used a modified version of the method developed by Maunsell and Van Essen (1987), and used by Sherk and Mulligan (1993) for extrastriate areas containing disorderly representations of the visual field. A grid with 250 μm X 250 μm squares was drawn over the reconstructions of recordings in Ssy. Relative to each grid square a line was drawn connecting adjacent penetration sites to each other that were within a 1 mm radius of the center of the grid square. The MF between the two sites was calculated. All receptive fields were included as we did not wish to exclude sites falling along isoazimuth or isoelevation lines. If the line connecting the penetration sites crossed a grid square then the center point on the portion of the line segment that fell within the grid square was determined. The distance in cortex between that point on the line segment and the closest of the penetration sites of a given pair that the line connected was divided by the MF. This gave us the distances in degrees of azimuth and elevation from the point within the square along the line that connected the recording sites and closest recording site. This distance in visual space was then added to the value of azimuth or elevation of the RF center corresponding to the respective recording site. If RF positions reversed in visual space then these distances from the point within the square were subtracted from the RF position at the recording site. The resulting coordinates were considered to be the location in visual space to which the location in cortex within the square responds. For example if one penetration site in a pair had a RF center located 20° of elevation along the HM, and the RF center at the second site was located at 10° of azimuth along the HM, a point within a grid square that fell midway between the 2 penetrations would respond to 15° of azimuth and 0° of elevation.

This method resulted in most squares of the grid having several interpolated values of azimuth and elevation. These values were averaged to find the mean retinotopic location within each grid square. These mean values of azimuth and elevation for each square were used to generate contour maps in Matlab. The numerical values in azimuth and elevation of the contour lines were then expressed as relative retinotopic distances from the VM and HM, respectively.

This method does smooth the retinotopic representation and can be inaccurate if there are several large discontinuities in the representation of the visual field. Maunsell and Van Essen (1987) defined discontinuities in the maps as adjacent penetration sites with nonoverlapping RFs. Since 3° is the accuracy with which we were able to map fields, we modify this criterion and consider RFs whose borders are separated by less than 3° to be overlapping. We found few discontinuities in each of the cases mapped with penetration sites separated by 400 μm. Another consideration is that this method does not account for reversals of azimuth in the representation of the visual field. We tried to account for this by using only closely spaced recording sites that were within a 1mm radius from the center of the grid square crossed by the line connecting the sites. Since there is only a weak relationship between MF and eccentricity we feel a linear interpolation provides reasonably accurate maps. Despite these considerations, the maps generated from this method are consistent with recording data.

Figure 1. Photomicrographs showing anatomical characteristics of Suprasylvian cortex (Ssy) in tangential sections. Areal boundaries (dashed lines) evident in tangential sections across upper layers of cortex after staining for myelin (A) and cytochrome oxidase (B). Dashed box in inset represents enlarged areas shown in A, B. SSyS = suprasylvian sulcus; LS = lateral sulcus; A1 = auditory cortex; LT= lateral temporal areas. LS = lateral sulcus; D = dorsal; P = posterior. Scales = 1 mm.

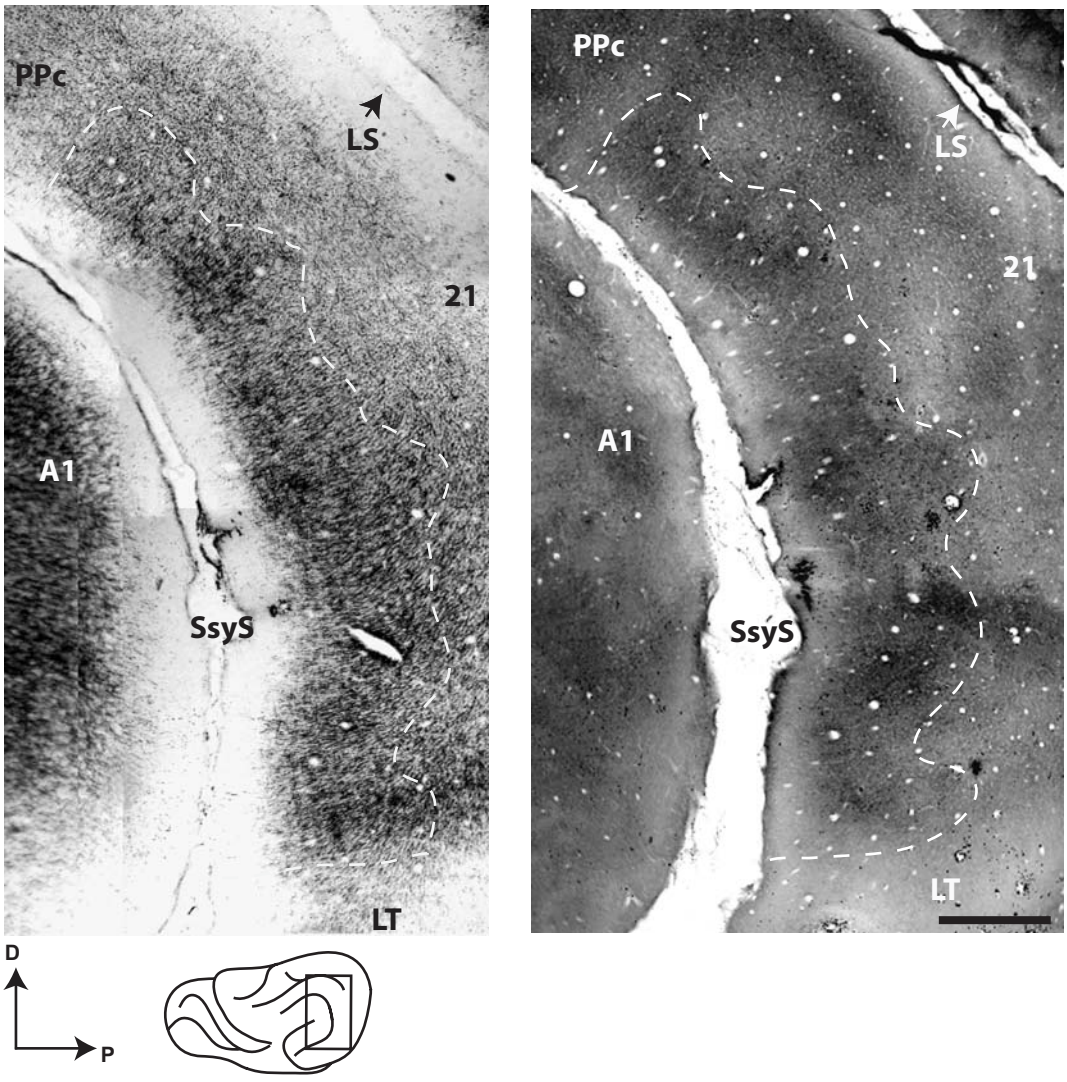
PPc
LS
21
A1
SsyS
LT
PPc
LS
21
A1
SsyS
LT
D
P

4.3 RESULTS

Size and boundaries of Suprasylvian cortex

Suprasylvian cortex (Ssy) occupies on average 8 mm^2, spanning approximately 2 mm rostrocaudally and 4 mm mediolaterally along the posterior bank of the suprasylvian sulcus (SsyS), on the suprasylvian gyrus rostral to visual area 21. It borders the caudal posterior parietal area (PPc) laterally, and lateral temporal visual areas PS (posterior suprasylvian) and 20b medially. Although a small portion lies within the suprasylvian sulcus, the majority of Ssy is on the exposed cortical surface.

Ssy can be distinguished from adjoining areas in tangential sections across the upper layers (II/III) of partially flattened cortex (Fig. 1A, B). There is an increase in staining for myelin and cytochrome oxidase (CO) in Ssy as compared to PPc, PS, and areas 20b, and 20b. In myelin stained sections the change from radial fasical to tangential fibers can be seen at the transition from area 21 to Ssy. These anatomical distinctions are also described by Innocenti et al. (2002) and Manger et al. (2002b, 2004). Despite the curvature of cortex, the difference in staining and distinct lamination can be seen in Ssy in the parasagittal plane of near adjacent sections. All of these histological stains reveal that all cortical layers become thinner at the rostral border of Ssy (Fig. 2). Although myelination is denser in Ssy, the thin radial fascicles seen in area 21 (Innocenti et al., 2002) are not as pronounced (Fig. 2A). The rostral border of Ssy is clearly discernible by the cortical layers being less myelinated. CO staining reveals Ssy contains a greater number of large pyramidal cells in the lower layers, a more prominent band in layer

IV, and darker staining in upper layers than its adjoining areas (Fig 2B). The Nissl stained section reveals more densely packed cells in the upper layers of Ssy than in what is seen in area 21. Innocenti et al (2002) also report that Ssy has larger pyramidal cells in layer III relative to area 21. There are larger pyramidal cells in layer V of area 21 than those found in Ssy. In Ssy layer VI becomes more distinguishable from layer V, which contains loosely packed cells, and becomes slightly thicker compared to area 21.

These anatomical borders correspond to particular receptive field (RF) positions and changes in RF characteristics. Responses become progressively weaker approaching the rostral border of Ssy. At the border cells in cortex become unresponsive to visual stimuli. In PPc, responses are weaker than those in Ssy. The representation of peripheral azimuths (beyond 20° from the vertical meridian) and elevations within 20° of the horizontal meridian (HM) are represented at the border between Ssy and PPc. RFs dramatically increase in size in areas PS and 20b. In most cases peripheral fields are represented at the border between Ssy and the lateral temporal areas. However, RFs can in rare cases approach the vertical meridian (VM) in this region. These findings are in agreement with those of Manger et al (2002a,b, 2004). The visual field representation in Ssy appears continuous with that in adjoining areas PPc, PS and 20b. Although the representation of the visual field is variable at the Ssy/21 border and may appear discontinuous at the border with area 21, RFs in the two areas do overlap at this border.

Figure 2. Photomicrographs showing areal boundaries (dashed lines) and distinct lamination of Ssy in parasagittal sections stained for myelin (A) cytochrome oxidase (B) and Nissl (C). Conventions same as in figure. WM = white matter.

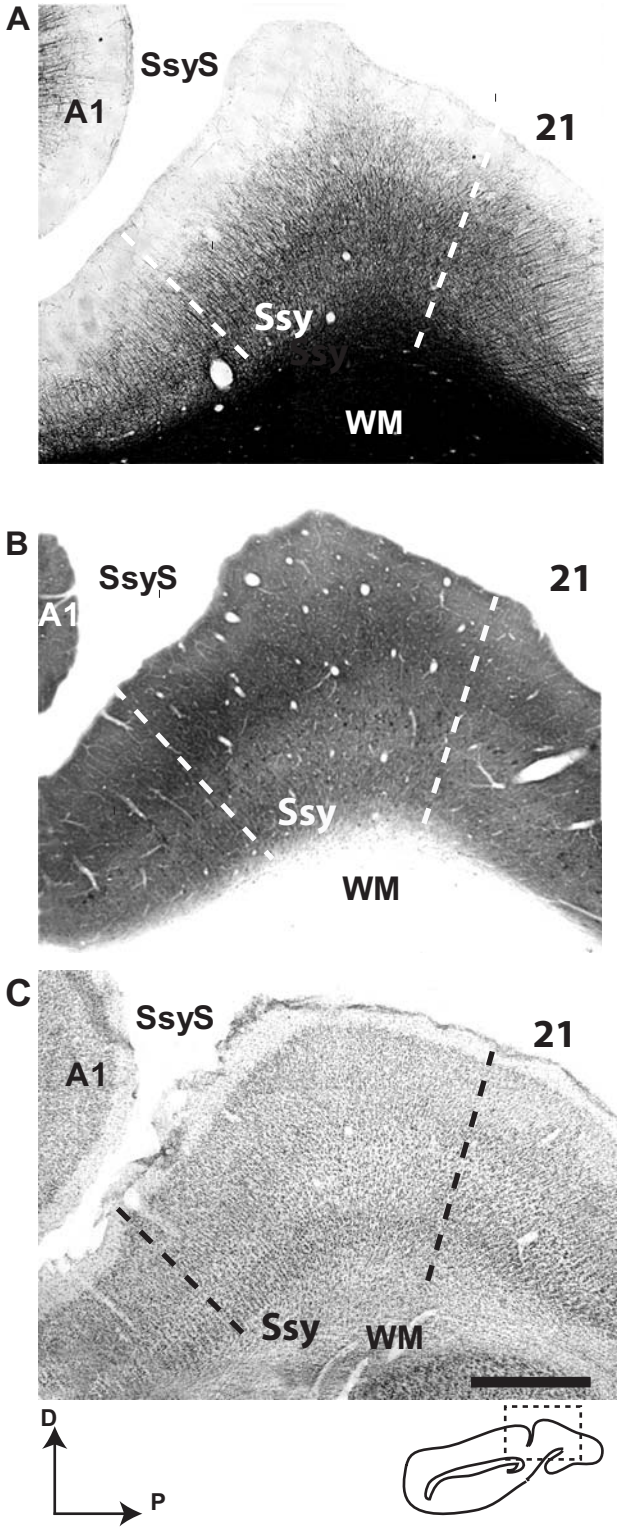
A
SsyS
A1
21
Ssy
WM
B
SsyS
A1
21
Ssy
WM
C
SsyS
A1
21
Ssy
WM
D
P

Receptive fields in Ssy

We found Ssy neurons were generally selective for stimulus orientation, direction, and velocity, with quickly adapting responses (although this may be due to the isoflurane anesthesia). In general, Ssy was less responsive than areas 17, 18, 19 and 21, and contains a representation of the contralateral visual field that varies across animals. The positions of recording sites in cortex and their corresponding receptive fields in three of the most complete mapping experiments are shown in Figures 3-5. In the case shown in Figure 3, the most medial regions of Ssy contain RFs in peripheral locations in the visual field (Fig 4B). Moving laterally, RFs become more centrally located (Fig. 3 C, D) and then reverse back to peripheral locations in the lateral portion of the area (Fig. 3E, F). In the case shown in Figure 4 the RFs show the same general progression through visual space moving laterally through Ssy (Fig. 4B-E). However, in contrast to the case in Figure 4, the RFs we find in the most lateral regions of Ssy are located centrally within the visual field (Fig. 4E).

There are irregularities in the progression of RFs. For example, in Figure 3 the RFs are continuous or overlap as one moves sequentially along each of the rows of recording sites labeled 19-23 and 24-27. However, there is a jump in RF position from upper to lower visual fields between adjacent sites 23 and 24. The case shown in Figure 4 shows the same shift of position in elevation of RFs corresponding to adjacent sites 20 and 21. Thus, there appear to be discontinuities in the representation of visual space in these regions of Ssy. The retinotopic organization is also coarse as a result of locations of RFs centers deviating from a general, continuous progression through the visual field as one moves through Ssy. For example in each of the cases shown in Figures 3E and 4E the

RFs corresponding to recording site 13 seem displaced from those at neighboring sites. There are also cases in which Ssy contains irregularities such that one can move large distances across cortex without moving in the visual field (Fig. 5). In this case, the small number of RFs encountered within 10° of the VM is unlikely due to sampling. The medial region without recording sites corresponds to the injection site described in Figure 6B. RFs recorded at the time of the injection were found to be about 30° from the VM, but are not included in the reconstruction in Figure 5.

Figure 3. Progression of receptive fields (RFs) in Ssy cortex. (A) Location of area Ssy on posterior bank of suprasylvian sulcus (gray area). Dashed square in inset indicates enlarged region in (A). (B)-(E) RFs at different mediolateral locations in Ssy. Numbers indicate penetration sites corresponding to illustrated RFs. RFs at penetration sites outside of Ssy are indicated by dashed squares and gray numbers. RFs are grouped in panels based on recording rows. The SsyS is drawn further rostral to show the entire Ssy. PPc = caudal posterior parietal area; PS = posterior suprasylvian area; 20a = area 20a; 20b = area 20b; 21 = area 21; VM = vertical meridian; HM = horizontal meridian. Scale = 1 mm. Other conventions as figure 1.

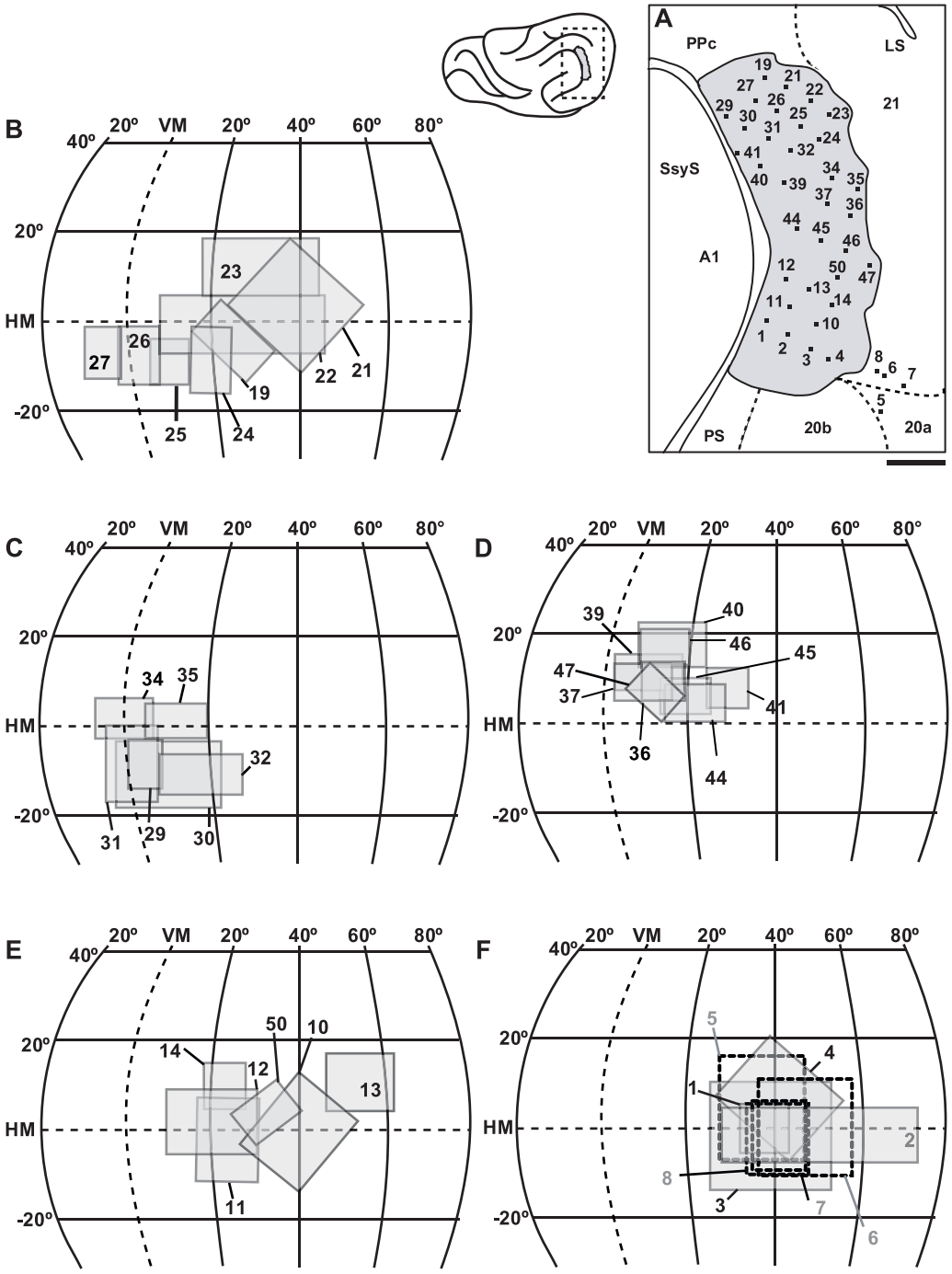
A
PPc
LS
21
SsyS
A1
PS
20b
20a
B
C
D
E
F
VM
HM
20°
40°
60°
80°
-20°

Figure 4. Progression of receptive fields in Ssy cortex in a second case. Conventions as in Figure 2.

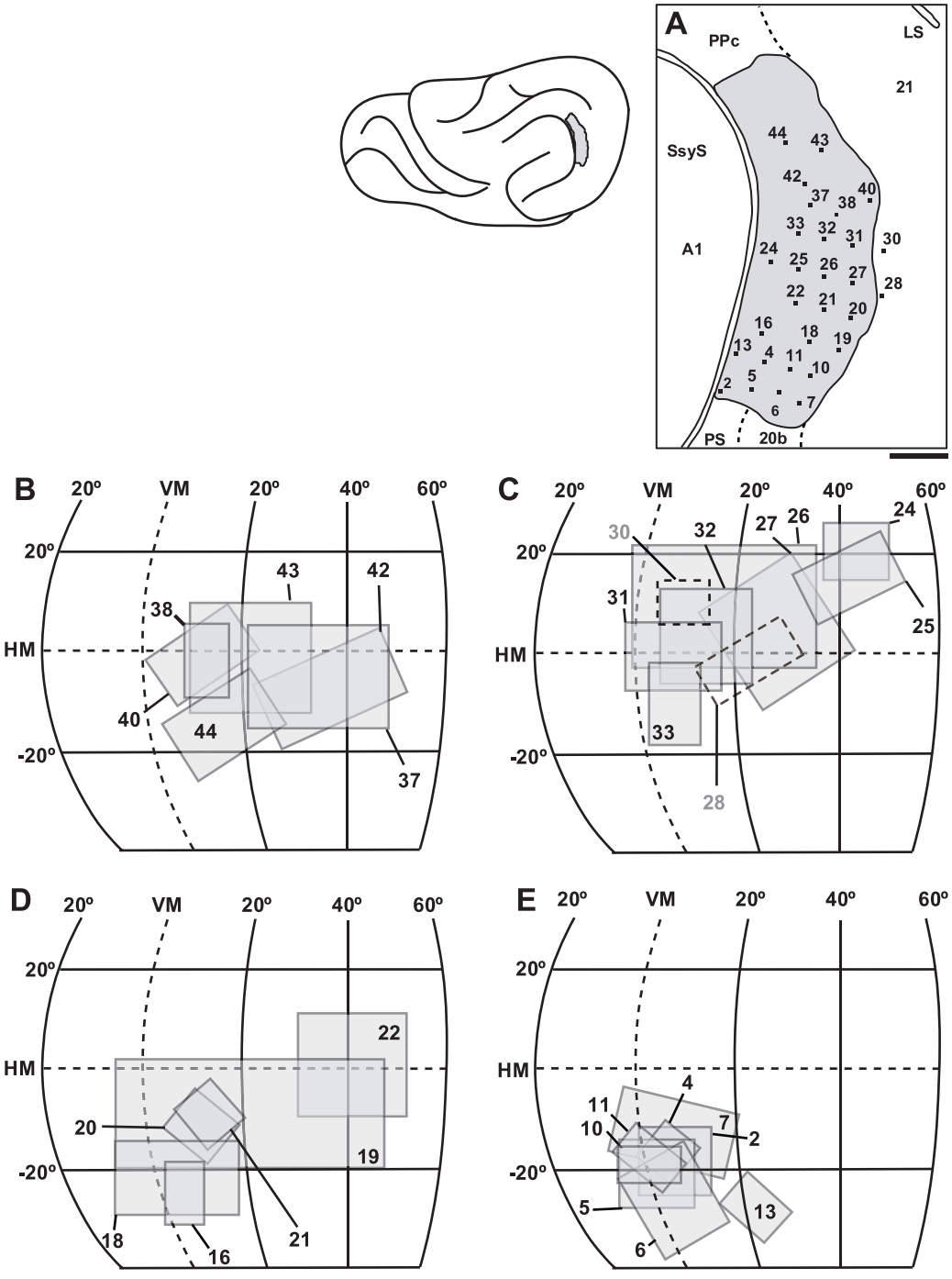
A
PPc
LS
21
SsyS
A1
PS
20b
B
C
D
E
VM
HM
20°
40°
60°
-20°

Figure 5. Progression of receptive fields in Ssy cortex in a third case. Conventions as in Figure 2. Widely separated cortical locations can have overlapping RFs.

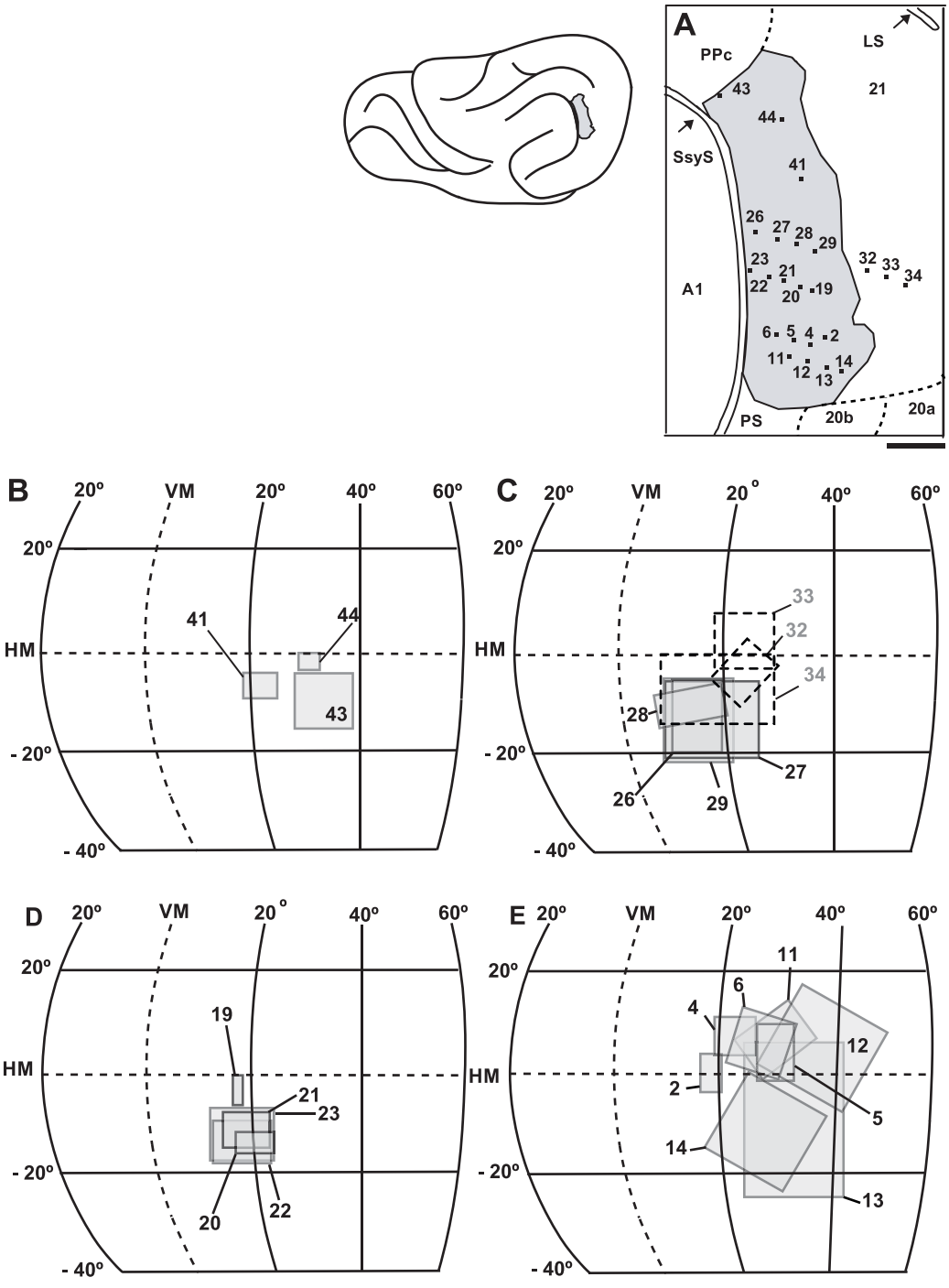
A
PPc
LS
21
43
44
SsyS
41
26
27
28
29
32
33
34
23
21
22
20
19
A1
6
5
4
2
11
12
13
14
PS
20b
20a
B
20°
VM
20°
40°
60°
20°
HM
- 20°
- 40°
41
44
43
C
20°
VM
20°
40°
60°
20°
HM
- 20°
- 40°
33
32
34
28
27
26
29
D
20°
VM
20°
40°
60°
20°
HM
- 20°
- 40°
19
21
23
20
22
E
20°
VM
20°
40°
60°
20°
HM
- 20°
- 40°
11
6
4
12
2
5
14
13

General trends in retinotopic organization of Ssy

We interpolated retinotopic maps for two of the most detailed mapping experiments. The maps shown in Figure 6A and B were derived from the case in Figure 3, while the maps shown in Figure 6C and D were derived from the case in Figure 4. Figures 3 and 4 show the detailed organization of RFs within Ssy for each case. In contrast these interpolated maps plot the average retinotopic location represented at a given location in cortex, and therefore show general trends in the retinotopy. Although the retinotopic organization differs among the animals enough that data from these 2 cases cannot be generalized, there are some similarities across cases that these maps illustrate. Six of nine cases have a retinotopic organization reflective of that in the case shown in Figure 6A and B. Peripheral azimuths are represented in the most medial and lateral regions. Central fields are represented in the middle portion of Ssy, spanning the full rostrocaudal extent of Ssy (Fig. 6A). Elevations within 15° of the HM dominate the visual field representation, with more of Ssy devoted to upper fields (Fig. 6B). Retinotopic organization in 3 of 9 cases resemble that shown in Figure 6C and D. Peripheral azimuths are represented midway along the SsyS. Isoazimuth lines progress to more central locations in visual space as they approach the medial, caudal and lateral borders of Ssy. Most of the area is dedicated to lower visual fields (Fig. 6D).

Figure 6. Interpolated retinotopic maps in Ssy. Representation of isoazimuth lines (A) and of isoelevation lines (B) for the case shown in Figure 2. (C and D) show the representation of rekative distance in visual space from the HM and VM isoazimuth and isoelevation lines for the case shown in Figure 3. Scale = 1 mm. other conventions as in Figure 1.

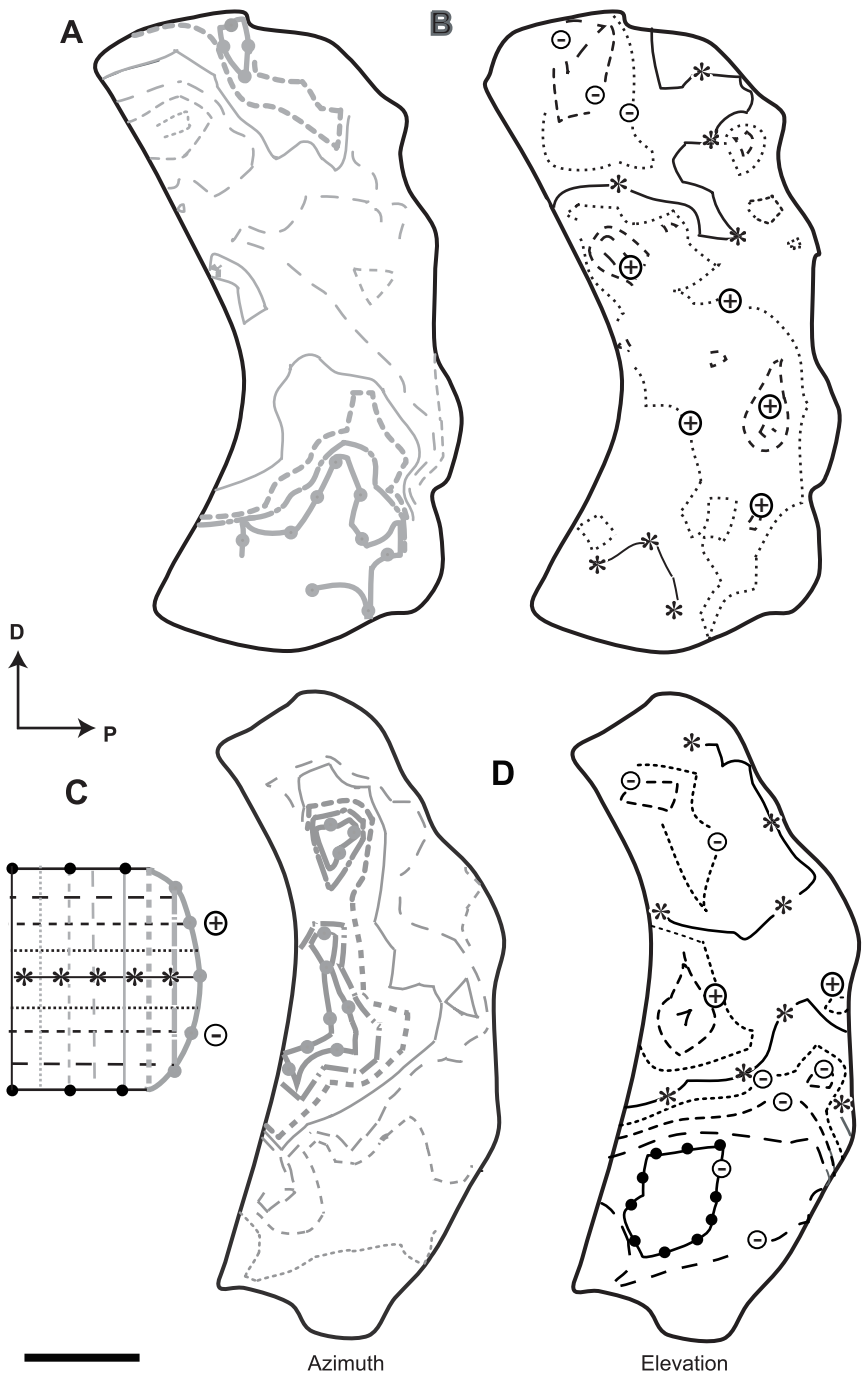
A
B
D
P
C
D
Azimuth
Elevation

As with the plots of RF positions, these maps also show certain complexities of the retinotopy found in this area. For example, in both cases there is a violation of the typical retinotopic pattern that the lower visual field maps onto medial cortical locations, with upper visual fields represented further lateral. Furthermore, there often appears to be a split or multiple representations of the HM. Figure 6D provides a clear example of this; lower fields are represented both medially and laterally while upper fields are represented centrally. In both Figure 6B and 6D, the HM representation located in the most medial aspect of the area curves considerably. In Figure 6B there also appears to be a separate HM representation further laterally. Both irregularities result in higher elevations in the visual field being represented in more medial regions of cortex relative to lower field locations.

There are other consistencies among all maps. Isoazimuth and elevation lines can span large distances both rostrocaudally and mediolaterally. They can run both perpendicular and parallel to each other, and they can form closed contours, as previously described in other ferret extrastriate areas (Manger et al., 2002a). Most of Ssy is dedicated to a band of visual space within 20° of the horizontal meridian. Ssy appears to contain only a small central representation, with an over-representation of 15°-30° in eccentricity relative to that of the *area centralis.* However, across animals the number of RFs is greater within the central 15° as compared to those between 15° and 30°. However, the latter comparison may be biased by our sampling within Ssy.

Extent of the representation of visual space

Pooling data across 9 cases, we fiund roughly the same proportion of RFs located in the upper and lower visual fields: 36% and 40% respectively, with 24% falling within 3° of the HM. However, there is a bias. The majority of the RFs located at central azimuths were in the lower visual field, while the majority of those located at peripheral azimuths were in the upper visual field. Overall, the representation of visual space in Ssy extends up to 70° in azimuth (with an incursion of roughly 10° into the ipsilateral hemifield), and roughly 35° in elevation above and below the horizontal meridian (Fig. 7). Ssy contains a limited representation of the vertical meridian (VM), which appears anisotropic. It extends up to 30° in the lower visual hemifield, but only 15° in the upper hemifield. Although RFs can also extend up 10° into the ipsilateral visual field, the representation of the VM results mainly from large RFs with centers more than 5° off the VM that overlap it.

Figure 7. Extent of visual field representation in Ssy. Gray area represents the region of visual space encompassed by the combined RFs of 9 cases.

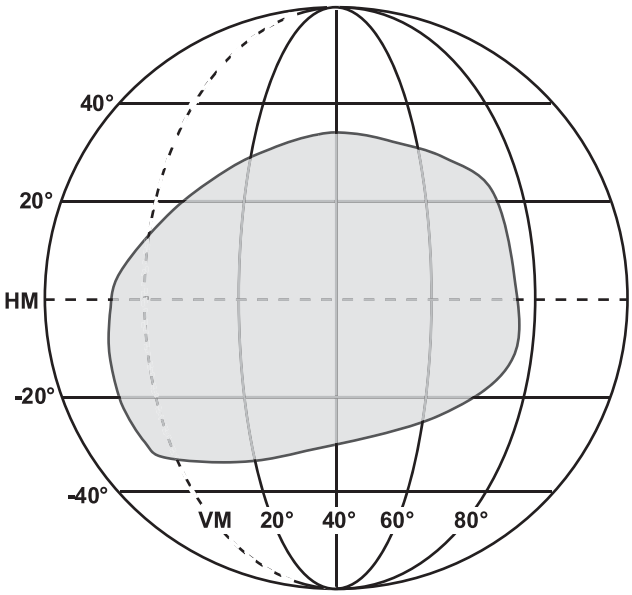
40°
20°
HM
-20°
-40°
VM
20°
40°
60°
80°

These conclusions are based on two cases in which we mapped RFs throughout the entire extent of Ssy, and 7 with incomplete mapping. Although in these 7 cases we encountered regions within Ssy that were unresponsive, in aggregate we did sample all portions of Ssy. In most cases we have successful recordings within the posterior bank of the sulcus abutting a large blood vessel lying within the suprasylvian sulcus (SsyS). However, we must consider that our mapping along the anterior border of Ssy may be incomplete due to this vessel impeding access to this region. In one case we were able to record RF locations within the SsyS. This indicates that we can access this region, and its unresponsiveness actually represents the rostral border of Ssy. To further determine if Ssy extended into the SsyS or underneath primary auditory cortex (A1) we made penetrations through the caudal portion of A1 aimed at underlying gray matter, and did not find visually responsive cells. We are therefore confident that we mapped the full visuotopic extent represented in Ssy.

Connectional evaluation of retinotopic organization in Ssy

To confirm our electrophysiological mapping data, in separate cases we made CTb injections at two different locations in Ssy. We then determined the retinotopic location of retrogradely labeled cells in area 17. If feedforward projections from area 17 to Ssy are topographic (Tigges et al., 1973; Spatz, 1977; Sherk and Ombrellaro, 1988; Shipp and Grant 1991; Mulligan and Sherk 1993), injections made at different retinotopic locations in Ssy should result in patches of labeling in different portions of area 17. We find no labeled cells in the dorsal lateral geniculate nucleus (LGN). We do find labeled cells in areas 17, 18, 19 and 21, as well as posterior parietal and lateral temporal areas.

The labeled cells providing intrinsic connections to the injection site fill the full area of Ssy, indicated by the abrupt end of label, which reflects the medial, lateral, and posterior borders described in Figure 1 (Fig 8A). Because the retinotopic organization is so regular and consistent in area 17 across animals (Law et al., 1988), we consider the retinotopic location of labeled cells in this area only.

Figure 8. Serial reconstructions and photomicrographs of tangential sections showing retrogradely labeled cells in area 17 after CTb injections in two different cases made at different retinotopic locations in Ssy. The full pattern of retrogradely labeled cells (small black dots) across extrastriate cortex is shown in (A). Injection in (A) was located more laterally along the SsyS than the injection shown in (B). For clarity, only labeled cells in area 17 are shown in reconstructions in (B). Large black circles represent CTb injection cores. Dashed lines represent areal border between 17 and 18. Box in insert represents the area enlarged in A, B. Gray boxes in A and B represent the area enlarged in C and D, respectively. Dashed boxes represent the area enlarged in E and F, respectively. Photomicrographs of injection cores (C, D) and retrogradely labeled cells (E, F). Dotted lines represent areal borders. scale in A-D = 1mm. scale in E,F = 100 μm. SVA = splenial visual area; SplS = splenial sulcus; II/III = surpagranular layers V/VI = infragranular layers; IV= layer IV; other conventions as in Figure 1.

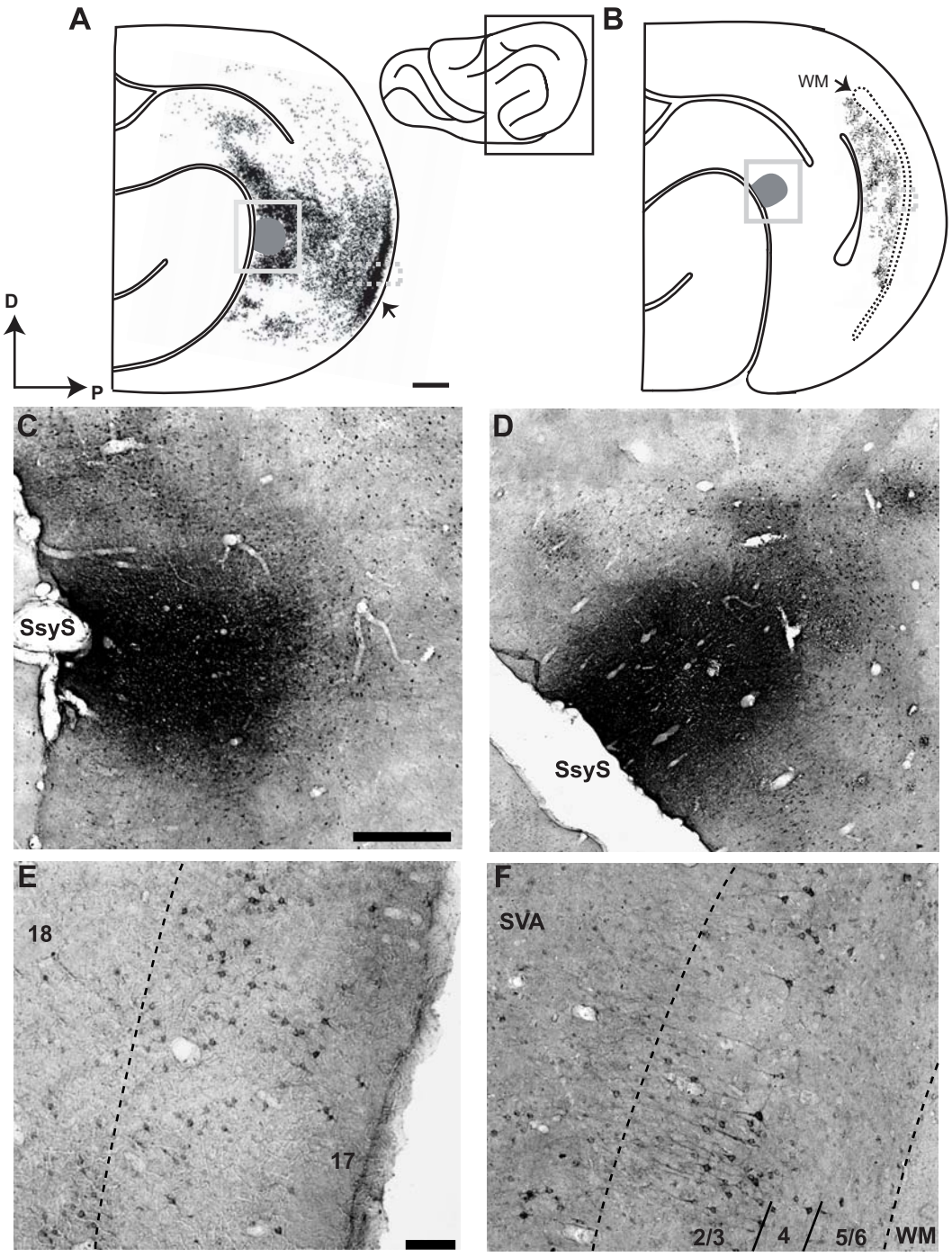
A
B
WM
D
P
C
SsyS
D
SsyS
E
18
17
F
SVA
2/3
4
5/6
WM

The distribution of label resulting from each of the injections reflects the aspects of retinotopic organization of Ssy shown in Figure 3 and 4. The injection shown in Figure 8A is located centrally along the SsyS; RFs recorded at this injection site were centered at 12° from the VM and 12° above the HM. However, the core encompasses regions of Ssy in which we mapped RFs centered at 36° in azimuth and 18° above the HM. The zone of retrogradely labeled cells in area 17 is continuous with labeled cells in area 18 and is located ventrally on the lateral surface (fig 8B, C) and caudal pole of the brain. Because of the plane of section of the reconstructions the extent around the caudal pole is appears as the dense region of cells in area 17. The spread of label extends 4-5 mm in cortex along the mediolateral axis in area 17. This location in cortex can respond to about 20° above the HM (Law et al., 1988; Manger et al. 2002a), and region of cortex spanning the caudal pole has been shown in some animals to respond to azimuths as far as 40° from the VM (Law et al., 1988). Therefore the extent of label in area 17 found in a region that contains a representation of the visual field is similar to that at the restricted injection site (Law et al., 1988; Manger et al., 2002a) (Fig. 8), and is consistent with the more common retinotopic organization shown in Figure 3.

In a different animal the CTb injection in Ssy is located more dorsally along the SsyS near the PPc border and is centered at 30° in azimuth, just below the HM. The core encompasses locations in Ssy that responded to 65° out from the VM and 20° above the HM. The pattern of retrogradely labeled cells in area 17 is not continuous with 18. Instead, label is located medially within the splenial sulcus. This area of area 17 contains a representation of peripheral azimuths that can potentially respond to 70° from the VM

(Law et al., 1988), similar to the retinotopic location at the injection core. Elevations in the upper visual field are represented at relatively more dorsal locations along the tentorial surface of area 17 than corresponding locations on the lateral surface (Law et al., 1988). Therefore, the spread of label along the medioloateral axis in area 17 in more dorsal locations also corresponds to the retinotopic location of our injection core. Retrogradely labeled cells are also found in separate cortical area adjacent to area 17 within the splenial sulcus, which is known to contain a representation of peripheral visual fields (Law et al., 1988). The pattern of labeled cells reflects the retinotopic organization shown Figure 4.

The dense injection core in Ssy covers a smaller extent in cortex than that of retrogradely labeled cells in area 17. This large spread of label in area 17 also suggests that MFs are smaller in Ssy than in area 17. We cannot state the exact convergence of visual space onto our injections site from area 17 through feedforward connections. Since we did not directly map the location of area 17 which contained label the estimation of the convergence would not be accurate.

Receptive field size and cortical magnification factor as a function of eccentricity

We examined whether eccentricity affects the representation of the visual space in Ssy. Multiunit receptive fields in Ssy range in size from 2°x4 ° to 52°x21°, and on average span 15°x15°. There is no significant relationship between RF size and eccentricity (Fig. 9). We also calculated the cortical magnification factors (MFs) in Ssy to confirm that they are lower in Ssy than those in area 17. The mean MFs are 0.063±0.003 mm/deg. of azimuth, and 0.078±0.004 mm/deg. of elevation. Both values are smaller than

the mean MF in area 17, which is approximately 0.2 mm/deg. in both azimuth and elevation (Law et al., 1988, Cantone et al., 2005).

Figure 9. Relationship between receptive field size and eccentricity. Eccentricity is defined as the absolute distance in degrees of visual space from RF center to the estimated location of the *area centralis*. Solid line shows the least squares linear regression line.

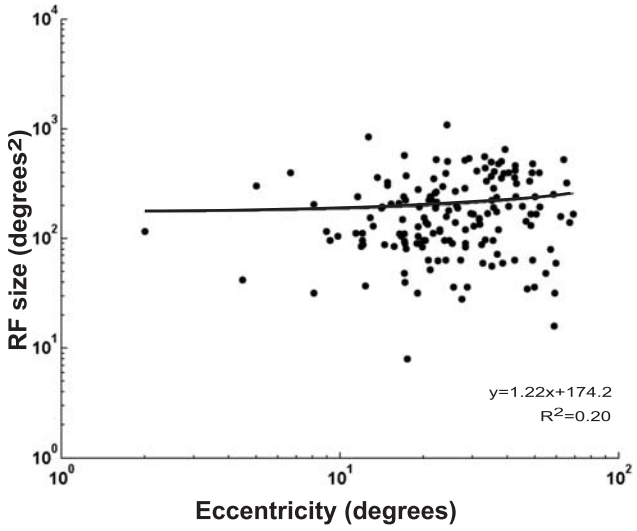
RF size (degrees2)
Eccentricity (degrees)
y=1.22x+174.2
R2=0.20

In examining in detail cortical magnification factors (MFs) in Ssy, aggregate data from 9 cases showed no significant correlation between MFs in mm/deg. of elevation and azimuth (Fig. 10). If MFs measured in azimuth and elevation both decrease with increasing eccentricity, these measures will be positively correlated, and will therefore fall along the diagonal in Figure 10. The lack of any significant correlation indicates that there is no consistent relationship between the spacing of isoazimuth and isoelevation contours. In cases in which two cortical loci have receptive fields that differ in azimuth or elevation but not both, it is not possible to calculate a MF along the axis of visual space along which receptive field position did not change. Therefore, we plot such unpaired MFs in Figure 10 outside the axes. The MFs along both axes in Ssy areas cover the same range, with no significant difference in mean MF values.

Figure 10. Relationship between cortical magnification factors (MF) along different axes of visual space. Data points without a corresponding MF along the opposing axis of visual space were plotted outside the range of MFs, indicated by dotted lines. The arrows outside the box indicate the mean MF in mm/deg. of azimuth or elevation, respectively.

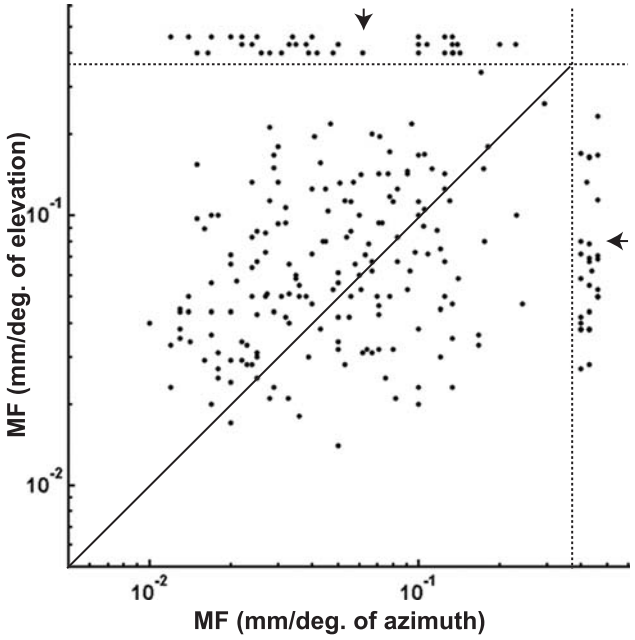
MF (mm/deg. of elevation)
10-1
10-2
10-2
10-1
MF (mm/deg. of azimuth)

We also assess the relationship between cortical magnification factors and eccentricity by plotting MFs in mm/deg. of azimuth and of elevation as functions of changes in degrees of azimuth and elevation. MFs in mm/deg. azimuth significantly decrease with increasing azimuth (Fig. 11A), and do not change significantly with changes in elevation (Fig. 11B). MFs in mm/deg. of elevation significantly decrease with increasing azimuths (Fig. 11 C, D). There is also a significant decrease in MFs that occurs as elevations progress from lower visual fields to upper visual fields, which suggests more of cortex is devoted to lower visual fields in Ssy. Any significant relationships ($p<0.01$) have only weak correlations (correlation coefficient = 0.2). This again confirms that spacing of isoazimuth and isoelevation contours does not change as consistently with retinal eccentricity.

Figure 11. Relationship of cortical magnification factors (MF) to eccentricity. Changes in MF in mm/deg. azimuth as a function of changes in degrees of azimuth (A) and elevation. (B), Changes in MF in mm/deg. elevation as a function of changes in degrees of azimuth (C), and elevation (D). Solid lines are the least squares regression lines using a second order polynomial.

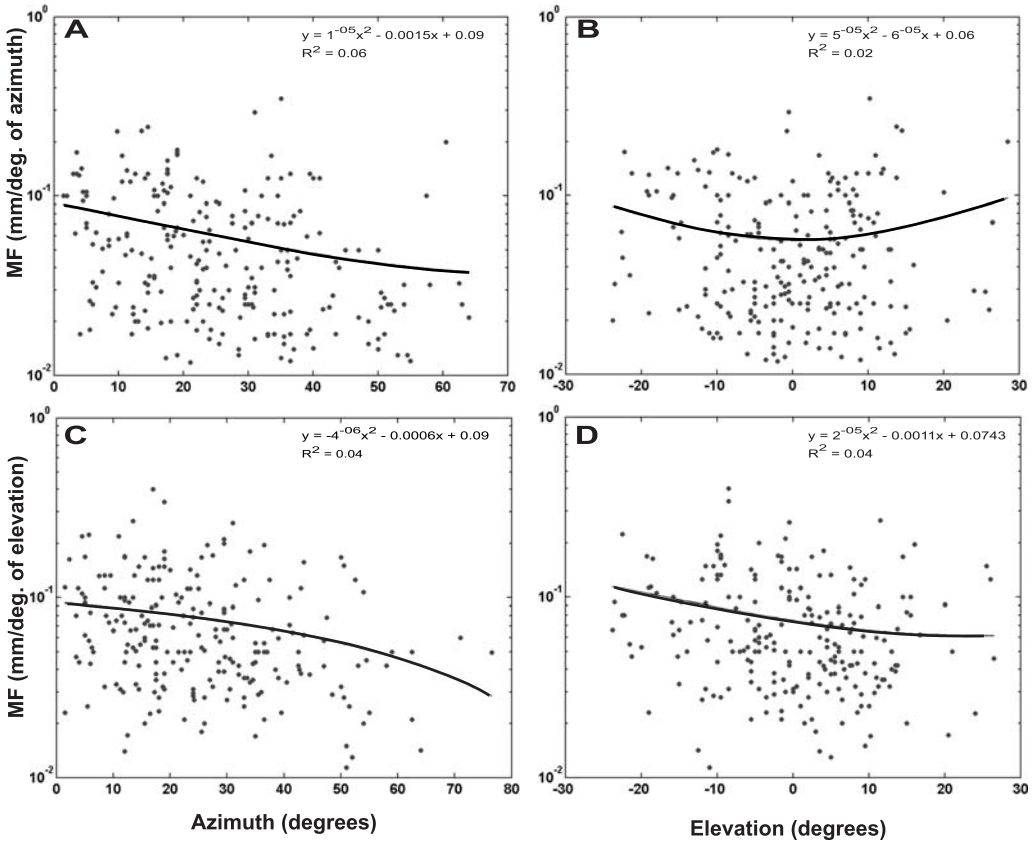
A
y = 1^-05x^2 - 0.0015x + 0.09
R^2 = 0.06
B
y = 5^-05x^2 - 6^-05x + 0.06
R^2 = 0.02
C
y = -4^-06x^2 - 0.0006x + 0.09
R^2 = 0.04
D
y = 2^-05x^2 - 0.0011x + 0.0743
R^2 = 0.04
MF (mm/deg. of azimuth)
MF (mm/deg. of elevation)
Azimuth (degrees)
Elevation (degrees)

4.4 DISCUSSION

Summary

The suprasylvian cortex (Ssy) is a visually responsive region in ferret cortex distinct in topography, and nissl-, myelo- and cytoarchitecture from surrounding cortical areas. It receives direct input from visual areas 17, 18, 19 and 21, and caudal posterior parietal (PPc) and lateral temporal visual areas (LT). It receives no input from the dorsal lateral geniculate nucleus (LGN). However, this evidence is based on only two injection cases. Ssy contains a limited representation of the contralateral visual field that extends up to 10° into the ipsilateral visual field. The area contains a limited representation of the contralateral visual field in which the map contains irregularities and varies among animals. Most of suprasylvian cortex is dedicated to the central 20° in elevation above and below the horizontal meridian, of which there often appears to be multiple representations. The size of multiunit receptive fields does not change with eccentricity and cortical magnification factors decrease only slightly with increasing eccentricity.

Defining suprasylvian cortex as a single visual area

Anatomical architecture, topography, RF properties, and connectivity are all criteria that are used to classify a cortical area (reviewed in Sherk, 1986). We find changes in RF size and neuronal responsiveness that coincide with anatomical boundaries. Anatomical evidence suggests that Ssy is a distinct cortical area. Innocenti et al. (2002) and Manger et al. (2002b, 2004) all report similar anatomical characteristics marking the borders of Ssy and neighboring areas. Our connectional data also support this. After making CTb injections into a restructed locus in Ssy there are breaks in the

pattern label of labeled cells at the Ssy/ PPc border and the Ssy/LT border. The label is only continuous with area 21 at regions adjacent to the injection core and is not continous along the entire posterior anatomical border of Ssy/21. In all cases in which we made injections of CTb into area 17 the resulting spread of labeled cells is continuous across area 17, 18,19, and 21. This pattern of label also reflects the retinotopic organization across these areas (Cantone et al., 2005). A break in the spread at the 21/Ssy border suggests the retinotopic maps are discontinuous between Ssy and area 21, marking an areal boundary. Although, the borders of the PPc and the LT also show changes in RF responsiveness and size, the location and size do not vary notably across the Ssy/21 border. Also, our physiological evidence does not reveal a reversal or discontinuity in the retinotopic map. Therefore, we cannot exclude the possibility that Ssy is a rostral extension of area 21.

We do not find that this region of cortex contains more than one complete representation of the visual field. Reversals in receptive field position occurring either at the representation of the VM or the periphery are often considered to be areal boundaries (Allman and Kaas, 1975; Manger et al., 2002a). However in Ssy, the location of the VM representation and the reversals in the map of visual space are not consistent across animals. In addition, neither coincides with any anatomical landmarks. Therefore they are unlikely to represent areal borders.

Another indication of areal boundaries is a discontinuity in the map (Gattass et al., 1988). We find very few discontinuities in cases with closely spaced recording sites, and they also do not correspond to anatomical borders or changes in RF characteristics. However, we do commonly find regions of Ssy with expanded representations of visual

space adjacent to regions where the retinotopic representation is compressed. Thus, one can move from regions in which large distances on cortex translate to small movements in the visual field to region in which short distance on cortex translate to large distances in the visual field. As suggested by Sherk and Mulligan (1993), regions of low MFs could be interpreted as discontinuities in the map. More closely spaced sampling can distinguish between apparent discontinuities in the map, such as regions of continuous but compressed representations of visual space as opposed to genuine areal borders.

Some studies suggest that discrete cortical areas contain a single and complete representation of the visual field (Daniel and Whitteridge, 1961; Allman and Kaas, 1971, 1974a; Tusa et al., 1978, 1979; Van Essen and Zeki 1978; Gattass et al., 1981). This is not always true in higher order extrastriate areas where there are often incomplete or double representations of the visual space (Palmer et al., 1978; Tusa and Palmer, 1980; Gattass et al., 1988). Within Ssy in ferret there are duplicate representations of both isoelevation lines and isoazimuth contours. However, because of how isoelevation and isoazimuth contours are organized relative to one another Ssy does not contain multiple complete representations of the visual field.

Our anatomical data from injections of CTb into area 17 also suggest that Ssy is a single cortical area with a single representation of the visual field. We consistently find a single cluster of retrogradely labeled cells in Ssy resulting from restricted injections in area 17 (Cantone et al., 2005). If Ssy were actually more than one area or had multiple representations of regions of the visual field, we might expect to see more than one patch of labeled cells. We did not examine the anatomical connections Ssy makes with cortical and subcortical structures in detail. The unique connectivity can also be a mode of

classifying an area as a functional unit. However, we feel the histological data, and electrophysiological mapping data cases are sufficient to classify Ssy as a distinct visual area.

Comparisons of Ssy with other visual areas in ferret cortex

Similar to the representations in areas 17, 18, 19 and 21, upper and lower visual fields are represented equally in Ssy. In contrast, areas PPr and PPc (which are located dorsal to Ssy) both have a bias towards the lower visual field, while areas 20a and 20b (which lie lateral to Ssy) each over-represent the upper hemifield (Manger et al., 2002b, 2004). The total extent of visual space represented in Ssy is smaller than that in all other previously described ferret visual areas (Law et al., 1988; Manger 2002a,b, 2004). The largest difference is with areas 17 and 18. This most likely can be attributed to the larger area of cortex both of these areas occupy relative to Ssy. MFs are considerably smaller in Ssy (0.071 mm/deg.) than in area 17 (0.2 mm/deg.) (Law et al., 1988), and slightly smaller than in extrastriate areas 18 (0.1 mm/deg.), 19 (0.1 mm/deg) and 21 (0.09 mm/deg.) (Cantone et al., 2005). Since the Ssy is roughly the same size as areas 19 and 21, the smaller amount of visual space represented in Ssy is not obviously reflected in the MFs. The mean RF diameter in Ssy is about 15°; this is larger than in area 17, about the same as in area 18, and smaller than in areas 19, 21, PPr, PPc, 20a, and 20b. These parietal and temporal visual areas have a larger visuotopic representation despite being smaller in cortical area than Ssy. Although MFs have not been reported for these areas, the larger visuotopic extent may be attributed to their larger RF sizes.

There are several factors that make Ssy unique from other extrastriate areas in

ferret cortex. There is limited representation of the vertical meridian (VM). In contrast, the representation of the VM forms a border between 17 and 18, 19 and 21, PPr and PPc, and 20b and PS (Manger et al., 2002a,b, 2004). As in areas like 18, 19 and 21, the isoazimuth lines in Ssy can form closed contours. The representation of isoelevation lines in Ssy differs greatly from most other areas. These contours run roughly parallel to each other rostrocaudally across areas 17, 18, 19, PPr, PPc and lateral temporal areas. In Ssy isoelevation lines can span substantial rostrocaudal and mediolateral distances in cortex sometimes forming closed contours. The MFs also do not change greatly with eccentricity. Although, this is similar to other extrastriate areas (Cantone et al., 2005), Ssy's retinotopic organization is most similar to area 21. The maps in both areas can vary across animals. The isoelevation lines in 21 can also run mediolaterally, and there can be multiple representations of the horizontal meridian (Manger et al., 2002a).

Despite the similarities with 21, the retinotopic organization within Ssy is more irregular than any other mapped visual area in ferret cortex. Since scatter of RF centers within column increases proportionately with RF size (Hubel and Wiesel, 1962), it is suggested that the coarse representation of the visual field within areas with large RFs may be a result of scatter (Albus 1975; Albright and Desimone, 1987). Although we did not explicitly measure it, we do not believe scatter alone can account for the coarseness of the maps in Ssy. The average RF size in Ssy is no larger than RFs in extrastriate areas with more orderly retinotopic organizations (Manger et al., 2002a, b, 2004). In addition, studies show that scatter was not proportional to RF size in medial temporal area (MT) of primates and the lateral suprasylvian cortex in cat (Gattass and Gross, 1981; Sherk and Mulligan 1992). The later study suggests that the disorderly maps are a result of the

coarseness of afferent inputs. Ssy is similar to areas 18, 19 in that more of cortex in Ssy contains a representation of 15°-30° in azimuth than that of central fields. The same is true in area 21 for azimuths between 25°-45° (Manger et al., 2002a). The representation of 15°-30° in eccentricity relative to that of the *area centralis* is greater in Ssy than in other areas. Ssy receives input from areas 18, 19, and 21. Therefore this bias in the visuotopic representation in Ssy reflects retinotopic afferent inputs from areas 18, and 19, as opposed to reflecting the density of retinal ganglion cells through direct input from LGN (as suggested by Palmer et al., 1978).

Comparisons with other species

Based on anatomical architecture, retinotopy, and our limited analysis of connectivity, Ssy appears homologous to the posteromedial lateral suprasylvian area (PMLS) (Clare and Bishop, 1954; Palmer et al. 1978). As in Ssy, this region of cortex in the cat is also densely myelinated (Sanides and Hoffmann, 1969). PMLS in cat has complex retinotopy and direct input from area 17, and 18 (Sherk, 1986; Shipp and Grant 1991). The lateral suprasylvian areas of cat is a region for which there are varying reports as to the number of functional areas that lie within it as well as their retinotopic organization (reviewed in Payne, 1993). More recent descriptions of the topography in the lateral suprasylvian area which includes PMLS show the VM is not strongly represented, and there is substantial variation among animals (Grant and Shipp, 1991; Sherk and Mulligan, 1993). Both Palmer et al. (1978) and Grant and Shipp (1991) show that the majority of RFs lie on or near the horizontal meridian just as we find in Ssy.

There are differences between Ssy in ferret and PMLS in cat. PMLS gets C

layer input from the LGN. Ssy also differs from this area in that it contains a slightly more extensive representation of the upper visual field. MFs have a stronger relationship to eccentricity than we find in Ssy (Palmer et al., 1978; Grant and Shipp, 1991). This could be because we have few recordings within the central 10°. In these previous studies the largest change in MF size is found within the central 10°. We also find that unlike most other extrastriate areas in ferret, cat and primate (Gattass et al., 1981, 1988; Grant and Shipp, 1991; Pinon et al., 1998; Manger et al. 2002a,b, 2004,) there is little relationship between RF size and eccentricity. However, this is similar to ferret areas 19, 20b, PPc and PPr.

It is arguable if visual areas in primate can be considered homologous to areas in non-primate species. However, studies do consider PMLS to be homologous with the middle temporal area (MT) in primates (Payne 1993; Dreher et al., 1996). Like MT Ssy is heavy myelination (Maunsell and Van Essen, 1987) and given Ssy's topography it is possible that ferret Ssy is also analogous to MT. Some studies report the topographic organization in MT is disorderly and varies between individual animals (Van Essen et al., 1981), while others report that MT has a more orderly representation of the visual field than what we describe in Ssy (Fiorani et al., 1989). MT also lacks a true representation of the VM (Gattass and Gross, 1981; Van Essen et al., 1981). Although Ssy contains a larger representation of the upper visual field than MT, Ssy shows several similarities with MT. However, Ssy receives no direct LGN input while MT does (Sincich et al., 2004).

Functional relevance of Ssy

Given that that strict ordely representation of the visual field on Ssy is not maintained, this area may have other functional relevance besides providing reintopic information to linked cortical areas. Preliminary physiological studies by (Phillipp et al., 2004) show cells in Ssy are direction selective and are connected to the nucleus of the optic tract and the dorsal terminal nucleus. Both structures are involved in the optokinetic system. Therefore, Ssy may have a similar role as MT (Zeki, 1974; Baker et al., 1981; Maunsell and Van Essen 1983 a, b). The lack of RF centers on the VM could simply be a way of limiting the intrusion of RFs onto the ipsilateral visual field by relatively large RFs (Gattass and Gross, 1981). However, the emphasis on the representation of more peripheral fields, the limited representation of the VM, and the anisotropic representation of the VM relative to that of the HM are all consistent with the idea that Ssy is involved in motion and direction processing. Both nonhuman primate electrophysiological, and human psychophysical studies report biases against motion detection near or towards the VM, where none are found along the HM (Maunsell and VanEssen, 1983b; Van de Grind et al., 1993).

Ssy is reciprocally linked with area 17. Both Bullier et al. (1988) and Katsuyama et al. (1996) suggest that neurons in cat lateral suprasylvian cortex can provide excitatory input to their targets in area 17. Given the smaller MFs and the larger RFs in ferret Ssy relative to those in area 17, larger extents of visual space can converge onto smaller RFs in area 17. Therefore, feedback connections arising from Ssy may have a functional role in shaping the responses of area 17 neurons. Other physiological studies show that response latencies of neurons in cat lateral suprasylvian area and primate MT

are very similar to those of neurons in area 17 (Dinse and Krüger, 1994; Katsuyama et al., 1996; Raiguel et al., 1989). There is also evidence that the modulatory effects arising from the nonclassical receptive field surround have response latencies similar to both responses within the classic receptive field of area 17 cells and those of cells within extrastriate areas (Knierim and Van Essen, 1992). This correlative evidence suggests that feedback connections arising from Ssy can contribute to the modulatory surround of area 17 neurons as in other species (Bullier et al., 2001; Angelucci and Bullier, 2003). Further studies addressing the functional characteristics of Ssy neurons are needed to clarify Ssy's role in visual processing.

CHAPTER 5: SUMMARY AND CONCLUSIONS

General Discussion

In examining the cortical connections of area 17 in ferret we find strong feedback connections arising from areas 18, 19, 21 and Ssy. Fewer projections arise from the posterior parietal areas PPr and PPc, and lateral temporal areas (LT). In all areas examined, feedback originates largely from the infragranular layers, with smaller contributions arising from the supragranular layers. Intrinsic connections within area 17, and feedback connections arising from extrastriate cortex to area 17, both link cells with non-overlapping receptive fields. However, the extent of visual space to which cells providing feedback to a restricted locus in area 17 respond is larger than that of intrinsic connections to that same locus. This confirms that these circuits allow for the convergence of signals from larger visuotopic regions onto smaller receptive fields of cells in area 17.

The minimum response fields (MRF) of cells, most within the central 20° of visual space, range from 1.66° to 33° in diameter. The majority of these cells have summation fields considerably larger than their MRF. This indicates that these cells have extensive regions beyond the MRF from which responses to stimuli within the classic receptive field can be modulated. For the majority of cells the extent in visual space that these surround regions encompass is commensurate with local connections. For cells that summate visual signals over a larger extent of visual space, feedback connections are a more plausible circuit. Therefore, neurons in area 17 of ferret derive their summation fields from both intrinsic and feedback connections.

A substantial proportion of feedback connections arise from Suprasylvian cortex

(Ssy). The retinotopic organization in this area can be quite irregular, and does vary across animals. However, in all cases Ssy contains smaller cortical magnification factors (MF) and larger receptive fields (RFs) than those in area 17. Based on the spread of label in Ssy resulting from injections of CTb into area 17 it is likely that larger extents of visual space can converge onto smaller RFs in area 17. Further studies addressing the functional characteristics of Ssy neurons are needed to clarify Ssy's role in visual processing. However, there are similarities between Ssy and PMLS in cat, and MT in primates, both of which are associated with motion and direction processing (Zeki, 1974; Baker et al., 1981; Maunsell and Van Essen 1983a, b; Dreher et al., 1996). Phillipp et al. (2004) provide both anatomical and physiological evidence that suggest Ssy may also be involved motion processing. Therefore, Ssy may have a functional role in shaping the responses of area 17 neurons other than providing for the retinotopic extent from which surround modulatory effects arise.

There is evidence that other functional aspects besides retinotopy may govern feedback connections arising from areas 18, 19, and 21. Clustering of connections reflects grouping of cells with similar RF properties (reviewed in Gilbert, 1992; Callaway, 2004; Chisum and Fitzpatrick, 2004). We find that locations where there are high densities of labeled cells are not restricted to similar retinotopic locations as their target neurons. Connectional strength may also be an indication of the functional influence each area has over the response properties of neurons in area 17. Based on the proportion of feedback connections arising from area 18, it may have the strongest influence on the response properties of area 17 neurons. We find all areas from which prominent feedback arises provide roughly the same retinotopic input. This also reveals

interspecies differences regarding the hierarchical organization of ferret visual areas. In primate, which has well established hierarchical arrangement among visual areas the increasingly larger extents of visual space converge into target neurons in area 17 through feedback connections as one moves up in the hierarchy (Angellucci et al., 2002b).

Our anatomical data also suggest there is not a strictly hierarchical arrangement among extrastriate areas providing prominent feedback to area 17. Based on the percentage of feedback connections arising in the supragranular layers of areas 18, 19, 21 and Ssy, they would all be considered to be on the same level of visual processing. Consistent with this evidence, areas 18 and 19 receive direct input from the Lateral Geniculate Nucleus (LGN) (Baker et al., 1998; Cantone et al., 2002). We do note that areas 18 and 19 in cat receive input from the LGN and are still placed at different levels within a hierarchy (Scannell et al., 1995). Baker et al. (1998) find that areas 17 and 18 in ferret receive afferent connections from different cell types, with varying proportions arising from different layers of the LGN. They suggest these areas are processing different information in parallel as opposed to serially. Neurons providing feedback connections to area 17 in cat can drive cells' responses as opposed to only modulating them (Bullier et al., 1988). In primate the specificity of clustering of feedback connections to area 17 relative to orientation domains in area 17 remains arguable (Stettler et al., 2002; Shmuel et al., 2005). Therefore, it remains unclear if they have a role in non-specific global integration of the visual field or in producing tuned modulatory surround effects. Collectively, evidence suggests that feedback connections in ferret may have a different role in the integration of visual space as compared to primate. If it is the case that feedback connections terminate diffusely in area 17 of ferret,

the lack of tuning of surround effects may be a result of feedback connections meditating surround modulation in neurons with smaller summation fields for which intrinsic connections can account.

Local connections are clustered, suggesting that surrounds are tuned for orientation. However, to some detail anatomical and physiological properties differ in ferret from cat and primate. Ferrets have similar anatomical and physiological features to cat and primate (Lund, 1973; Gilbert and Wiesel, 1979; Rockland and Lund, 1982; Rockland, 1985; Weliky et al., 1996; reviewed in Lamme et al., 1998; Tucker and Katz, 2003, Roerig and Chen, 2002; White et al., 2002), but surround inhibition when the center and surround match appears rare. In addition the CV values for individual cells were all above 0.6, indicating the surrounds of individual cells are not strongly orientation tuned. Orientation domains in ferret overlap (Rao et al., 1997). If these domains are not as organized in ferret as they are in primate, the effects on a cell's receptive field properties by its recruitment of cells linked through horizontal connections may not be as specific. The functional architecture in ferret in area 17 may be organized well enough to produce tuning within the classic receptive field, but intrinsic connections may not capable of producing well-tuned modulation arising from the surround.

Significance

Our findings expand on the uses of ferret in studies addressing adult visual processing. Many MRFs have more than one locus of peak activity, and are quite large which allows for the study of the interactions of regions within the classical receptive field, such as loci of high activity and low activity or with stimuli that span the center and

surround. These types of studies may provide information that is more applicable to understanding how the visual system processes natural scenes. Both the similarities and differences it has with cat and primate are important for making it useful for interspecies comparisons. These comparisons aid in determining the type of functional information that must be provided through anatomical inputs to a given cell to produce its RF properties. By looking at how different cortical areas of the brain are functionally organized across species, we can determine what adaptations of visual processing influence the anatomical and functional characteristics of cortex.

Relating the anatomical connection to physiological properties in area 17 cells only provides a correlative association between the two. Although this alone does not conclusively determine the role of feedback connections in ferret, this study provides additional information regarding several cortical areas, such as the corticocortical connectivity of area 17 in ferret, the nature of retinotopic convergence onto area 17 and the response properties of cells within area 17. It also establishes these cortical characteristics in adult to which developmental or inactivation studies can be compared. These types of studies can more clearly resolve the issue of which circuits underlie the larger summation properties of cells by at least eliminating a given anatomical circuit as underlying substrate. For example intrinsic connections within area 17 formed but feedback connections from areas 18, 19 and 21 are not present at a certain developmental stage. At this same stage, area 17 neurons summate information over the same visuotopic extents then connections from extrastriate areas are not necessary to produce adult like summation properties. Expanding the findings in visual cortex to other areas of the brain will also help in understanding what circuits are involved in higher processes that shape

learning and reorganization in adult cortex, and how these dynamic changes in adult cortex occur.

This study describes the plausible anatomical substrates that integrate information across space to form perception. Although these properties described here are specific to vision, features of visual cortex such as anatomical structure and connectivity, cell type, topographical mapping are common to prefrontal cortex, association cortex, motor cortex and somaotosensory cortex (Tusa et al., 1978; Barbas, 1995; Levitt et al., 1993; Pucak et al., 1996, McLaughin et al, 1998; Barbas and Rempel-Clower, 1997; Sonty and Juliano, 1997). In fact the columnar organization of the cortex was first described in sensory motor cortex by Mountcastle (1957), and since has been established as a basic property of cortical architecture. Given these similarities, clarifying issues in visual cortex can be useful in understanding the rest of cortex. Therefore, these studies provide information about the general connectivity of cortex, and how it governs higher sensory processing. They also address questions pertaining to how individual anatomical circuits integrate information throughout the cortex, the dynamic changes in receptive field properties and the way in which visual cortex processes stimuli in the natural world. Crick and Jones (1993) state that understanding functional connectivity of cortex is a foundation of many of the neurophysiological techniques, such as brain imaging, that will eventually show how the brain functions. In addition studies used to develop cortically controlled neuroprosthetic systems analyze neural activity to decode natural behaviors and brain controlled movement (Tillery et al., 2002; Tillery and Taylor, 2004). Thus, the knowledge of how neural circuitry results in neuronal function will eventually aid in restoring damaged cortex.

LITERATURE CITED:

Albright TD. 1984. Direction and orientation selectivity of neurons in visual area MT of the macaque. J Neurophysiol 52:1106-30.

Albright TD, Desimone R. 1987. Local precision of visuotopic organization in the middle temporal area (MT) of the macaque. Exp Brain Res 65:582-92.

Albus K. 1975. A quantitative study of the projection area of the central and the paracentral visual field in area 17 of the cat. I. The precision of the topography. Exp Brain Res 24:159-79.

Alitto HJ, Usrey WM. 2004. Influence of contrast on orientation and temporal frequency tuning in ferret primary visual cortex. J Neurophysiol 91:2797-808.

Allman JM, Kaas JH. 1971.Representation of the visual field in striate and adjoining cortex of the owl monkey (Aotus trivirgatus). Brain Res 35:89-106.

Allman JM, Kass JH. 1974a. The organization of the second visual area (V II) in the owl monkey: a second order transformation of the visual hemifield. Brain Res 76:247-65.

Allman JM, Kaas JH. 1974b. A crescent-shaped cortical visual area surrounding the middle temporal area (MT) in the owl monkey (Aotus trivirgatus). Brain Res 81:199-213.

Allman JM, Kaas JH. 1975. The dorsomedial cortical visual area: a third tier area in the occipital lobe of the owl monkey (Aotus trivirgatus). Brain Res 100: 473-87.

Allman JM, Kaas JH. 1976. Representation of the visual field on the medical wall of occipital-parietal cortex in the owl monkey. Science 191:572-5.

Allman J, Miezin F, McGuinness E. 1985. Direction- and velocity-specific responses from beyond the classical receptive field in the middle temporal visual area (MT). Perception 14:105-26.

Alonso J M, Cudiero J, Perez R, Gonzalez F, Acuña C. 1993a. Influence of layer V of area 18 of the cat visual cortex on responses of cells in layer V of area 17 to stimuli of high velocity. Exp Brain Res 93:363-66.

Alonso JM, Cudeiro J, Perez R, Gonzalez F, Acuna C. 1993. Orientational influences of layer V of visual area 18 upon cells in layer V of area 17 in the cat cortex. Exp Brain Res 96:212-20.

Anderson JS, Lampl I, Gillespie DC, Ferster D. 2001. Membrane potential and conductance changes underlying length tuning of cells in cat primary visual

cortex. J Neurosci 21:2104-12.

Angelucci A, Clasca F, Sur M. 1996. Anterograde axonal tracing with the subunit B of cholera toxin: a highly sensitive immunohistochemical protocol for revealing fine axonal morphology in adult and neonatal brains. Neurosci Methods 65:101-112.

Angelucci A, Levitt JB, Lund JS. 2002a. Anatomical origins of the classical receptive field and modulatory surround field of single neurons in macaque visual cortical area V1. Prog Brain Res 136:373-388.

Angelucci A, Levitt JB, Walton EJ, Hupé JM, Bullier J, Lund JS. 2002b. Circuits for local and global signal integration in primary visual cortex. J Neurosci 22:8633-8646.

Angelucci A, Bullier J. 2003. Reaching beyond the classical receptive field of V1 neurons: horizontal or feedback axons? J Physiol Paris 97:141-154.

Baker JF, Petersen SE, Newsome WT, Allman JM. 1981. Visual response properties of neurons in four extrastriate visual areas of the owl monkey (Aotus trivirgatus): a quantitative comparison of medial, dorsomedial, dorsolateral, and middle temporal areas. J Neurophysiol 45:397-416.

Baker GE, Thompson ID, Krug K, Smyth D, Tolhurst DJ. 1998. Spatial-frequency tuning and geniculocortical projections in the visual cortex (areas 17 and 18) of the pigmented ferret. Eur J Neurosci 10:2657-68.

Barbas H. 1995. Pattern in the cortical distribution of prefrontal directed neurons with divergent axons in rhesus monkey. Cereb Cortex 2:158-165.

Barbas H, Rempel-Clower N. 1997. Cortical structure predicts the pattern of corticocortical connections. Cereb Cortex 7:635-46.

Barlow HB, Blakemore C, Pettigrew JD. 1967. The neuronal basis of binocular depth discrimination. J Physiol Lond 193:327-42.

Barone P, Batardiere A, Knoblauch K, Kennedy H. 2000. Laminar distribution of neurons in extrastriate areas projecting to visual areas V1 and V4 correlates with the hierarchical rank and indicates the operation of a distance rule. J Neurosci

20:3263-81.

Barone P, Dehay C, Berland M, Bullier J, Kennedy H. 1995. Developmental remodeling of primate visual cortical pathways. Cereb Cortex 5:22-38.

Batardiere A, Barone P, Dehay C, Kennedy H. 1998. Area-specific laminar distribution of cortical feedback neurons projecting to cat area 17: quantitative analysis in the adult and during ontogeny. J Comp Neurol 396:493-510.

Bartfeld E, Grinvald A, 1992. Relationships between orientation-preference piinwheels, cytochrome oxidase blobs, and ocular-dominance columns in primate striate cortex. Proc. Natl Acad Sci U.S.A 89:11905-9.

Batardière A, Barone P, Dehay C, Kennedy H. 1998. Area-specific laminar distribution of cortical feedback neurons projecting to cat area 17: quantitative analysis in the adult and during ontogeny. J Comp Neurol 396:493-510.

Bolz J, Gilbert C. 1989. The role of horizontal connections in generating long receptive fields in the cat visual cortex. Eur J Neurosci 1:263-67.

Bosking WH, Zhang Y, Schofield B, Fitzpatrick D. 1997. Orientation selectivity and the arrangement of horizontal connections in tree shrew striate cortex. J Neurosci 17:2112-27.

Bringuier V, Chavane F, Glaeser L, Fregnac Y. 1999. Horizontal propagation of visual activity in the synaptic integration field of area 17 neurons. 283:695-9.

Brown HA, Allison JD, Samonds JM, Bonds AB. 2003. Nonlocal origin of response suppression from stimulation outside the classic receptive field in area 17 of the cat. Vis Neurosci 20:85-96.

Bullier J, McCourt ME, Henry GH. 1988. Physiological studies on the feedback connections to the striate cortex from cortical areas 18 and 19 of the cat. Exp Brain Res 70:90-98.

Bullier J. 2001. The role of feedback connections in shaping the responses of visual cortical neurons. Prog Brain Res 134:193-204.

Calderone JB, Jacobs GH. 2003. Spectral properties and retinal distribution of ferret ones. Vis Neurosci 20:11-7.

Cantone G, McFarlane N, Levitt JB. 2002. Corticocortical connections among

ferret visual areas. Soc Neurosci Abstr 28, 159.3.

Cantone G, Xiao J, Levitt JB. 2003. Retinotopic organization of ferret suprasylvian cortex. Soc Neurosci Abstr 29:818.9.

Cantone G, Xiao J, Levitt JB. 2004. Direct measurement of the visuotopic extent of feedback connections to ferret primary visual cortex. Soc Neurosci Abstr 30:300.8.

Cantone G, Xiao J, McFarlane N, Levitt JB. 2005. Feedback connections to ferret striate cortex: Direct evidence for visuotopic convergence of feedback inputs. J Comp Neurol 2005 487:312-31.

Callaway EM. 2004. Feedforward, feedback and inhibitory connections in primate visual cortex. Neural Netw 17:625-32.

Cavanaugh JR, Bair W, Movshon JA. 2002. Selectivity and spatial distribution of signals from the receptive field surround in macaque V1 neurons. J Neurophysiol 88:2547-2556.

Chapman B, Godecke I. 2002. No ON-OFF maps in supragranular layers of ferret visual cortex. J Neurophysiol 88:2163-6.

Chisum HJ, Mooser F, Fitzpatrick D. 2003. Emergent properties of layer 2/3 neurons reflect the collinear arrangement of horizontal connections in tree shrew visual cortex. J Neurosci 23:2947-60.

Chisum HJ, Fitzpatrick D. 2004.The contribution of vertical and horizontal connections to the receptive field center and surround in V1. Neural Netw 17:681-93.

Clare MH, Bishop GH. 1954. Responses from an association area secondarily activated from optic cortex. J Neurophysiol 27: 620-634.

Crick F, Jones E. 1993. Backwardness of human neuroanatomy. Nature 361:109-10.

Crook JM, Eysel UT Machemer HF. 1991. Influence of GABA-induced remote inactivation on the orientation tuning of cells in area 18 of feline visual cortex: A comparison with area 17. Neruosci 40:1-12.

Crook JM, Eysel UT. 1992. GABA-induced inactivation of functionally characterized sites in cat visual cortex (area 18): effects on orientation tuning. J Neurosci 12:1816-25.

Daniel PM, Whitteridge D. 1961. The representation of the visual field on cerebral cortex in monkeys. J Physiol Paris 159:203-201.

Das A, Gilbert CD. 1995. Long-range horizontal connections and their role in cortical reorganization revealed by optical recording of cat primary visual cortex. Nature 375:780-4.

DeAngelis GC, Robson JG, Ohzawa I, Freeman RD. 1992. Organization of suppression in receptive fields of neurons in cat visual cortex. J Neurophysiol 68:144-63.

DeAngelis GC, Freeman RD, Ohzawa I. 1994. Length and width tuning of neurons in the cat's primary visual cortex. J Neurophysiol 71:347-74.

Dinse HR, Kruger K. 1994. The timing of processing along the visual pathway in the cat. Neuroreport 5:893-7.

Dow BM, Snyder AZ, Vautin RG, Bauer R. 1981. Magnification factor and receptive field size in foveal striate cortex of the monkey. Exp Brain Res 44:213-228.

Dreher B, Wang C, Turlejski KJ, Djavadian RL, Burke W. 1996. Areas PMLS and 21a of cat visual cortex: two functionally distinct areas. Cerebral Cortex 6:585-99.

Engel AK, Kreiter AK, Konig P, Singer W. 1991. Synchronization of oscillatory responses between striate and extrastriate visual cortical areas of the cat. Proc Natl Acad Sci USA 88:6048-6052.

Einstein G. 1996. Reciprocal projections of cat extrastriate cortex: I. Distribution and morphology of neurons projecting from posterior medial lateral suprasylvian sulcus to area 17. J Comp Neurol 376:518-529.

Eysel UT, Shevelev IA, Lazareva NA, Sharaev GA. 1998. Orientation tuning and receptive field structure in cat striate neurons during local blockade of intracortical inhibition. Neurosci 84:25-36.

Felleman DJ, Van Essen DC. 1991. Distributed hierarchical processing in the primate cerebral cortex. Cereb Cortex 1:1-47.

Ferster D. 1988. Spatially opponent excitation and inhibition in simple cells of the cat visual cortex. J Neurosci 8:1172-80.

Fitzpatrick D. 1996. The functional organization of local circuits in visual cortex: insights from the study of tree shrew striate cortex. Cereb Cortex 6:329-41.

Fitzpatrick D. 2000. Seeing beyond the receptive field in primary visual cortex. Curr Opin Neurobiol 10:438-43.

Gallyas F. 1979. Silver staining of myelin by means of physical development. Neurol Research 1:203-209.

Gattass R, Gross CG. 1981. Visual topography of striate projection zone (MT) in posterior superior temporal sulcus of the macaque. J Neurophysiol 46, 621-38.

Gattass R, Gross CG, Sandell JH. 1981.Visual topography of V2 in the macaque. J Comp Neurol 201:519-39.

Gattas R, Sousa AP, Gross CG. 1988.Visuotopic organization and extent of V3 and V4 of the macaque. J Neurosci 8:1831-45.

Gegenfurtner KR, Kiper DC, Levitt JB. 1997. Functional properties of neurons in macaque area V3. J Neurophysiol 77:1906-23.

Gilbert CD. 1977. Laminar differences in receptive field properties of cells in cat primary visual cortex. J Physiol 268:391-421.

Gilbert CD, Wiesel TN. 1979. Morphology and intracortical projections of functionally characterised neurones in the cat visual cortex. Nature 280:120-125.

Gilbert CD, Wiesel TN. 1990. The influence of contextual stimuli on the orientation selectivity of cells in primary visual cortex of the cat. Vision Res 30:1689-1701.

Gilbert CD. 1992. Horizontal integration and cortical dynamics. Neuron 9:1-13.

Grant S, Shipp S. 1991. Visuotopic organization of the lateral suprasylvian area and of an adjacent area of the ectosylvian gyrus of cat cortex: a physiological and connectional study. Vis Neurosci 6:315-38.

Hata Y, Tsumoto T, Stao H, Hagiahara K, Tamura H. 1998. Inhibition contributes to orientation selectivity in visual cortex of cat. Nature 27:815-7.

Hartline, HK 1940. The receptive fields of optic nerve fibers. Am J Physiol 130: 690-699.

Henderson Z. 1985. Distribution of ganglion cells in the retina of adult pigmented ferret. Brain Res 358:221-228.

Henry GH, Salin PA, Bullier J. 1991. Projections from areas 18 and 19 to cat striate cortex: divergence and laminar specificity. Eur J Neurosci 3:186-200.

Hilgetag CC, Grant S. 2000. Uniformity, specificity and variability of corticocortical connectivity. Phil Trans R Soc Lond B Biol Sci 355:7-20.

Hirsch JA. 1995.Synaptic integration in layer IV of the ferret striate cortex. J Physiol 483:183-99.

Hirsch J, Gilbert C. 1991. Syanaptic Physiology of horizontal connections in the cat's visual cortex. J Neurosci 11:1800-09.

Hupe JM, James AC, Payne BR, Lomber SG, Girard P, Bullier J. 1998. Cortical feedback can improve discrimination between figure and background by V1, V2, and V3 neurons. Nature 394:784-87.

Hupe JM, James AC, Girard P, Bullier J. 2001a. Response modulations by static texture in area V1 of the Macaque monkey do not depend on feedback connections from V2. J Neurophysiol 85:146-163.

Hubel DH, Wiesel TN. 1962. Receptive fields, binocular interaction and functional architecture in the cat's visual cortex. J Physiol 160:106-154.

Hubel DH, Wiesel TN. 1968. Receptive fields and functional architecture of monkey striate cortex. J Physiol 195:215-243.

Hubel DH, Wiesel TN. 1974. Uniformity of monkey striate cortex: a parallel relationship between field size, scatter, and magnification factor. J Comp Neurol 158:295-306.

Hubel DH, Wiesel TN, Stryker MP. 1978. Anatomical demonstration of orientation columns on Macaque monkey. J Comp Neurol 177:361-80.

Hubener M, Shoham D, Grinvald A, Bonhoeffer T. 1997. Spatial relationships among three columnar systems in cat area 17. J Neurosci 17:9270-84.

Hupé JM, James AC, Girard P, Bullier J. 2001a. Response modulations by static texture in area V1 of the Macaque monkey do not depend on feedback connections fromV2. J Neurophysiol 85:146-163.

Hupé JM, James AC, Girard P, Lomber SG, Payne BR, Bullier J. 2001b. Feedback connections act on early part of the responses in monkey visual cortex . J Neurophysiol 85:134-145.

Hupé JM, James AC, Payne BR, Lomber SG, Girard P, Bullier J. 1998. Cortical feedback can improve discrimination between figure and background by V1, V2, and V3 neurons. Nature 394:784-787.

Hupe JM, James AC, Girard P, Lomber SG, Payne BR, Bullier J. 2001b. Feedback connections act on early part of the responses in monkey visual cortex. J Neurophysiol 85:134-45.

Innocenti GM, Manger P, Masiello I, Colin I, Tettoni L. 2002. Architecture and callosal connections of visual areas 17, 18, 19 and 21 in the ferret (Mustella putorius). Cereb Cortex 12:411-422.

Jackson CA, Hickey TL. 1985. Use of ferrets in studies of the visual system.Lab Anim Sci 35:211-5.

Jones HE, Grieve KL, Wang W, Sillito AM. 2001.Surround suppression in primate V1. J Neurophysiol 86:2011-28.

Kalia M, Whitteridge D. 1972. A splenial visual area. J Physiol 222:142-143.

Kaas JH, Lin CS. 1977. Cortical projections of area 18 in owl monkeys. Vision Res 17:739-41.

Katsuyama N, Tsumoto T, Sato H, Fukuda M, Hata Y. 1996. Lateral suprasylvian visual cortex is activated earlier than or synchronously with primary visual cortex in the cat. Neurosci Res 24: 431-5.

Knierim JJ, Van Essen DC. 1992. Neuronal responses to static texture patterns in area V1 of the alert macaque monkey. J Neurophysiol 67:961-80.

Kuffler S. 1953. Discharge patterns and functional organization of mammalian retina J Nuerophysiol 16:37-68.

Kuypers HG, Szwarcbart MK, Mishkin M, Rosvold HE. 1965. Occiptotemporal corticortical connections in the rhesus monkey. Exp Neurol 11:245-262.

Lanciego JL, Wouterlood FG, Erro E, Gimenez-Amaya JM. 1998. Multiple axonal tracing: simultaneous detection of three tracers in the same section. Histochem

Cell Biol 110:509-515.

Law M I, Zahs K, Stryker M. 1988. Organization of primary visual cortex (area 17) in the ferret. J Comp Neurol 278:157-180.

Lagae L, Gulyas B, Raiguel S, Orban GA. 1989. Laminar analysis of motion information processing in macaque V5. Brain Res 496:361-7.

Lamme VAF, Super H, Spekreijse H. 1998. Feedforward, horizontal, and feedback processing in the visual cortex. Curr Opin In Neurobiol 8:529-35.

Levitt JB, Lewis DA, Yoshika T, Lund JS. 1993. Topography of pyramidal neuron intrinsic connections in macaque monkey prefrontal cortex (areas 9 and 46). J Comp Neurol 338:360-76.

Levitt JB, Kiper DC, Movshon JA. 1994. Receptive fields and functional architecture of macaque V2. J Neurosci 71: 2517-41.

Levitt JB, Lund JS, Yoshioka T. 1996. Anatomical substrates for early stages in cortical processing of visual information in macaque monkey. Behavioral Brain Res 76:5-19.

Levitt JB, Lund JS. 1997. Contrast dependence of contextual effects in primate visual cortex. Nature 387:73-76.

Levitt JB, Lund JS. 2002. The spatial extent over which neurons in macaque striate cortex pool visual signals. Vis Neurosci 19:439-452.

Li C, Li W. 1994. Extensive integration field beyond the classic receptive field of cat's striate cortical neurons-classification and tuning properties. Vision Res 34:2337-2355.

Livingston, MS, Hubel, DH. 1984. Specificity of intrinsic connections in primate primary visual cortex. J Neurosci 4:2830-5.

Lund JS. 1973. Organization of neurons in the visual cortex, area 17, of the monkey (Macaca mulatta). J Comp Neurol 147:455-496.

Lund JS. 1988. Anatomical organization of macaque monkey striate visual cortex. Annu Rev Neurosci 11:253-88.

Lund JS, Lund RD, Hendrickson AH, Fuchs AF. 1975. The origin of efferent pathways from the primary visual cortex of the macaque as shown by retrograde transport of horseradish peroxidase. J Comp Neurol 164:287-304.

Lund JS, Yoshioka T, Levitt JB. 1993. Comparison of intrinsic connectivity in different areas of the macaque monkey cerebral cortex. Cerebral Cortex 3:148-62.

Maffei R, Fiorentini A. 1976. The unresponsive regions of visual cortical receptive fields. Vision Res 16:1131-1139.

Malach R, Amir Y, Harel M, Grinvald A. 1993. Relationship between intrinsic connections and functional architecture revealed by optical imaging and in vivo targeted biocytin injections in primate striate cortex. Proc Natl Acad Sci 90:10469-10473

Manger P, Kiper D, Masiello I, Murilo L, Tettoni, Hunyadi Z, Innocenti GM. 2002a. The representation of the visual field in three extrastriate areas of the ferret (Mustella putorius). Cereb Cortex 12:411-422.

Manger P, Masiello I, Innocenti GM. 2002b. Areal organization of the posterior parietal cortex of the ferret (Mustella putorius). Cereb Cortex 12:1280-1297.

Manger PR, Nakamura H, Valentiniene S, Innocenti GM. 2004. Visual areas in the lateral temporal cortex of the ferret (Mustela putorius). Cereb Cortex 14:676-89.

Martin KA, Whitteridge D. 1984. Form, function and intracortical projections of spiny neurones in the striate visual cortex of the cat. J Physiol 353:463-504.

Martinez-Conde S, Cudeiro J, Grieve KL, Rodriguez R, Rivadulla C, Acuña C. 1999. Effects of feedback projections from area 18 layers 2/3 to area 17 layers 2/3 in the cat visual cortex. J Neurophysiol 82:2667-2675.

Martinez-Millan L, Hollander H. 1975. Cortico-Cortcal projections from striate cortex of the squirrel monkey (Saimiri Sciureus). A radioautographic study. Brain Res 83:405-417.

Matsubara JA, Cyander MS, Swindale NV. 1987. Anatomical properties and physiological correlates of the intrinsic connections in cat area 18. J Neurosci 7:1428-46.

Maunsell JH, Van Essen, DC 1983a. The connections of the middle temporal visual area (MT) and their relationship to a cortical hierarchy in the macaque monkey. J Neurosci 3:2563-86.

Maunsell JH, Van Essen DC. 1983b. Functional properties of neurons in middle temporal visual area of the macaque monkey. I. Selectivity for stimulus direction, speed, and orientation. J Neurophysiol 49:1127-47.

Maunsell JH, Van Essen DC. 1987. Topographic organization of the middle temporal visual area in the macaque monkey: representational biases and the relationship to callosal connections and myeloarchitectonic boundaries. J Comp Neurol 266:535-55.

McGuire BA, Gilbert CD, Rivlin PK, Wiesel TN. 1991. Targets of horizontal connections in macaque primary visual cortex. J Comp Neurol 395:370-92.

McLaughlin DF, Sonty RV, Juliano SL. 1998. Organization of the forepaw representation in ferret somatosensory cortex. Somatosens Mot Res 15:253-68.

Merrill EG, Ainsworth A. 1972. Glass-coated platinum-plated tungsten microelectrodes. Med Biol Eng 10:662-72.

Moore Iv BD, Alitto HJ, Usrey WM. 2005 Orientation tuning, but not direction selectivity, is invariant to temporal frequency in primary visual cortex. J Neurophysiol. In press.

Mountcastle VB. 1957. Modality and topographic properties of single neurons of cats somatic sensory cortex. J Neurophysiol 20:408-434.

Morley JW, Yuan L, Vickery RM. 1997. Corticocortical connections between area 21a and primary visual cortex in the cat. Neuroreport 8:1263-1266.

Movshon JA. 1974. Velocity preferences of simple and complex cells in the cat's striate cortex. J Physiol 242: 121-23.

Movshon JA, Thompson ID, Tolhurst DJ. 1974a. Spatial Summation in the receptive fields of simple cells in the cat striate cortex. J Physiol (Lond) 283: 53-77.

Movshon JA, Thompson ID, Tolhurst DJ. 1974b. Receptive field organization of complex cells in cat striate cortex. J Physiol (Lond) 283: 79-99.

Mulligan K, Sherk H. 1993. A comparison of magnification functions in area 19 and the lateral suprasylvian visual area in the cat. Exp Brain Res 97:195-208.

Nelson JI, Frost BJ, 1978. Orientation-selective inhibition from beyond the classic receptive field. Brain Res 139: 359-65.

Nelson JI, Salin PA, Munk MH, Arzi M, Bullier J. 1992. Spatial and Temporal coherence in cortico-cortical connections: A cross correlation study in areas 17 and 18 in cat. Vis Neurosci 9:21-37.

Nowak LG, Munk MH, Girard P, Bullier J. 1995. Visual latencies in areas V1 and V2 of the macaque monkey. Vis Neurosci 12:371-84.

Obermayer K, Blasdel GG. 1993. Geometry of orientation and ocular dominance columns in monkey striate cortex. Neurosci 13:4114-29.

Ozeki H, Sadakane O, Aksaki T, Naito T, Shimegi S, Sato H. 2004. Relationship between excitation and inhibition underlying size tuning and contectual response modulation in the car primary visual cortex. J Neurosci 24:1428-1438.

Palmer LA, Rosenquist AC, Tusa RJ. 1978. The retinotopic organization of lateral suprasylvian visual areas in the cat. J Comp Neurol 177:237-256.

Payne BR. 1993. Evidence for visual cortical area homologs in cat and macaque monkey. Cerebral Cortex 3:1-25.

Philipp R, Distler C, Hoffmann KP. 2004. Characterization of motion specific areas in ferret visual cortex. Soc Neurosc Abstr 30:526.5.

Pinon MC, Gattass R, Sousa AP. 1998. Area V4 in Cebus monkey: extent and visuotopic organization. Cerebral Cortex 8: 685-701.

Polat U, Norcia AM, 1996. Neurophysiological evidence for contrast dependant long-range facilitation and suppression in the human visual cortex. Vision Res 36:2099-109.

Pucak M, Levitt JB, Lund JB, Lewis D. 1996. Patterns of intrinsic and associational circuitry in monkey prefrontal cortex. J Comp Neurol 376:614-630.

Ramsay AM, Meredith MA. 2004. Multiple sensory afferents to ferret pseudosylvian sulcal cortex. Neuroreport 15:461-5.

Raiguel, SE, Lagae, L, Gulyas, B, Orban, GA. 1989. Response latencies of visual cells in macaque areas V1, V2 and V5. Brain Res 493:155-9.

Ringach DL, Shapley RM, Hawken MJ. 2002. Orientation selectivity in macaque V1: diversity and laminar dependence. J Neurosci 22:5639-51.

Rockland KS, Lund JS. 1982. Wide spread periodic intrinsic connections in the tree

shrew visual cortex. Brain Res 169:19-40.

Rockland KS, Lund JS. 1983. Intrinsic laminar lattice connections in primate visual cortex. J Comp Neurol 216:303-318

Rockland KS. 1985. Anatomical organization of primary visual cortex (area 17) in the ferret. J Comp Neurol 241:225-236.

Rockland KS, Pandya DN. 1979. Laminar origins and terminations of cortical connections of the occipital lobe in rhesus monkey. Brain Res 179:3-20.

Rockland KS, Van Hoesen GW. 1994. Direct temporal-occipital feedback connections to striate cortex (V1) in the macaque monkey. Cereb Cortex 4:300-313.

Ruthazer ES, Stryker MP. 1996. The role of activity in the development of long-range horizontal connections in area 17 of the ferret. J Neurosci 15:7253-7569.

Rodieck RW, Stone J. 1965. Analysis of receptive fields of cat retinal ganglion cells. J Neurophysiol 28:832-49.

Roerig B, Chen B. 2002. Relationships of local inhibitory and excitatory circuits to orientation preference maps in ferret visual cortex. Cereb Cortex 12:187-98.

Salin PA, Bullier J, Kennedy H. 1989. Convergence and divergence in the afferent projections to cat area 17. J Comp Neurol 283:486-512.

Salin PA, Girard P, Kennedy H, Bullier J. 1992. Visuotopic organization of corticocortical connections in the visual system of the cat. J Comp Neurol 320:415-434.

Salin PA, Bullier J. 1995. Corticocortical connections in the visual system: Structure and function. Physiol Rev 75:107-154.

Samonds JM, Allison JD, Brown HA, Bonds AB. 2003.Cooperation between area 17 neuron pairs enhances fine discrimination of orientation. J Neurosci 23:2416-25.

Sanides F, Hoffmann, J. 1969. Cyto- and myelo-architecture of the visual cortex of the cat and of the surrounding integration cortices. J Hirnforschung 11:79-104.

Scannell JW, Blakemore C, Young MP. 1995. Analysis connectivity in the cat cerebral cortex, J Neruosci 15:1463-1483.

Sceniak, MP, Ringach, DL, Hawken, MJ, Shapley R. 1999. Contrast's effect on spatial summation by macaque V1 neurons. Nat Neurosci 2:733-9.

Sceniak MP, Hawken MJ, Shapley R. 2001. Visual spatial characterization of macaque V1 neurons. J Neurophysiol 85:1873-1887.

Sengpiel F, Sen A, Blakemore C. 1997. Characteristics of surround inhibition in the cat. Exp Brian Res 116:216-228.

Sherk H. 1986. Coincidence of patchy inputs from the lateral geniculate complex and area 17 to the cat's Clare-Bishop area. J Comp Neurol 253:105-20.

Sherk H, Ombrellaro M. 1988. The retinotopic match between area 17 and its targets in visual suprasylvian cortex. Exp Brain Res 72:225-36.

Sherk H, Mulligan KA. 1992. Retinotopic order is surprisingly good within cell columns in the cat's lateral suprasylvian cortex. Exp Brain Res 91:46-60.

Sherk H, Mulligan KA. 1993. A reassessment of the lower visual field map in striate-recipient lateral suprasylvian cortex. Vis Neurosci 10:131-58.

Shipp S, Grant S. 1991. Organization of reciprocal connections between area 17 and the lateral suprasylvian area of cat visual cortex. Vis Neruosci 6:339-355.

Shipp S, Zeki S. 2002. The functional organization of area V2, I: specialization across stripes and layers. Vis Neurosci 19:187-210.

Shmuel A, Korman M, Sterkin A, Harel M, Ullman S, Malach R, Grinvald A. 2005. Retinotopic axis specificity and selective clustering of feedback projections from V2 to V1 in the owl monkey. J Neurosci 25:2117-31.

Sillito AM, Grieve KL, Jones HE, Cudeiro J, Davis J. 1995. Visual cortical mechanisms detecting focal orientation discontinuities. Nature 378:492-496.

Sonty RV, Juliano SL. 1997. Development of intrinsic connections in cat somatosensory cortex. J Comp Neurol 384:501-16.

Spatz WB. 1977. Topographically organized reciprocal connections between areas 17 and MT (visual area of superior temporal sulcus) in the marmoset Callithrix jacchus. Exp Brain Res 27:559-572.

Stettler DD, Das A, Bennet J, Gilbert CD. 2002. Lateral connectivity and contextual

interactions in macaque primary visual cortex. Neuron 36:739-750.

Schwartz C, Bolz J. 1991. Functional specificity of a long-range horizontal connection in cat visual cortex: a cross correlation study. J Neurosci 11:2995-3007.

Schwartz TH. 2003. Optical imaging of epileptiform events in visual cortex in response to patterned photic stimulation. Cereb Cortex 13:1287-98.

Symonds LL, Rosenquist AC. 1984a. Corticocortical connections among visual areas in the cat. J Comp Neurol. 229:1-38.

Symonds LL, Rosenquist AC. 1984b. Laminar origins of visual corticocortical connections in the cat. J Comp Neurol 229:39-47.

Talbot SA, Marshall WH. 1941. Physiological studies on neural mechanisms of visual localization and discrimination. Am J Opthamol 24:1255-63.

Ts'o DY, Gilbert CD, Wiesel TN 1986. Relationships between horizontal interactions and functional architecture in cat striate cortex as revealed by cross-correlation analysis. J Neurosci 6:1160-70.

Tucker TR, Katz LC. 2003. Recruitment of local inhibitory networks by horizontal connections in layer 2/3 of ferret visual cortex. J Neurophysiol 89:501-12.

Tusa RJ, Palmer LA, Rosenquist AC. 1978. The retinotopic organization of area 17 (striate cortex) in the cat. J Comp Neurol 177: 213-35.

Tusa RJ, Rosenquist AC, Palmer LA. 1979. Retinotopic organization of areas18 and 19 in the cat. J Comp Neurol 185:657-78.

Tusa RJ, Palmer LA. 1980. Retinotopic organization of areas 20 and 21 in the cat. J Comp Neurol 193: 147-64.

Usrey WM, Sceniak MP. 2003. Chapman B. Receptive fields and response properties of neurons in layer 4 of ferret visual cortex. J Neurophysiol 89:1003-15.

Van de Grind WA, Koenderink JJ, Van Doorn AJ, Milders MV, Voerman H. 1993. Inhomogeneity and anisotropies for motion detection in the monocular visual field of human observers. Vis Res 33:1089-107.

Van Essen DC, Zeki SM. 1978. The topographical organization of rhesus monkey prestriate cortex. J Physiol 277:193-226.

Van Essen DC, Maunsell JH, Bixby JL. 1981. The middle temporal visual area in the macaque: myeloarchitecture, connections, functional properties and topographic organization. J Comp Neurol 199:293-326.

Van Essen DC, Maunsell JH. 1983. Hierarchial organization and functional streams in the visual cortex. Trends in Neurosci 6:370-375.

Van Essen, DC. Newsome, WT., Mansuell, JHR. 1984. The visual field representation in striate cortex of the macaque monkey: asymmetries, anisotropies, and individual variability. Vision Res 24:429-48.

Vitek DJ, Schall JD, Leventhal AG. 1985. Morphology, central projections, and dendritic field orientation of retinal ganglion cells in the ferret. J Comp Neurol 241:1-11.

Walker GA, Ohzawa I, Freeman R. 1999. Asymmetric suppression outside the classic receptive field of the visual cortex. J Neurosci 19:10536-53.

Wang C, Waleszczyk WJ, Burke W, Dreher B. 2000. Modulatory influence of feedback projections from area 21a on neuronal activities in striate cortex of the cat. Cereb Cortex. 10:1217-32.

Weliky M, Katz LC. 1994. Functional mapping of horizontal connections in developing ferret visual cortex: experiments and modeling. J Neurosci 14:7291-7305.

Weliky M, Kandler K, Fitzpatrick D, Katz LC. 1995. Patterns of excitation and inhibition evoked by horizontal connections in visual cortex share a common relationship to orientation columns. Neuron 15:541-52.

Weliky M, Bosking WH, Fitzpatrick D. 1996. A systematic map of direction peference in primary visual cortex. Nature 379(6567): 725-8.

White LH, Bosking WH. Fitzpatrick D. 2001. Consistent mapping of orientation preference across irregular functional domains in ferret visual cortex. Vis Neurosci 18: 65-78.

White LE, Basole A Fitzpatrick D. 2002a. Functional and anatomical characterization of an extrastriate area in ferret visual cortex. Soc Neurosci Abs 28, 159.5.

Wong-Riley M. 1979. Reciprocal connections between striate and prestriate cortex in the squirrel monkey as demonstrated by combined peroxidase histochemistry and autoradiography. Brain Res 147:159-164.

Worgotter F, Eysel UT. 1991. Topographical aspects of intracortical excitation and inhibition contributing to orientation specificity in area 17 of the cat visual cortex. Eur J Neurosci 3:1232-44.

Yoshioka T, Blasdel GG, Levitt JB, Lund JS. 1996. Relation between patterns of intrinsic lateral connectivity, ocular dominance, and cytochrome oxidase-reactive regions in macaque monkey striate cortex. Cereb Cortex 6:297-310.

Zeki SM. 1974. Functional organization of a visual area in the posterior bank of the superior temporal sulcus of the rhesus monkey. J Physiol 236:549-73.

Zeki SM. 1978. Functional specialization in visual cortex of rhesus monkey. Nature 274:423-28.

Zipser K, Lamme VAF, Schiller PH. 1996. Contextual modulation in primary visual cortex. J Neurosci 16:7376-89.